AD-776 349

MICROWAVE EXCITATION OF LASER GASES

David R. Durham

Air Force Institute of Technology
Wright-Patterson Air Force Base, Ohio

March 1974

SECURITY CLASSIFICATION OF THIS PAGE (When Data Entered)

REPORT DOCUMENTATION PAGE		READ INSTRUCTIONS BEFORE COMPLETING FORM
1. REPORT NUMBER GEP/PH/74-5	2. GOVT ACCESSION NO.	3. RECIPIENT'S CATALOG NUMBER AD 776349
4. TITLE (and Subtitle) Microwave Excitation of Laser Gases		5. TYPE OF REPORT & PERIOD COVERED Thesis
		6. PERFORMING ORG. REPORT NUMBER
7. AUTHOR(s) David R. Durham Captain, USAF		8. CONTRACT OR GRANT NUMBER(s)
9. PERFORMING ORGANIZATION NAME AND ADDRESS Air Force Institute of Technology (AFIT/EN) Wright-Patterson AFB, Ohio		10. PROGRAM ELEMENT, PROJECT, TASK AREA & WORK UNIT NUMBERS
11. CONTROLLING OFFICE NAME AND ADDRESS Aerospace Research Laboratory (ARL/LU) Wright-Patterson AFB, Ohio		12. REPORT DATE March, 1974 13. NUMBER OF PAGES 112
14. MONITORING AGENCY NAME & ADDRESS(if different from Controlling Office)		15. SECURITY CLASS. (of this report) Unclassified 15a. DECLASSIFICATION/DOWNGRADING SCHEDULE

16. DISTRIBUTION STATEMENT (of this Report)

Approved for public release; distribution unlimited

17. DISTRIBUTION STATEMENT (of the abstract entered in Block 20, if different from Report)

Approved for public release; distribution unlimited

18. SUPPLEMENTARY NOTES

Approved for public release;
IAW AFR 190-17.

JERRY C. HIX, Captain, USAF
Director of Information

19. KEY WORDS (Continue on reverse side if necessary and identify by block number)

Microwave Excitation
Helium Metastables
Gas Ionization
Penning Ionization

20. ABSTRACT (Continue on reverse side if necessary and identify by block number)

The goal of this experiment was the creation of large numbers of electrons and helium (2^3S) metastables through the use of four microwave cavity discharges. The desire for gas ionization independent of the exciting field stems (1) from the increased efficiency available when lower exciting fields can be used, and (2) from the stabilizing effect of independent electron density control. The desire for helium metastable production stems from (1) additional electron creation via Penning ionization in a helium

DD FORM 1 JAN 73 1473 EDITION OF 1 NOV 65 IS OBSOLETE

UNCLASSIFIED

SECURITY CLASSIFICATION OF THIS PAGE (When Data Entered)

Abstract (Continued)

afterglow, and (2) increased metal-vapor laser pumping efficiency. The microwave cavity discharge technique is shown to produce on the order of 5×10^{10} helium metastables per cubic centimeter and 5×10^{10} helium metastables per cubic centimeter and 5×10^{10} electrons per cubic centimeter. The effective increase of the recombination coefficient due to electron cooling by added nitrogen was shown. And the discovery of negative absorption of the 3889A line in a pure helium afterglow was made.

MICROWAVE EXCITATION OF LASER GASES

THESIS

GEP/PH/74-5

DAVID R. DURHAM
CAPTAIN, USAF

MICROWAVE EXCITATION

OF LASER GASES

THESIS

Presented to the Faculty of the School of Engineering

of the Air Force Institute of Technology

Air University

In Partial Fulfillment of the

Requirements for the Degree of

Master of Science

by

David R. Durham, B.E.S.
Captain USAF

Graduate Engineering-Physics

January, 1974

ic

Preface

This work is a study of microwave excitation of laser gases done with the cooperation and guidance of the Plasma Physics Group at the Aerospace Research Laboratories at Wright-Patterson Air Force Base, Ohio.

Thanks is not a sufficient word to describe the appreciation I feel toward the Plasma Physics personnel. I am especially grateful to Dr. Peter Bletzinger, Dr. Alan Garscadden, and Captain Bailey who seem to have endless patience with questions. Rod Darrah spent many late hours assisting. C. Van Sickle helped build the tube and knew where to look for that missing part. Glen Hubka always took his time to lathe that extra piece. J. Ray re-built the inlet tubes time after time and Lt Colonel Dettmer solved an equal pressure problem I couldn't.

Thanks also to Captain Bailey for his advice on solutions to the mobility problem. And a special thanks to Dr. Merrill Andrews of Wright State University who read the rough draft and helped clarify my thoughts.

My wife [redacted] spent much time alone wondering if it would end. And my son [redacted] showed me that learning is built from small steps.

Contents

List of Figures

List of Figures

Abstract

The goal of this experiment was the creation of large numbers of electrons and helium (2^3S) metastables through the use of four microwave cavity discharges. The desire for gas ionization independent of the exciting field stems (1) from the increased efficiency available when lower exciting fields can be used, and (2) from the stabilizing effect of independent electron density control. The desire for helium metastable production stems from (1) additional electron creation via Penning ionization in a helium afterglow, and (2) increased metal-vapor laser pumping efficiency. The microwave cavity discharge technique is shown to produce on the order of 5×10^{10} helium metastables per cubic centimeter and 5×10^{10} electrons per cubic centimeter. The effective increase of the recombination coefficient due to electron cooling by added nitrogen was shown. And the discovery of negative absorption of the 3889Å line in a pure helium afterglow was made.

10 to the 1500 power

MICROWAVE EXCITATION

OF LASER GASES

I. Introduction

The CO_2 laser was limited to low power until Terrill A. Cool first researched the advantages (Ref 11) of a flowing gas laser system and who, with Shirley, showed marked gain increases in a CO_2 system by flowing the gas mixture at high velocities (Ref 12). Investigation revealed that the wall dominated laser plasma had an electrical to optical conversion efficiency limited by the wall temperature. The convective laser, however, utilized gas convective cooling to maintain cool gas translational temperature while still allowing high vibrational temperature. Since Cool's discovery, power levels up to 27 kilowatts of continuous power have been reported using convective subsonic systems (Ref 6).

Convective flow has not been the complete answer to high power laser systems. The attempted scaling of the convective laser has resulted in the onset of plasma instabilities with increased gas pressures and/or volumes because at lower electric field to pressure ratios glow-to-arc transitions have become more probable. And with the onset of arc, laser power terminates because of gas heating and redistributed electron energies (Ref 13:733).

According to Nighan (Ref 41), plasma instabilities depend directly on the response of the electron density to plasma disturbances. Therefore if the electron density were controlled from outside the lasing region, higher power densities in lasers would be possible.

Such electron density control has been accomplished using electron beams operating independently of the primary plasma exciting field. Photoionization has been used by Levine and Javan to control electron density (Ref 31). And in 1971 Ganley, et al., reported electron density tailoring by neutron irradiation to enhance CO_2 laser output (Ref 20).

One important goal of this project has been to separate control of the electron density from the primary exciting field. With the ability to control independently the electron density one gains control over plasma instabilities that depend on the electron density. Additionally, the electron energy distribution can be optimized because independent control of the electron density allows the energizing source to be chosen to fit the specific transition reaction.

A second important goal of this project has been to optimize the density of the $He(2^3S)$ metastable. For many lasing media (He-Ne, He-Hg, He-Se, He-Cd, etc.), the population density of the $He(2^3S)$ determines the efficiency of the laser because the Penning ionization process (to be discussed later) is the pump for the upper laser level.

The approach for achieving independent electron density control and optimization of $He(2^3S)$ production was the same. The approach was to use a microwave cavity operating at 2.45 GHz to excite fast flowing He. This process gives large numbers of both electrons and $He(2^3S)$ metastables in the afterglow. The electron density may be multiplied by the Penning process with N_2 in the afterglow under the proper conditions. And the overall parameters of microwave power, flow velocity of helium, pressure in the reaction zone, and gas mixture must be

chosen to obtain the desired response.

Because the parameters for electron production were multiplied by the number of processes occurring simultaneously, the theory will be broken down into three parts: (1) a description of the glow discharge, (2) an introduction to Penning ionization, and (3) a description of the independent ionization control concept. Following the theory will be the analysis of the reactive species interaction, the methods for making the measurements of the interactions, the experimental results, and finally conclusions and recommendations.

II. Introduction to the Glow Discharge

As was stated, the theory will start with the glow discharge. A description of the position of the glow discharge on the current-voltage characteristic relation will be followed by a classification of parts, a graphic description, and finally the ionization balance equations.

The characteristic relation of current and voltage describes for some gas at some pressure the sum of all ionizing reactions occurring in that gas. A typical curve is given in Figure 1. Not all of the regions are of interest here and only the saturation currents leading to self-sustained discharge and subsequent glow will be discussed.

The saturation current region is characterized by a linear current ramp for which all electrons emitted by the cathode are ultimately collected by the anode. An external source of ionization must be provided at the cathode (such as photoionization) so current will flow. Should the external source be removed the saturation current would essentially cease. An inherent requirement on the electrons in the saturation region is that the drift velocity gained from the applied electric field be slow enough to avoid inelastic ionizing collisions with the background gas. Should the electron drift velocity become fast enough to produce large quantities of secondary electrons through inelastic ionizing collisions, a self-sustained discharge will result. The self-sustained discharge requires no external source of electron production and will increase in current to the limit of the external circuit. Ion-neutral collision processes and cathode processes dominate the discharge.

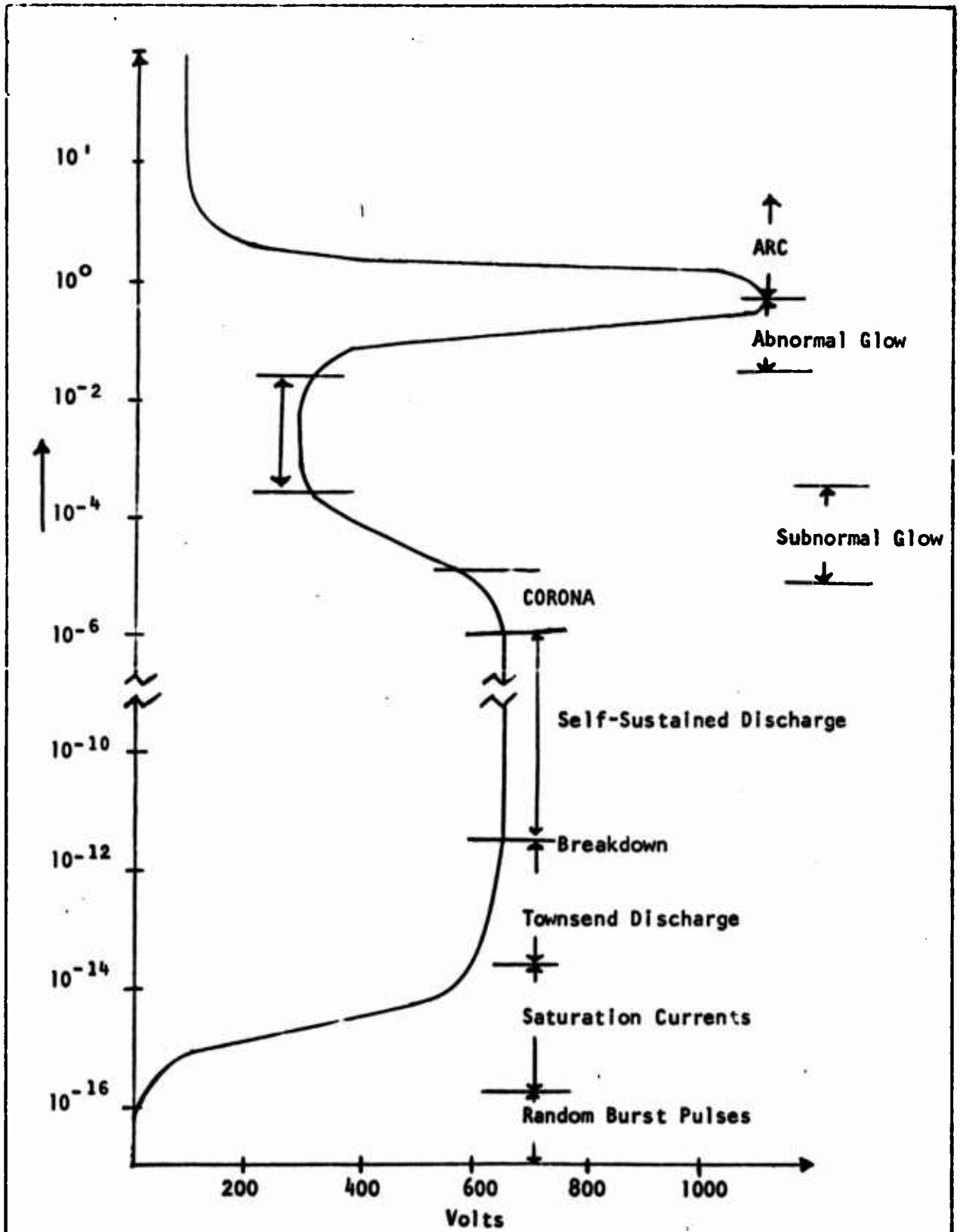

Fig. 1. A Typical Voltage Current Relation for an Enclosed Gas

If the external circuit will allow, the self-sustained discharge will become the glow discharge. The glow discharge is characterized by a nearly uniform current density and voltage in the positive column. As shown by Figure 2, the glow discharge is often divided into seven separate regions. Some glow discharges have all the regions readily discernible while others seem to have only the positive column. A brief description of the seven regions may be found in the references (Ref 7). For our purposes only the positive column has similar general parameters to the concepts to be described.

The positive column is a conducting path from the Faraday dark space to the anode. Much work has been done on the positive column because of its uniformity. As Figure 3 shows, the positive column is non-varying over its entire length. Charge density in the positive column is zero because the electron density equals the ion density. No net recombinations take place and do net negative ions exist.

From the brief description of the positive column and Figure 3, a short treatment of the reactions in that region is now undertaken. The discussion will be limited to the positive column and the following assumptions will be made to greatly simplify the equations:

1. No net charge density
2. Steady-state condition ($n_i = n_e$)
3. No negative ions.
4. Circular cross section with radius large compared to the electron mean free path.
5. No charge on the column's radial edge.
6. No end effects.

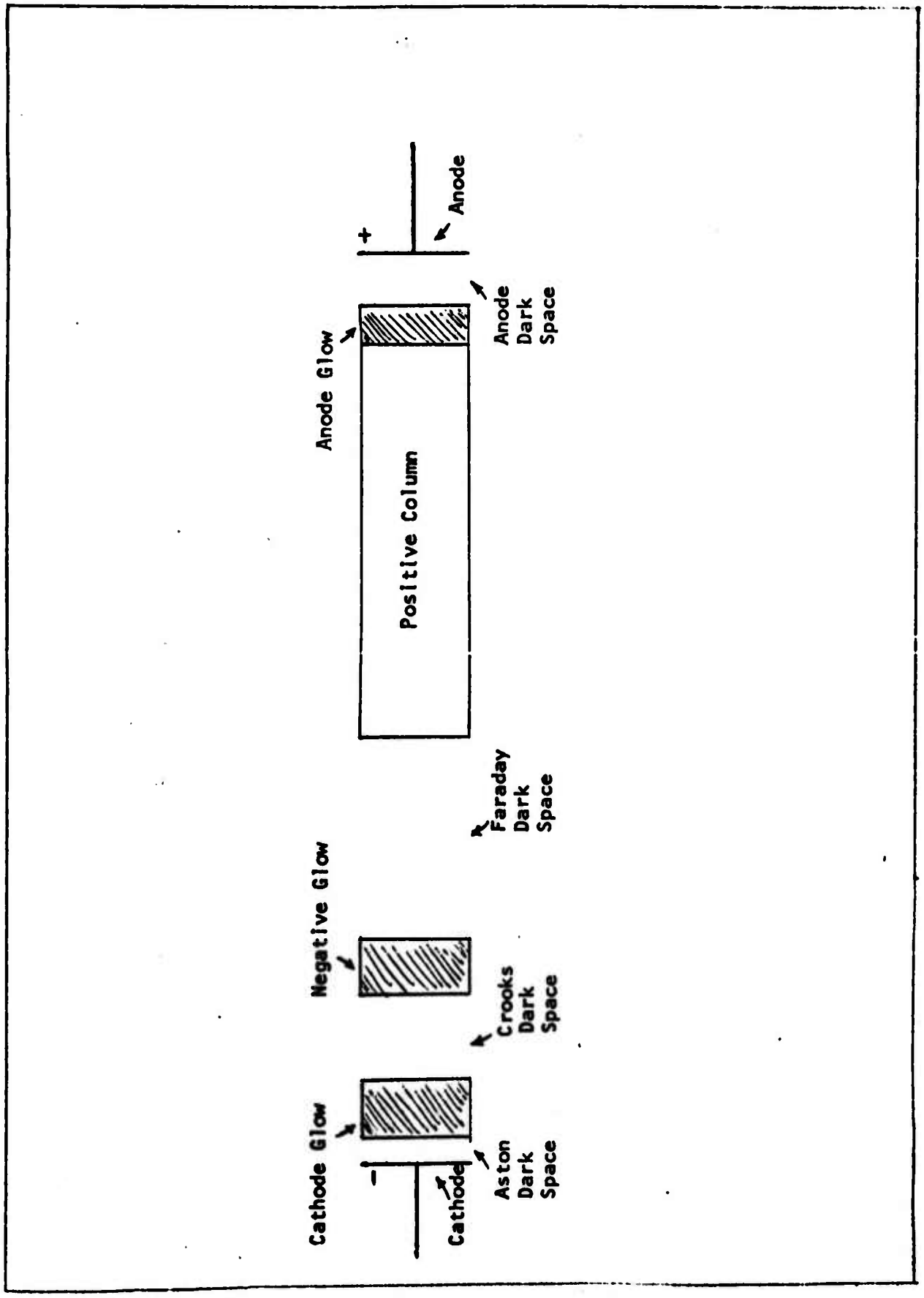

Fig. 2. Classification of the Parts of the Glow Discharge

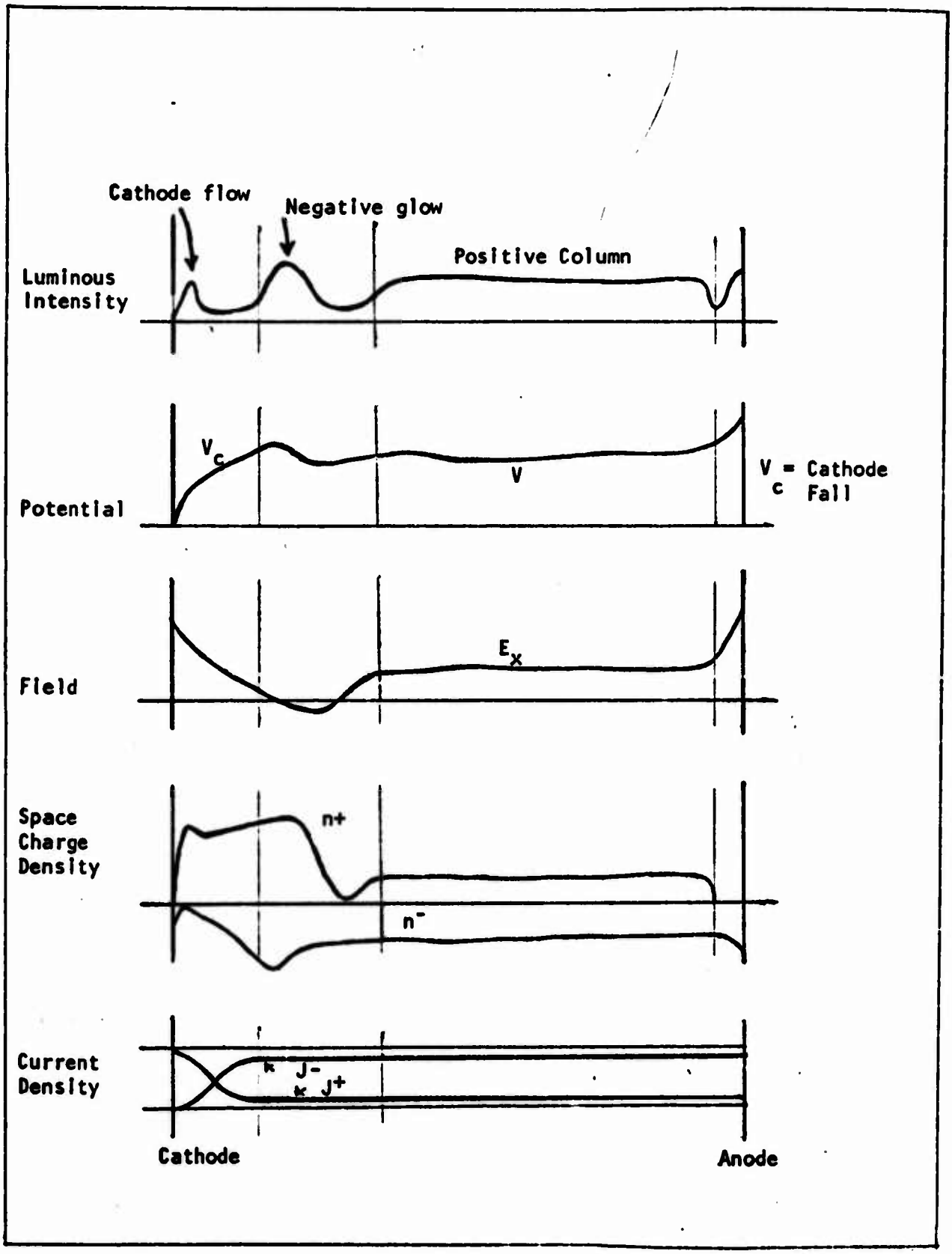

Fig. 3. Graphic Description of Glow Discharge

The first assumption allows one to set the time rate of change of electron (or ion) density to zero. Writing the first moment of the Boltzmann transfer equation for the species 'a' one gets

$$\dot{N}_a + \nabla \cdot N_a \vec{U}_a = \Sigma S_{coll}^{(a,b)} \qquad (1)$$

where $\dot{N}_a$ = time rate of change of species 'a' number density, N_a = species a number density, $\vec{U}_a$ = the average flow of species 'a; and $S_{coll}^{(a,b)}$ = the collisional process that creates or destroys species a through a collisional reaction with species 'b'. Using the first two assumptions equation (1) maybe written

$$\nabla \cdot N_a \vec{U}_a = \Sigma S_{coll}^{(a,b)} \qquad (2)$$

This could be the continuity equation for electrons if we knew the electron production and loss reactions that make up $\Sigma S_{coll}^{(a,b)}$. Some possible electron production and loss reactions are: (1) impact ionization and three body recombination, (2) associative ionization and dissociative recombination, (3) photoionization and radiative recombination.

Impact ionization and three body recombination can be written as a reversible reaction pair

$$X + Y \rightleftarrows X^+ + e + Y$$

where it is not necessary that the reaction proceed in both directions at the same rate. Two forward going special cases of this type of

reaction are important here: electron impact ionization and the Penning effect.

Electron impact ionization could be written as above by replacing "e*" for "Y". This impact is inelastic and occurs only for electrons of kinetic energy equal to or greater than the ionization potential of the gas particle "X".

The Penning effect is written by showing "Y" as a long-lived excited gas atom (or molecule) as Y*. When "X" is some atom (or molecule) with an ionization potential lower than the metastable energy level of "Y*" then the Penning reaction may proceed. This type of reaction has not been known to be directly reversible although three body recombination is an indirect reversal.

Associative ionization and dissociative recombination are written

$$X + Y \rightleftarrows XY^{+} + e$$

The forward going reaction is important in helium metastable collisions (sort of a self-Penning process) and for helium has been shown to transition into associative ionization from impact ionization with increasing pressure. The reverse reaction is an important electron loss mechanism for electrons of energy less than the ionization potential of "XY".

Photoionization is not highly probable when the ionization energy required is 25eV (corresponds to 504 Å light). However, the reverse reaction, radiative recombination, is a definite likelihood in helium ion states and is an electron loss mechanism.

The particular processes which occur among helium and electrons and which lead to electron creation or annihilation are the following:

(1) Ground state atom - energetic electron collisions

$$He(^1S_o) + e^* \rightarrow He^+ + 2e - \Delta E_e$$

Ionization from the ground state in helium requires 24.58 electron volts. A much easier ionization occurs from the next reaction.

(2) Excited atom - energetic electron collision

$$He^* + e^* \rightarrow He^+ + 2e - \Delta E_e'$$

In this case ionization from the lowest energy state above ground requires only about 4.8 eV.

(3) Excited atom - excited atom collision

$$He^* + He^* \rightarrow He(^1S_o) + He^+ + e + \Delta E_i$$

$$\rightarrow He_2^+ + e + \Delta E_i$$

This process has two possible product configurations but the net effect is still the production of an electron.

(4) Ion-slow electron capture and radiative recombination

$$He^+ + e \rightarrow He + h\nu$$

$$\rightarrow He^* + h\nu' \qquad \nu' < \nu$$

$$He_2^+ + e \rightarrow 2He^* + h\nu'$$

Obviously an electron loss process, the first formula could additionally lead to resonant radiation trapping for which no change in electron number could be detected. The last two processes would yield the same detectable information for electron number density: loss of an electron.

One might argue that the second ionization of helium is another production method of electrons. But since a total energy of 70eV is required for the second ionization (Ref 46:780), this process will be ignored.

Having discussed the possible processes for electron gains and losses, it is now possible to write an equation for $\sum_b S_{coll}^{(e,b)}$.

$$\sum_b S_{coll}^{(e,b)} = \nu_{ne} n_e + \nu_{me} n_e + \nu_{mm} n_m - \nu_{ie} n_e$$

where the symbols are defined as follows:

ν_{ne} = collision frequency for ionization of neutrals by electrons

ν_{me} = collision frequency for ionization of metastables by electrons

ν_{mm} = collision frequency for metastable-metastable ionization

ν_{ie} = collision frequency for electron capture by ions

n_e = number density of electrons

n_m = number density of metastables

For some general collision frequency ν_g the cross section for the appropriate reaction σ_r may be related by

$$\nu_g = n_r \bar{v}_{rg} \sigma_r$$

where n_r = reactant species, $\bar{v}_{rg}$ = average relative velocity between the reacting bodies. An an example, ν_{ne} should be written

$$\nu_{ne} = n_n \bar{v}_{ne} \sigma_i \quad \text{where } i = \text{ionization and}$$

n_n = neutral number density.

Then writing the summation again, one substitutes in the appropriate cross sections as follows:

$$\sum_b S_{(e,b)} = n_e (n_n \bar{v}_{ne} \sigma_i + n_m \bar{v}_{me} \sigma_i' - n_i \bar{v}_{ie} \sigma_c) + n_m^2 \bar{v}_{mm} \sigma_i''$$

For the above equation, n_i = number density of ions, σ_c = capture cross section, and the σ_i annotated with primes indicates that the particular ionizing cross sections for different reacting species are not in general the same.

The next subject should be the left side of equation (2) where if isothermal conditions are assumed ($p = nkT$) and Fick's law is used ($\Gamma = -D\nabla n$) one obtains

$$\nabla \cdot n\bar{u} = \nabla \cdot \Gamma = -\nabla \cdot (D\nabla n) = -D\nabla^2 n$$

for $\nabla D = 0$, where D = the diffusion coefficient.

Writing out the entire equation for electrons, one finds

$$\nabla^2 n_e = \frac{-1}{D_a} \left[\left(n_n \bar{v}_{ne} \sigma_i + n_m \bar{v}_{me} \sigma_i' - n_i \bar{v}_{ie} \sigma_c \right) n_e + n_m^2 \bar{v}_{mm} \sigma_i'' \right] \qquad (3)$$

The electron number density is coupled to the metastable density only because $\dot{n}_i = \dot{n}_e$ for zero net charge density and n_e, n_i, and $n_m \ll n_n$ for partially ionized gases. Assuming $n_n \approx$ constant then $\nabla^2 n_n \approx 0$. For the metastable continuity equation, one has

$$\nabla^2 n_m = -\frac{1}{D_t}\left[n_n n_e \bar{v}_{ne}\sigma_m + n_i n_e \bar{v}_{ie}\sigma_c - n_m n_e \bar{v}_{me}\sigma_s\right] \qquad (4)$$

where

D_t = thermal diffusion coefficient

σ_m = cross section for metastable production

σ_s = cross section for superelastic collision

σ_c = cross section for capture leading to metastable production

At this point one would be tempted to disregard the relative velocity and cross sections in the separate terms and say that since $n_n \gg n_e$, n_m, n_i, the last two terms could be dropped. And indeed for slightly ionized gases where $n_n \sim 10^{16}$ and $n_i = n_e \sim 10^{10}$, and where σ_m differs from σ_c, σ_s by less than two orders of magnitude, then the last two terms may be disregarded, since the relative velocity between an electron and ion or metastable is the same.

The equation for metastables becomes then

$$\nabla^2 n_m = -\frac{1}{D_t} n_n n_e \bar{v}_{ne}\sigma_m \qquad (5)$$

which can be solved by separation of variables. Assume $n_m = R(r)\Phi(\phi)Z(s)$ and the general solution is

$$n_m = 2 C_k J_o(ikr) e^{\pm ikz} \qquad (6)$$

where cylindrical coordinates have been used and angular symmetry assumed. The separation constant

$$k^2 = k'^2 - \frac{1}{D_t} n_n n_e \bar{\nu}_{ne} \sigma_m \tag{7}$$

follows directly from writing

$$-k'^2 = -\frac{Z''}{Z} - \frac{1}{D_t} n_n n_e \bar{\nu}_{ne} \sigma_m$$

Inspection of equations (3), (6) and (7) will show that a numerical solution to the continuity equation for electrons would be preferred.

At this point a discussion of the Penning ionization principle will be undertaken before returning to the ionization balance equations.

III. Introduction to Penning Ionization

Suppose that some given gas, A, has a higher metastable energy state (not ionized) than the ionization energy state of some second gas, B. The consequence of a collision between A in its excited metastable state A* and B in any state below its ionization energy state is the transfer of energy from A* to B resulting in ground state A and ionized B. This chemical reaction process may be symbolized:

$$A^* + B \rightarrow A + B^+ + e$$

Any energy in excess of the ionization energy of B may go into internal energy of B (if a molecule), or into electron gas heating (kinetic energy of e), or into both.

If the ejected electron has sufficient energy to escape the attraction of the ionized B, it diffuses rapidly through the neutral gas. And if the overall concentration of electrons and ions is low, the electron lifetime is long meaning it is available for further collisions with the neutral gas.

The process just described is called Penning ionization. Reveral of the Penning process is either through radiative recombination

$$B^+ + e \rightarrow B^* + h\nu$$

or dissociative recombination

$$B_2^+ + e \rightarrow B^* + B^*$$

or charge transfer

$$A^+ + B \rightarrow A^* + B^+$$

Because the Penning process is reversible and energy level dependent, it would be appropriate to discuss the various rates at which the Penning process proceeds and is reversed. Since the rates are dependent upon the reacting species and their probability of collision, a specific temperature will be picked for the reactant species chosen.

The first reactant will be helium. Helium has a Penning process with itself when the colliding molecules are both excited to as low as the first state above ground. The first state above ground is a 2^3S state and has an excitation energy of 18.8 eV. Obviously two $He(2^3S)$ atoms colliding have total energy in excess of the 24.58 eV that it takes to ionize one of the He atoms. The process is symbolized:

$$He^*(2^3S) + He^*(2^3S) \longrightarrow He^+ + He + e + \Delta E(0\text{-}i4.5eV) \quad \text{(Ref 28)}$$

$$He^*(2^3S) + He\ (g.s.) \longrightarrow He_2^+ + e + \Delta E(15eV)$$

(Hornbeck-Molnar Process)
(Ref 28 and 16)

The cross section for the above reactions was given by Phelps and Molnar (Ref 42) to be 10^{-14} cm^2 at 300^oK and the effective rate coefficient by Miller, Verdeyen and Cherrington (Ref 38) was given as 1.8×10^{-9} $\frac{cm^3}{sec}$.

The second reactant species will be the nitrogen molecule. Nitrogen was chosen for several reasons. First, it has a rather large cross section for ionization with the $He(2^3S)$ excited atom. Second, there are no reaction channels in competition with the Penning process as there are in O_2 (Ref 43). Third, a mixture of $He\text{-}N_2\text{-}CO_2$ has

important implications in high power lasers.

The specific Penning process with N_2 is the following:

$$He(2^3S) + N_2 \rightarrow N_2 + (B^2\Sigma_u^+) + He + e$$

For this reaction the ionizing transition occurs when an electron from nitrogen tunnels into the empty 1s helium orbital. The 2s electron escapes the helium and the electron exchange mechanism leaves a ground state helium, ionized nitrogen and a free energetic electron (Ref 43). Application of the Franck-Condon principle (Ref 23:194) to the reacting species implies that the free electron leaves with about 0.2eV for N_2^+ vibrational excitation to the v = 3 state.

According to Richardson and Setser (Ref 43) the statment that an He^*-N_2 collision leads to the $B^2\Sigma_u^+$ state of N_2^+ is incomplete. The relative electronic state populations of N_2^+ are divided among $X^2\Sigma_g^+$, $A^2\pi_u$, and $B^2\Sigma_u^+$ states in the percentages 35:24:41 respectively. That would say that the exiting electron may have energy from ~ 0 to 4+eV. The energy of the free electron is important when considering the electron energy distribution function, but for the purpose of generating electrons the mere fact of being free is sufficient. Therefore rather than use the rate coefficient for each specific electronic excitation, only the overall rate coefficient for the Penning process will be used. This coefficient from M. Cher and C. S. Hollingsworth is $k = (1.0 \pm 0.3) \times 10^{-10}$ cm^3/molecule sec at 300°K measured at 1-2 torr (Ref 10).

One last finding of Cher and Hollingsworth is noteworthy: the rate coefficients are not functions of pressure but depend on temperature. Their range of pressures covered .64 to 2.03 torr but their data

displayed no significant rate coefficient variation with pressure.

Reversal of the Penning self-ionization in helium is possible through the coupled process collisional-radiative recombination

$$He^+ + e \rightarrow He^* + h\nu$$

$$He^+ + e + e \rightarrow He^* + e$$

through dissociative recombination

$$He_2^+ + e \rightarrow He^* + He$$

or in the presence of another gas through charge transfer

$$He_2^+ + N_2 \rightarrow N_2^+ + He^* + He$$

For the charge transfer reaction above, Bolden, et al. (Ref 5) gives a reaction rate constant of 12.5×10^{-10} cm^3/sec. For dissociative recombination Johnson and Gerado (Ref 29) have shown that the effective rate coefficient for He_2^+ production from metastable-metastable collision includes the reversal (dissociative recombination) rate coefficient. As such small errors will be introduced when dissociative recombination is neglected. Lastly for the collisional-radiative recombination coefficient, Bates et al. (Ref 2) calculated it to be 1.8×10^{-8} cm^3/sec and Cher, et al. (Ref 9) experimentally determined it to be $8.9 \pm 0.5 \times 10^{-9}$ cm^3/sec at T_e of 300°K and n_e of 1.6×10^{11}/cm^3.

Reversal of the Penning process for nitrogen in the helium nitrogen mix would come from radiative recombination

$$N_2^+ + e \rightarrow N_2 + h\nu$$

but the process is too slow to effect large changes in the reaction region used here and will be ignored.

Knowing the applicable processes it is now worthwhile to discuss the external control concept.

IV. Description of Experimental Concept for Independent Ionization Control

Probably the first indication that tailoring of the electron density independent of the energizing field would increase the efficiency of lasers came from Ganley in 1971 (Ref 20), when he showed efficiency increase from neutron irradiation. Other external controls have been attempted including plasma jets, UV, and electron beams.

The experimental concept for ionization control independent of the energizing field came from A. Garscadden and P. Bletziner of the Aerospace Research Laboratories. The concept uses three separate processes: microwave discharge ionization, Penning ionization, and gas dynamic (convective) cooling.

Microwave discharge ionization is accomplished by flowing a gas (helium in this case) through an operating microwave cavity. Electron impact ionization occurs between the few naturally existing electrons and the gas particles. Subsequent electron impact ionization by the secondary electrons thus created leads to gas breakdown. Additional collisions lead to additional electron creation but the electron losses also increase until a steady state is reached. The steady state achieved is a function of pressure, flow velocity, impurity concentration, gas temperature, and microwave power.

Penning ionization has been discussed previously and only the reminder that in helium self-ionization via the Penning process is highly likely need be mentioned.

Convective cooling is somewhat complicated for the particular configuration used in this project, but for the purposes of this

explanation is simply the extraction of heat by removal of the unusable thermalized species.

The external control concept can best be demonstrated by an example. The obvious example of interest is the CO_2-N_2-He mixture. The discussion will proceed from knowing that the addition of N_2 increased the upper laser level pumping efficiencies and the addition of helium depopulates the lower CO_2 vibrational energy level.

For the given mixture, calculations by Fowler (Ref 17) have shown that optical power density is a function of the square of the neutral gas density at constant electron-neutral ratio and constant gas temperature. Scaling the power means scaling the density at constant gas temperature. However, to maintain gas temperature the excess heat must be conducted away. For closed non-flowing or slow-flowing systems conduction means wall-dominated thermal conduction where practical tubes sizes for short conduction times are of the order of 1 cm radius (Ref 41:10).

So, using a 1 cm radius tube and liquid nitrogen wall cooling scaling could be attempted at higher densities (hence higher pressures). For the optimum field to pressure ratio (E/P) of ten to fifty volts per cm-torr, a one meter laser at 200 torr requires 200,000 volts minimum. Arc discharges occur long before 200 kilovolts is reached and arc discharges do not efficiently pump the CO_2 laser.

One way to avoid the 200 kilovolt fields required for a 200 torr one meter laser would be to excite the gas transverse to the optic axis rather than along the axis. Transverse excitation reduces the required voltage by two orders of magnitude, but, because of the increased

particle number density with increased pressure, a glow-to-air transition becomes more probable at lower values of E/P (Ref 13:733).

Rather than increase E/P, a way to reactivate the upper laser levels of CO_2 is sought. The main problem is the deactivation of trapped energy. Convective cooling sweeps trapped energy in low lying excited states (specifically the 010 of CO_2) from the reacting region. The ground state CO_2 swept in can be activated and the lasing process repeated. By just such a technique continuous wave operation of the CO_2 laser at atmospheric pressure has been achieved (Ref 36). Further, T. Cool has demonstrated a 415% gain coefficient increase by convective cooling in CO_2 (Ref 12).

The next step is to change the gas impedance by utilizing preionization. As was mentioned, various techniques in addition to microwave discharge ionization are possible. Electron beams have given the best results to date. However, electron beams (e-beams) require extremely high voltages and massive equipment. Microwave (μw) discharge electron production presents a very attractive alternate since it requires lower voltages and much less massive equipment.

Either e-beam or μw electron production techniques offer essentially the same final result: maintenance of electron-ion pairs against volume losses in dense plasmas. The decoupling of electron production from the energizing electric field additionally leads to stability in the discharge.

This last statement may be seen by reference to Figure 1. It can be seen that for any saturation current curve that the number density of electrons remains approximately constant so long as breakdown voltages

are avoided. For current density J_e given by

$$J_e = -N_e q \mu_e E$$

the current becomes primarily a function of the electron number density N_e alone since the charge q and the electron mobility μ_e are constants and the applied electric field E is less than the breakdown field E_b. Therefore, fluctuations in E along the saturation current curve have little effect on the electron number density. In contrast, if the glow region is the region of operation (for a plasma dependent primarily on the applied field) small fluctuations in applied field lead to large fluctuations in electron number density.

The use of helium for electron production has two advantages. First, the metastable levels $He(2^3S)$ and $He(2^1S)$ are sufficiently energetic to ionize any atom or molecule except neon. Second, the electron-metastable reaction in helium leads to either He^+ and hence additional electrons or to ground state helium and a high energy electron, both beneficial responses.

By mixing helium metastables with nitrogen in the afterglow (a region where high temperature electrons and metastables are de-excited by collisional and radiative combinations after exiting an excitation region) additional electrons are produced. And as Benton, et al., have shown the additional electrons are not negligible (Ref 3:208).

Harkening back to the example then, the laser system proposed would be convectively cooled, pre-ionized by microwave discharge ionization in helium, then further ionized by Penning ionization in the after glow of the microwave discharge as in Figure 4.

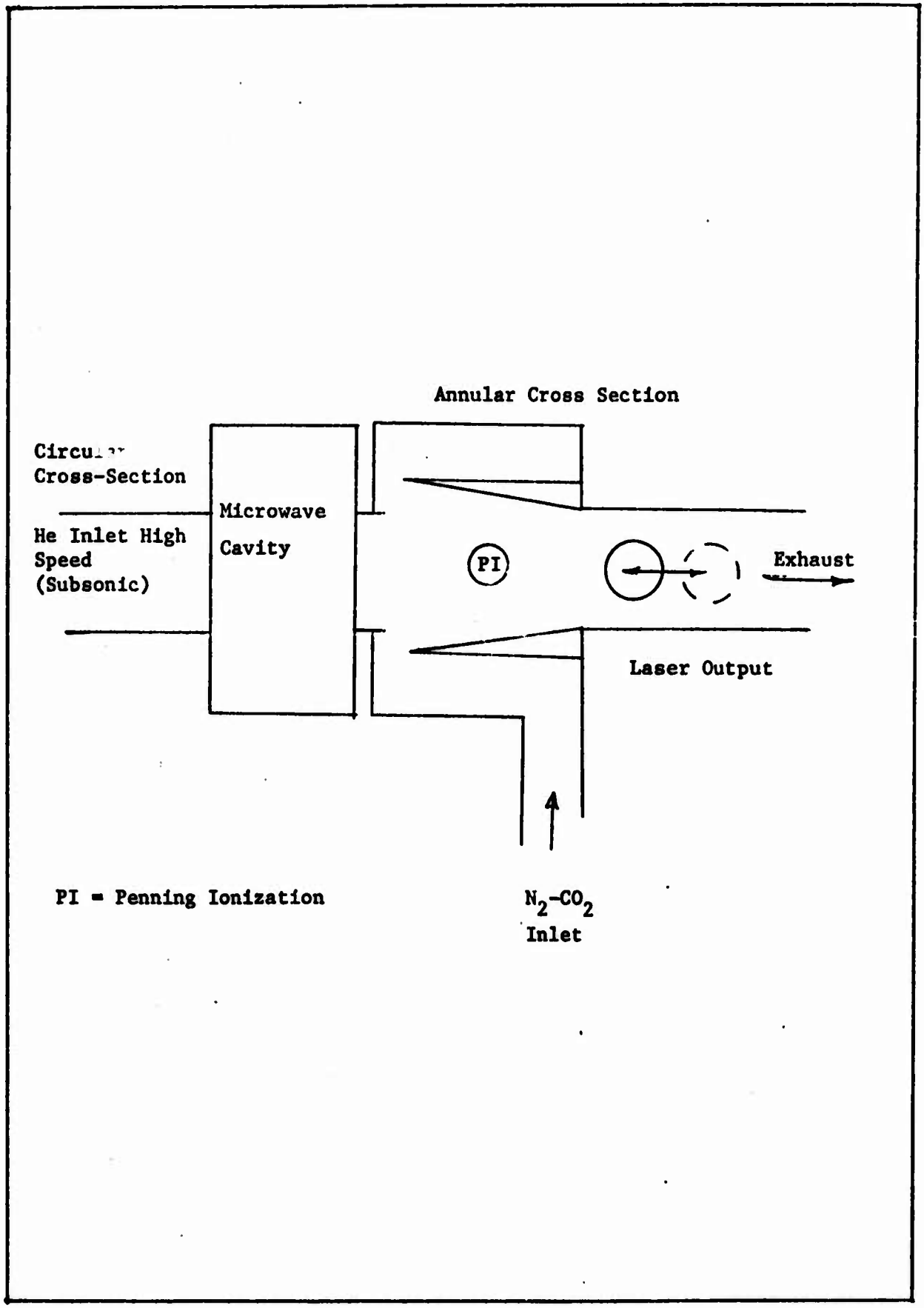

Fig. 4. A Proposed Laser System

The convective microwave-Penning ionization control technique has an additional advantage in molecular lasers worthy of mention: efficiency of vibrational population pumping. Because the electrons are produced independent of the laser exciting field, low distributed fields may be used to preferentially charge vibrational states through elastic collisions (Ref 41:16).

In order to better illustrate the last statement, Figures 5 and 6 are presented.

From Figure 5 one sees that pumping of the upper laser level of CO_2 is effected by a .29 eV vibrational energy N_2 molecule. Since (1) the relaxation time of $N_2(v = 1)$ at a few torr is greater than 8 seconds, (2) the average thermal energy (kT) of molecules is around .025eV, and (3) the energy difference between the $v = 1$ in N_2 and the (001) in CO_2 is about .0022eV, large cross sections for collisions of the second kind are possible due to near perfect energy coincidence.

As shown in Figure 6, for ionization the lowest field to number density (E/N) ratio is about 12×10^{-16} V-cm^2. At this E/N, thirty-four percent of the applied power is transferred into all vibrational states. At an E/N of 3×10^{-16} V-cm^2, the fractional power transferred into all vibrational states is ninety-nine percent. Therefore using the lower E/N, energy is not wasted pumping unwanted vibrational or electronic energy states.

Presuming that some justification for examining this external control concept has been shown, the experimental method of choice will be described and the results given.

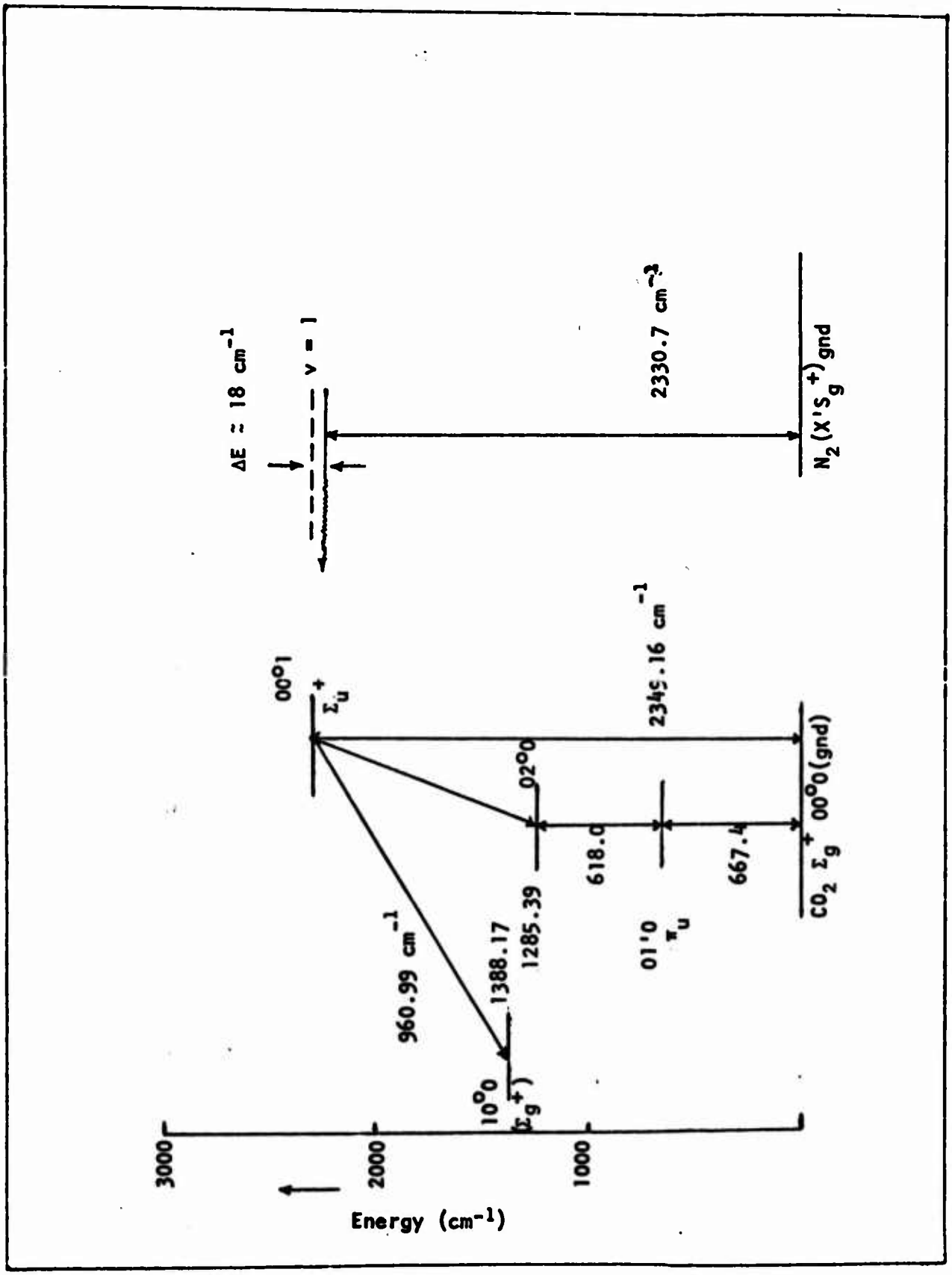

Fig. 5. Energy Level Diagram for N_2-CO_2 Energy Transfer

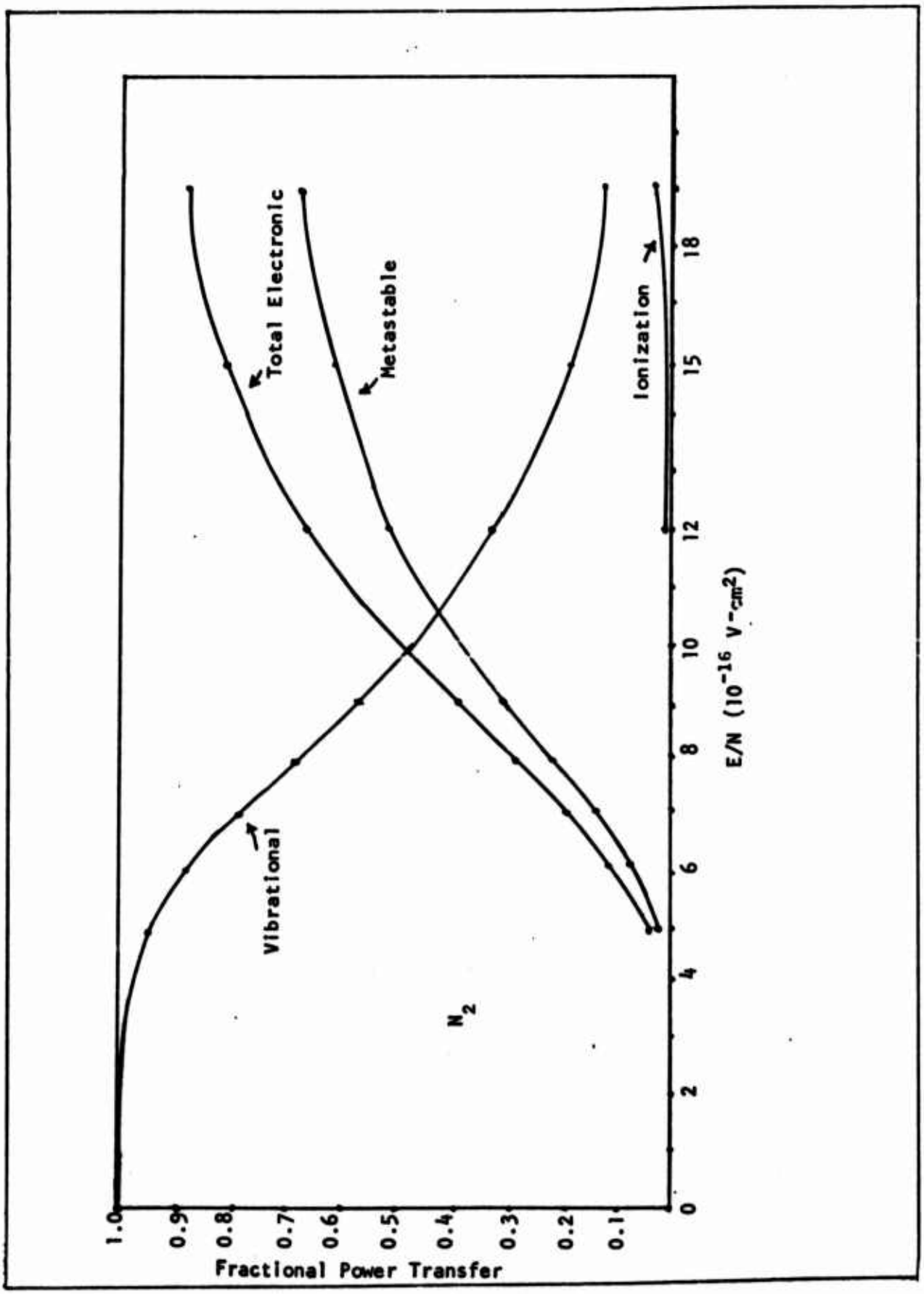

Fig. 6. Fractional Power Transfer in N_2

V. Analysis of Metastable $He(2^3S)$ in the Afterglow

Figures 7 and 8 describe the gas flow geometry. Complications in the flow arise from the discontinuous nature of the geometry, but these problems will be avoided in this treatment.

Bolden, et al, solved the basic high speed flowing problem (Ref 5:47), albeit subsonically, and the exhaust flow here (1.23×10^4 cm/sec) compares favorably with theirs (1.393×10^4 cm/sec) assuming both gases fill the tube. Therefore the Bolden, et al. solution for the axial variation of ion density will be used to describe the metastable and electron density variations substituting the appropriate diffusion coefficients where required.

The metastable density n_m may be described by a continuity equation of the form

$$\frac{\partial n_m}{\partial t} + \nabla \cdot n_m \bar{U}_m = \sum_b S_{coll}^{(m,b)}$$

Letting $\sum_b S_{coll}^{(m,b)} = n_m^2 k_m$ be the primary loss for metastables (Ref 28:A1019) and the metastable current density be given by

$$\bar{J}_m = (n_m \bar{v} - \frac{D_m P_z}{P_z} \nabla n_m) = n_m \bar{U}_m$$

Then the continuity equation is written for steady state conditions as

$$n_m \frac{\partial v}{\partial z} + v \frac{\partial nm}{\partial z} - \frac{D_m P_z}{P_z} \nabla^2 n_m - n_m^2 k_m = 0$$

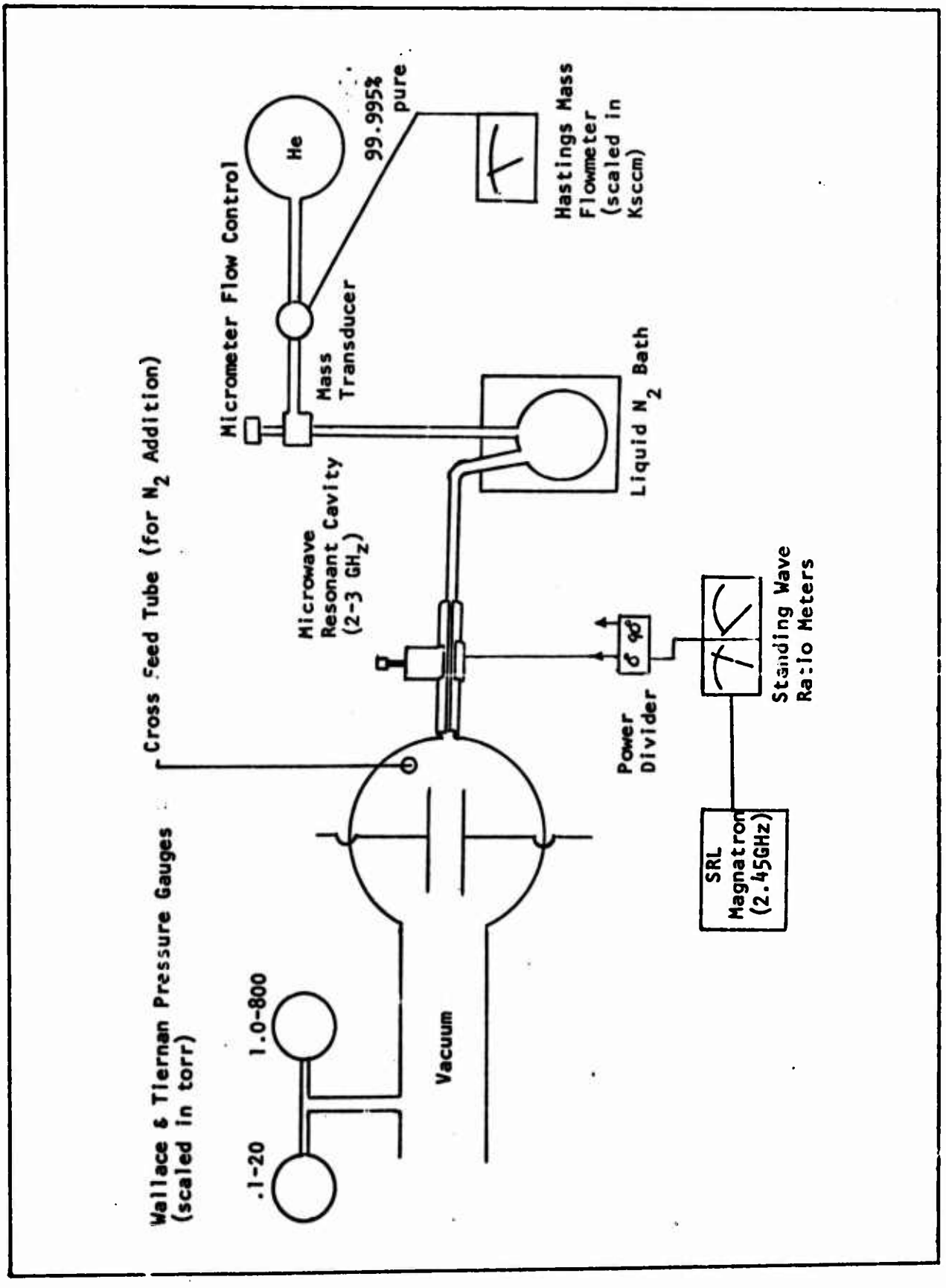

Fig. 7. Vacuum and Flow System

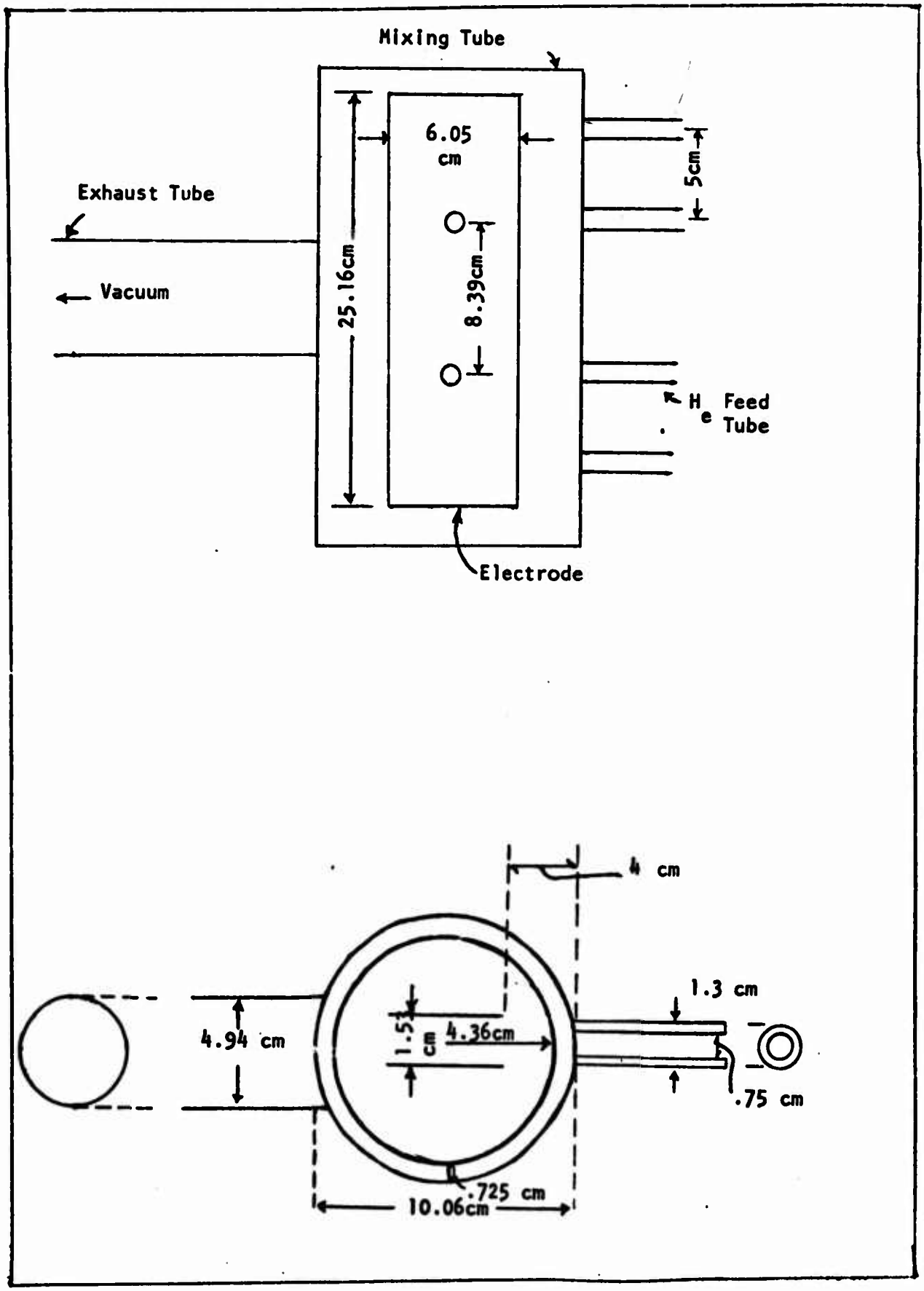

Fig. 8. Reaction Chamber

The solution for this equation is given by Bolden, et al (Ref 4:63) as (azimuthal symmetry assumed)

$$\left[n_m\right]_{\ell} = \left[n_m\right]_o \frac{\bar{v}_o}{\bar{v}_e} \exp\left\{ -\left[\left(\frac{\Delta(D_m P_z)}{P_{av} a^2} + \frac{\Gamma k_m \dot{n}_m}{\pi a^2 \bar{v}_{av}} \right) \frac{\ell - \ell_o}{\bar{v}_{av}} \right] \right\}$$

The terms are defined as follows:

$[n_m]_{\ell}$	-	metastable density at ℓ
$[n_m]_o$	-	metastable density from source at ℓ_o
$\frac{\bar{v}_o}{\bar{v}_{\ell}}$	-	ratio of bulk velocities at ℓ and ℓ_o
D_m	-	metastable diffusion coefficient
P_{av}	-	pressure at the midpoint of ℓ and ℓ_o
a	-	tube radius
$\dot{n}$	-	metastable flow rate
k_m	-	rate coefficient for metastable-metastable ionization
$\bar{v}_{av}$	-	average velocity between ℓ and ℓ_o
Δ	-	eigenvalue component (Ref 5:50)
Γ	-	eigenvalue component (Ref 5:50)

Similar equations may be written for the axial variation of electron density.

$$\frac{\partial n_e}{\partial t} + \nabla \cdot N_e \bar{U}_e = \sum_b S_{coll}^{(e,b)}$$

$$\sum_b S_{coll}^{(e,b)} = n_m^2 k_m - n_i n_e k_r$$

$$\bar{J} = n_e v - \frac{D_a P_z}{Pt} \nabla n_e$$

$$n_e \frac{\partial v}{\partial z} + \frac{v \partial n_e}{\partial z} - \frac{D_a P_z}{P_z} \nabla^2 n_e - \Sigma S_{coll}^{(e,b)} = 0 \quad \text{steady state}$$

$$[n_e]_\ell = [n_e]_o \frac{\bar{v}_o}{\bar{v}_e} \exp\left\{ - \left[\frac{\Delta D_a P_z}{a^2 P_{av}} + \frac{\Gamma}{\pi a^2 \bar{v}_{av}} (k_r n_i - k_m \hbar_m \right] \times \left(\frac{\ell - \ell_o}{\bar{v}_{av}} \right) \right\}$$

In the solution, it has been assumed that although the known electron creation destruction processes are more extensive than those given by $\sum_b S_{coll}^{(e,b)}$ only those shown contribute significantly to this experiment. The additional terms are defined as follows:

$[n_e]_\ell$	~	electron density at ℓ
$[n_e]_o$	~	electron density at ℓ_o
D_a	~	ambipolar diffusion coefficient for electrons
k_n	~	rate coefficient for ion-electron recombination
n_i	~	helium ion flow rate

An initial calculation of $[n_m]_\ell$ and $[n_e]_\ell$ was made to give some indication of the solution validity. The values used were

$[n_m]_o = 10^{11}\ cm^{-3}$ $\quad$ $\Delta = 3.66$

$\Gamma = .628$ (Ref 5:50)

$\frac{\bar{v}_o}{v_e} = 1.0$

$D_m P_z = 490\ \frac{cm^2}{sec}\ torr$ $\quad$ $P_{av} = 2\ torr$

$a^2 = .166\ cm^2$ $\quad$ $\dot{n}_m = 1.72 \times 10^6\ cm^{-3}\ sec^{-1}$

$k_m = 1.8 \times 10^{-9}\ \frac{cm^3}{sec}$ $\quad$ $v_{av} = 5.8 \times 10^4\ cm/sec$

$\ell - \ell_o = 4\ cm$ $\quad$ $D_a P_z = 588\ \frac{cm^2}{sec}\ torr$

$k_r = 8.9 \times 10^{-9}\ \frac{cm^3}{sec}$ $\quad$ $[n_e]_o = 10^{11}\ cm^{-3}$

$n_1 = 1.72 \times 10^6\ cm^{-2}\ sec^{-1}$

The solutions obtained were:

$[n_m]_4 = 6.9 \times 10^{10}$ at 2 torr

$[n_e]_4 = 6.4 \times 10^{10}$ at 2 torr

If the pressure is changed from 2 torr to 4 torr and the eigenvalues for this pressure are substituted, the solutions become:

$[n_m]_4 = 8.3 \times 10^{10}$ at 4 torr

$[n_e]_4 = 8.0 \times 10^{10}$ at 4 torr

It is seen that the solutions tend to the values of $[n_m]_o$ and $[n_e]_o$ for increasing pressure measured at the same point. for an increase in length of from 4 cm to 12 cm, the electron number density solution is for a uniform pressure of 2 torr

$$[n_e]_{12} = 2.6 \times 10^{10} \text{ at 2 torr}$$

This will be discussed later.

VI. Analysis of $He(2^3S)$ in Presence of Nitrogen in the Afterglow

The addition of nitrogen to the flowing afterglow has three distinct effects. One, it destroys helium metastables. Two, it destroys helium ions. Three, for the proper combination of parameters it enhances electron production. Therefore a new helium metastable continuity equation and solution are necessary. The new equation will change only in the term $\sum_b S_{coll}^{(m,b)}$. This has the effect of changing only the reactant term in the exponential of the solution. The final solution for the concentration of helium metastables is

$$[n_m]_\ell = [n_m]_o \frac{\bar{v}_o}{\bar{v}_\ell} \exp\left\{ -\left[\frac{\Delta D_m P_z}{P_{av} a^2} + \frac{\Gamma}{\pi a^2 \bar{v}_{av}} (k_m \dot{n}_m + k_p \dot{n}_n) \right] \frac{\ell - \ell_o}{\bar{v}_{av}} \right\}$$

The terms are as defined earlier and additionally k_p is the Penning ionization rate coefficient for N_2 in He* and $\dot{n}_n$ is the nitrogen flow rate.

The electron density requires a new solution because of the additional creation source. That solution is:

$$[n_e]_\ell = [n_e]_o \left(\frac{\bar{v}_o}{\bar{v}_e}\right) \exp\left\{ -\left[\frac{\Delta D_a P_z}{P_{av} a^2} + \frac{\Gamma}{\pi a^2 \bar{v}_{av}} -(k_p \dot{n}_n + k_r n_i - k_m \dot{n}_m) \right] \times \frac{\ell - \ell_o}{\bar{v}_{av}} \right\}$$

and k_r is the recombination rate coefficient for electrons with helium.

The value of k_p is from Cher and Hollingsworth $1 \times 10^{-10} \frac{cm^3}{sec}$. The nitrogen flow rate is from 6×10^{16} to 2×10^{19} cm^{-3} sec^{-1}.

It is easily seen then that the Penning process easily dominates its term and at slower velocities begins to dominate the system.

For the assumed values of the metastable solution in the last section, a calculation made for n_m with nitrogen introduced leads to

$$[n_m]_4 = 6.8 \times 10^{10} \text{ @ } 2 \text{ torr}$$

a decrease of 1.5%

This will be discussed later also.

VII. Absorption Technique for Measuring $He^1(2^3S)$ Density

The absorption technique for measuring the relative helium triplet metastable density is well known. Essentially the absorption is determined from the equation

$$I_\ell = I_o e^{-\alpha \ell}$$

where I_ℓ denotes the intensity of the transmitted light which travelled a distance ℓ through the absorbing medium, I_o, is the undiminished light intensity, and α is the absorption coefficient. The absorption coefficient of Zemansky (Ref 47) is

$$\alpha(\nu_o) = \frac{\lambda_o^2}{8\pi}\left(\frac{g_2}{g_1}\ \frac{1}{T}\right)\left(\frac{4\ell n 2}{\pi}\right)^{\frac{1}{2}}\ \frac{N}{\Delta\nu D}$$

where the Doppler line width $\Delta\nu_D = 7.17 \times 10^{-7}\nu_o(T/M)^{\frac{1}{2}}$, ν_o is the center of the line, N is the number density of absorbing bodies, and g_1T/g_2) is calculated from (Ref 4:63) to be 2.6096×10^{-8} sec @ 293^oK. The metastable density by re-arrangement is

$$n_m = \left(\frac{1}{\ell}\ell n\ \frac{I_o}{I\ell}\right)\left(\frac{8\pi c}{\lambda_o^3}\right)\left(\frac{Tg_1}{g_2}\right)(1.064)(7.16 \times 10^{-7})\left(\frac{T}{M}\right)^{\frac{1}{2}}$$

$$= \left(\frac{1}{\ell}\ell n\ \frac{I_o}{I_e}\right)\left(\frac{T}{M}\right)^{\frac{1}{2}}\ (2.5534 \times 10^{11})\ cm^{-3}$$

where $\lambda_o = 3889\text{Å}$.

The measurements for absorption were made with the equipment set-up in Figure 9. The first lens had the capillary at its focus.

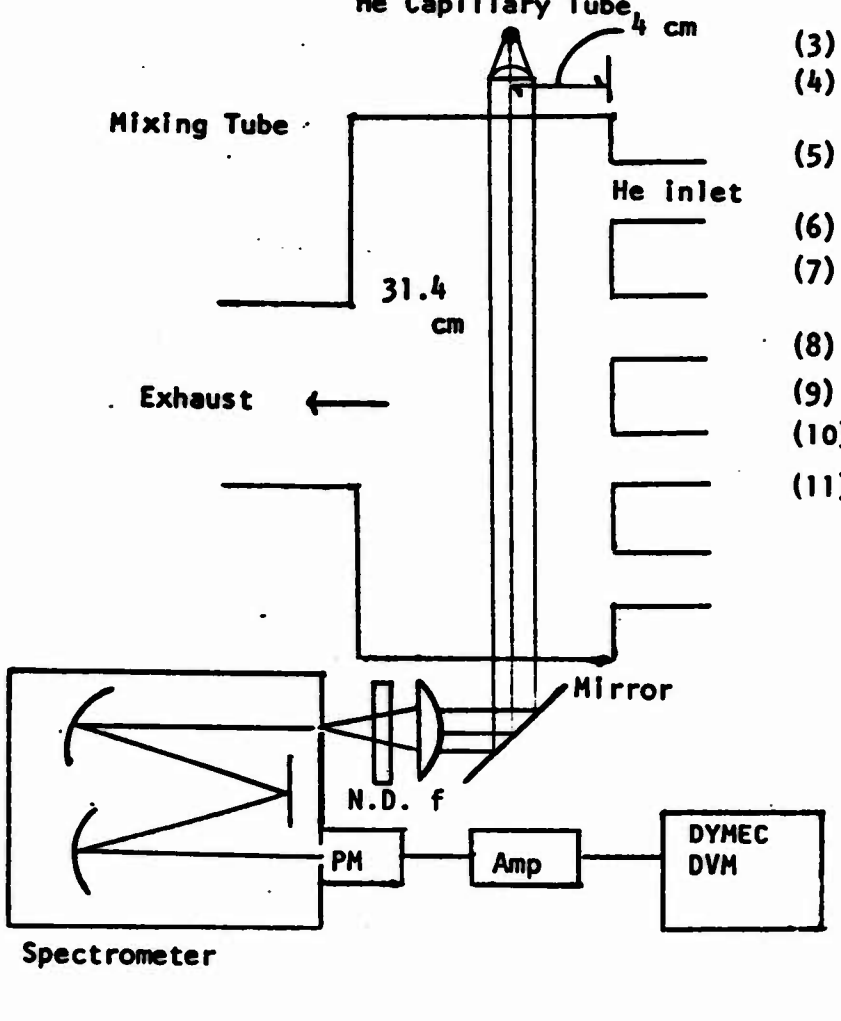

Notes:

(1) Both lenses same focal length f
(2) Neutral density filter (N.D.) Precision 10^{-1} attenuation (CORION)
(3) Mirror front face
(4) Photomultiplier tube (PM) EMI 7256B S-13 (quartz window)
(5) Jarrell-Ash one meter Czerny-Turner spectrometer
(6) Amplifier manufactured by ARL
(7) Dymec digital voltmeter (DVM) integrating 1 second sample
(8) Grating 3000Å blaze 11860 grooves/mm
(9) Mixing tube polystyrene TFE
(10) Helium inlets quarts
(11) Exhausted by 500 cfm pump

Fig. 9. Absorption Measurement Equipment

Parallel light entered the mixing tube, was partially absorbed, upon exit was reflected, and finally refocussed onto the spectrometer slit. The spectrometer acted as a bandpass filter for 3889Å light and fed the photomultiplier tube.

The 3889Å line is a $3^3P \rightarrow 2^3S$ transition in helium for which 3^3P has no other allowed transition. A check was made to insure any emission from the flowing afterglow at this wavelength was accounted for.

Runs were made using only helium at various pressures, mass flow rates, and applied microwave powers in order to characterize the $He(2^3S)$ density for these parameters. Then nitrogen was mixed by way of a cross feed tube and the helium metastable density (and electron density) taken to give the loss of metastable density for various nitrogen mass flows.

A check to verify that indeed the nitrogen 3914Å line was not adding to the 3889Å line (that the spectrometer had sufficient resolution) was made. No overlap was found and the absorption measurements were deemed valid.

Verification checks with the Ne 5689.8Å line for metastable density were run but are not included because of incomplete data. Additionally, the 3914Å line of the first negative in N_2^+ was taken for verification of Penning ionization and metastable destruction but are not included because of lack of time.

A sample calculation was made for the metastable density and the calculation with its assumed values are given as follows:

$$n_m = \left(\frac{1}{\ell} \ln \frac{I_o}{I_e}\right) (2.5534 \times 10^{11}) \left(\frac{T}{M}\right)^{\frac{1}{2}}$$

at $273^{o}k$

$$n_m = \left(\frac{1}{31.4} \ln \frac{I_o}{I_e}\right) (2.5534 \times 10^{11}) \left(\frac{273}{4}\right)^{\frac{1}{2}}$$

$$= \left(\ln \frac{I_o}{I_\ell}\right) (1.01 \times 10^{12}) \text{ cm}^{-3}$$

at $77^{o}k$

$$n_m = \left(\ln \frac{I_o}{I_\ell}\right) (5.35 \times 10^{11}) \text{ cm}^{-3}$$

To the accuracy of the first two decimals, the natural logarithm of the quotient I_o/I_ℓ and the decimal equivalent of the percent absorption are the same. Therefore, a first estimate may be obtained by taking the percent absorption decimal equivalent from one of the graphs and replacing the $\ln (I_o/I_\ell)$ by this number to obtain a metastable density.

The experimental results are discussed next.

VIII. Experimental Results - Electrical

The electron density was determined using the experimental set-up shown in Figure 10. Not shown is a times-ten attenuation probe that was used for some runs. When the probe was used the data was corrected accordingly.

The output data was a series of graphs which plotted voltage out vs. voltage in. Because a one thousand ohm resistor was used between the voltage out and ground, the plot for voltage out converts directly to current. Therefore the graphs read current out vs. voltage in. Using the relations

$$I = JA$$

$$J = n_e e \mu E$$

$$E = V/d$$

the equation for the number density of electrons is written

$$n_e = \frac{Id}{e\mu AV}$$

where μ is the electron mobility, d is the plate separation, e is the electron charge, A is the plate area, V is the applied voltage, and j is the electron current density. The electron mobility is given by

$$\mu = \frac{e}{m_e \nu_m}$$

with m_e the electron mass and ν_m the collision frequency which Brown (Ref 7:50) gives as $2.3 \times 10^9 p$ in helium with p in torr.

The same equation for electron number density applies in the helium-nitrogen mixtures except that the mobility must be determined

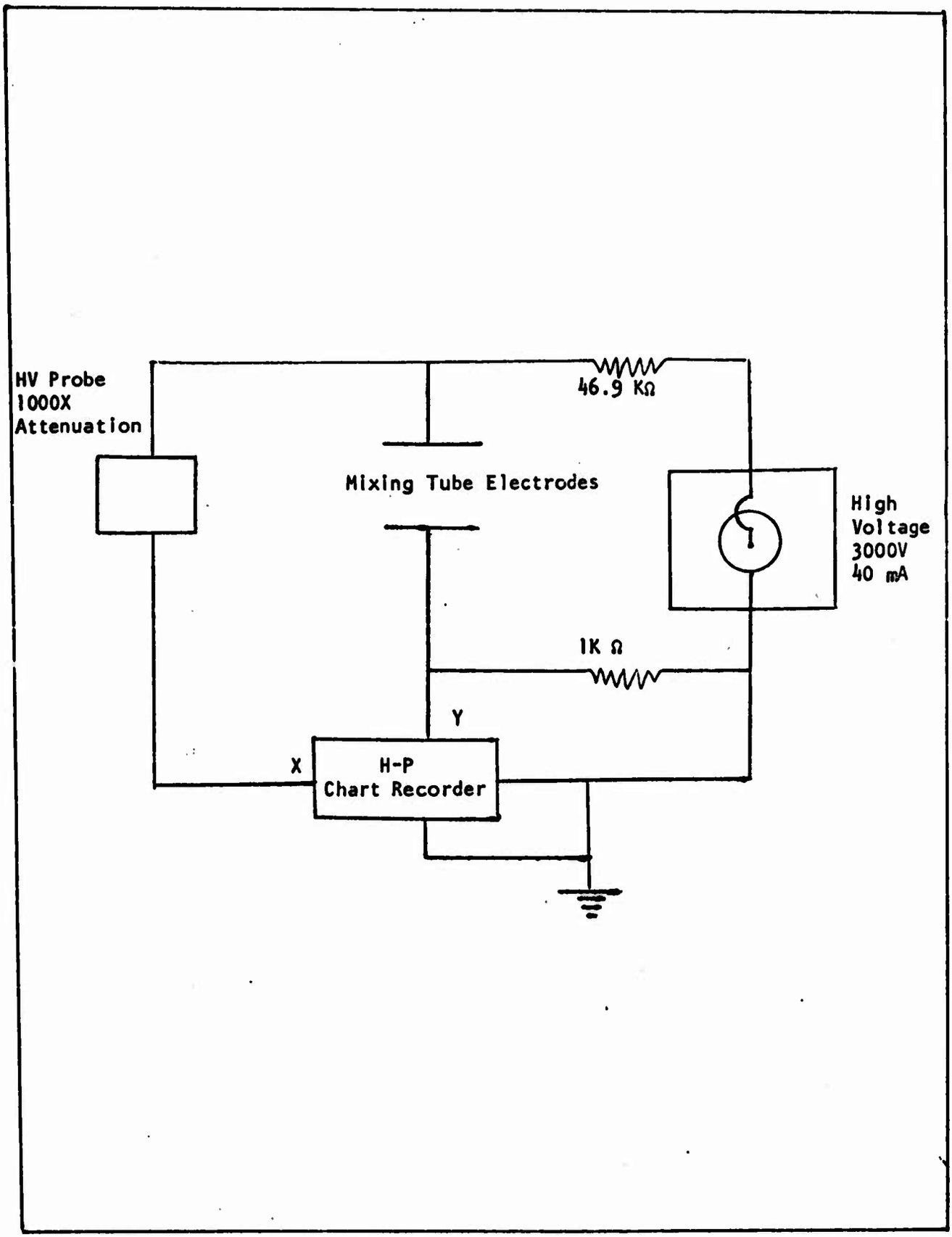

Fig. 10. Electrical Set-Up

for electrons in a helium-nitrogen mixture. The total mobility is assumed to follow Blanc's law from Acton & Swift (Ref 1:61)

$$\frac{1}{\mu_t} = \frac{f}{\mu_{N_2}} + \frac{(1-f)}{\mu_{He}}$$

where $f = P_{N_2} / (P_{N_2} + P_{He})$ is the partial pressure of N_2 in the total mixture, μ_t is the total mobility at unit pressure, μ_{n_2} is the nitrogen mobility at unit pressure, and μ_{He} is the helium mobility at unit pressure. The total mobility μ at some total pressure P_t is gained from

$$\mu = \frac{\mu_t}{P_t}$$

The choice of a particular point on the current-voltage characteristic curve obviously determines the calculated electron number density. For the point choice to give comparable results, the points must be taken from essentially comparable portions of the current-voltage curves.

Because the addition of nitrogen in minute amounts lowers the value of current for a given voltage but allows higher collection voltages prior to breakdown, comparable points between pure helium and a helium-nitrogen mixture would be the highest points in the saturation current region of each current-voltage curve prior to the onset of the Townsend region.

The transition from the saturation current curve to the Townsend discharge region is not well defined in these curves. Although it has been implicitly assumed that the mobility is a constant, the actual

mobility is a function of the field to number density ratio E/N. Since E/N is increasing as the applied voltage increases, the electron mobility is changing also.

Without making a correction for the electron mobility for each point on each curve, it is possible to make a best judgment of the particular point for each curve where the linear analysis for the electron number density has broken down. By picking such a point, call it P_1, on the helium I-V curve, the corresponding point, call it P_2, on the helium-nitrogen I-V curve may be chosen by matching the slope of the helium-nitrogen curve at P_2 to the slope of the helium curve at P_1.

This method of point choice was followed consistently for each pair of curves. From the chosen point the voltage and current were read corresponding to that point and the electron number density was calculated.

The experimental graphs are included in the appendix. The calculated number densities are included and are plotted against pressure as Figures 11 through 16.

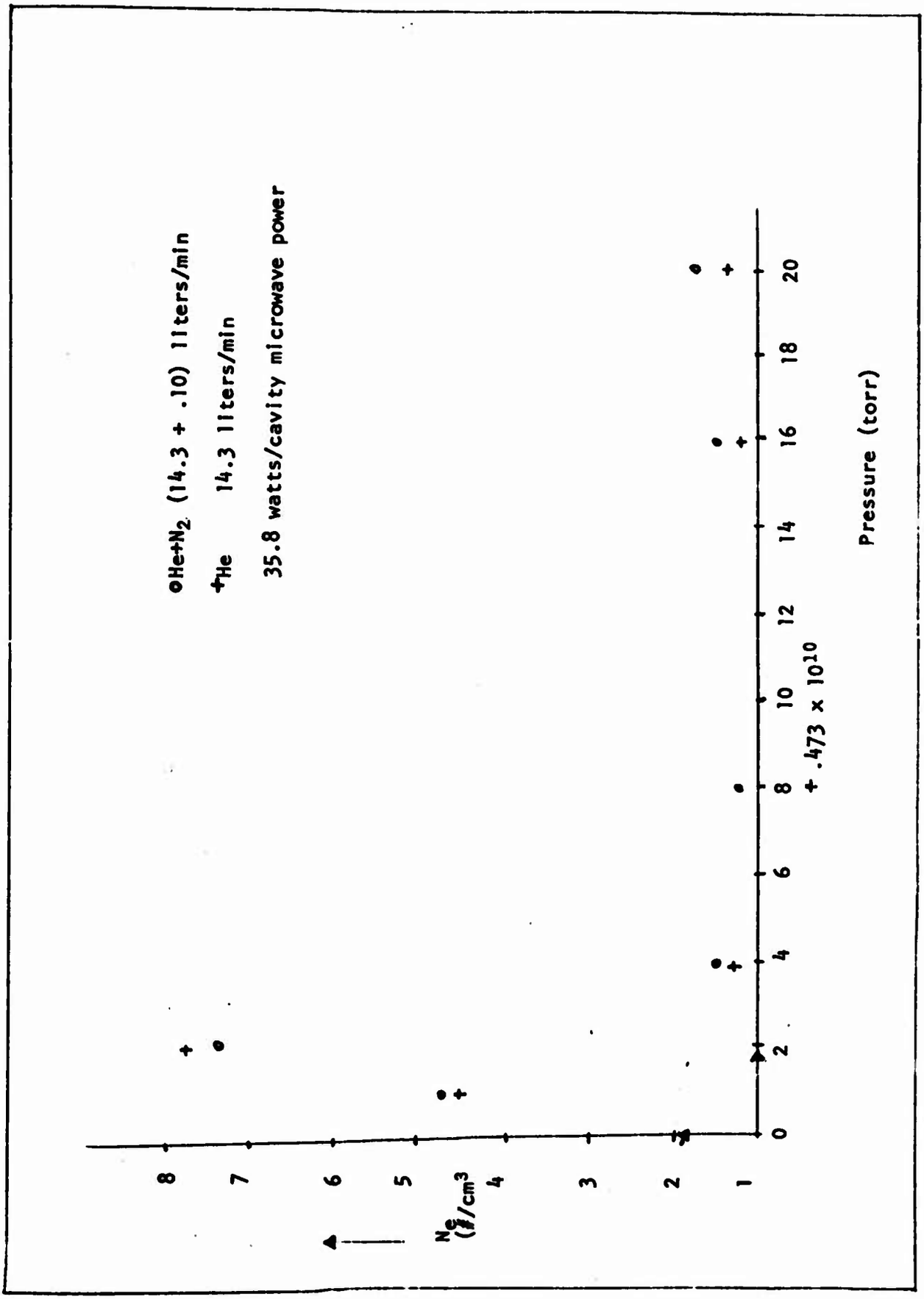

Fig. 11. Electron Number Density vs. Pressure for Helium-Nitrogen[-1]

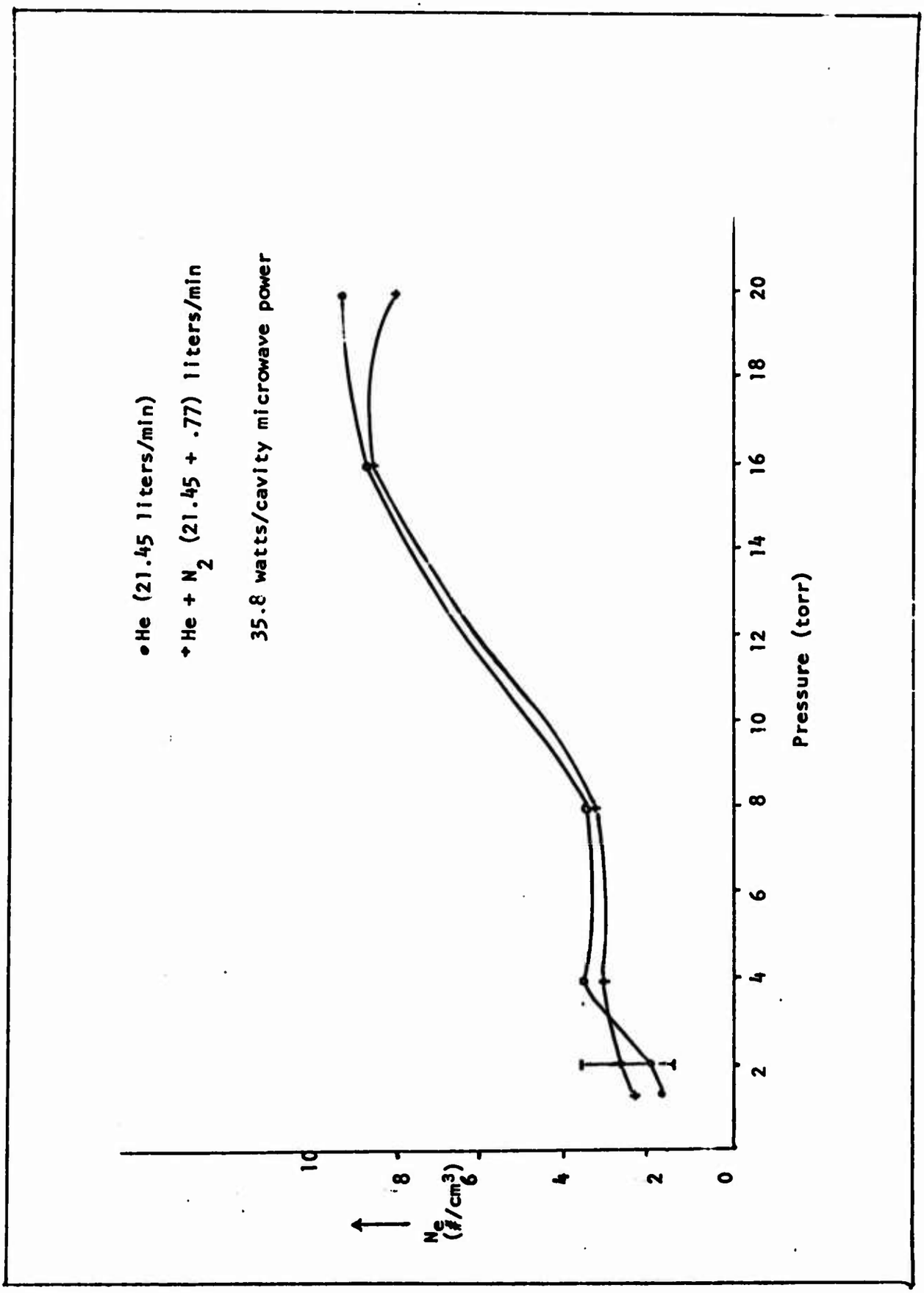

Fig. 12. Electron Number Density vs. Pressure for Helium-Nitrogen- II

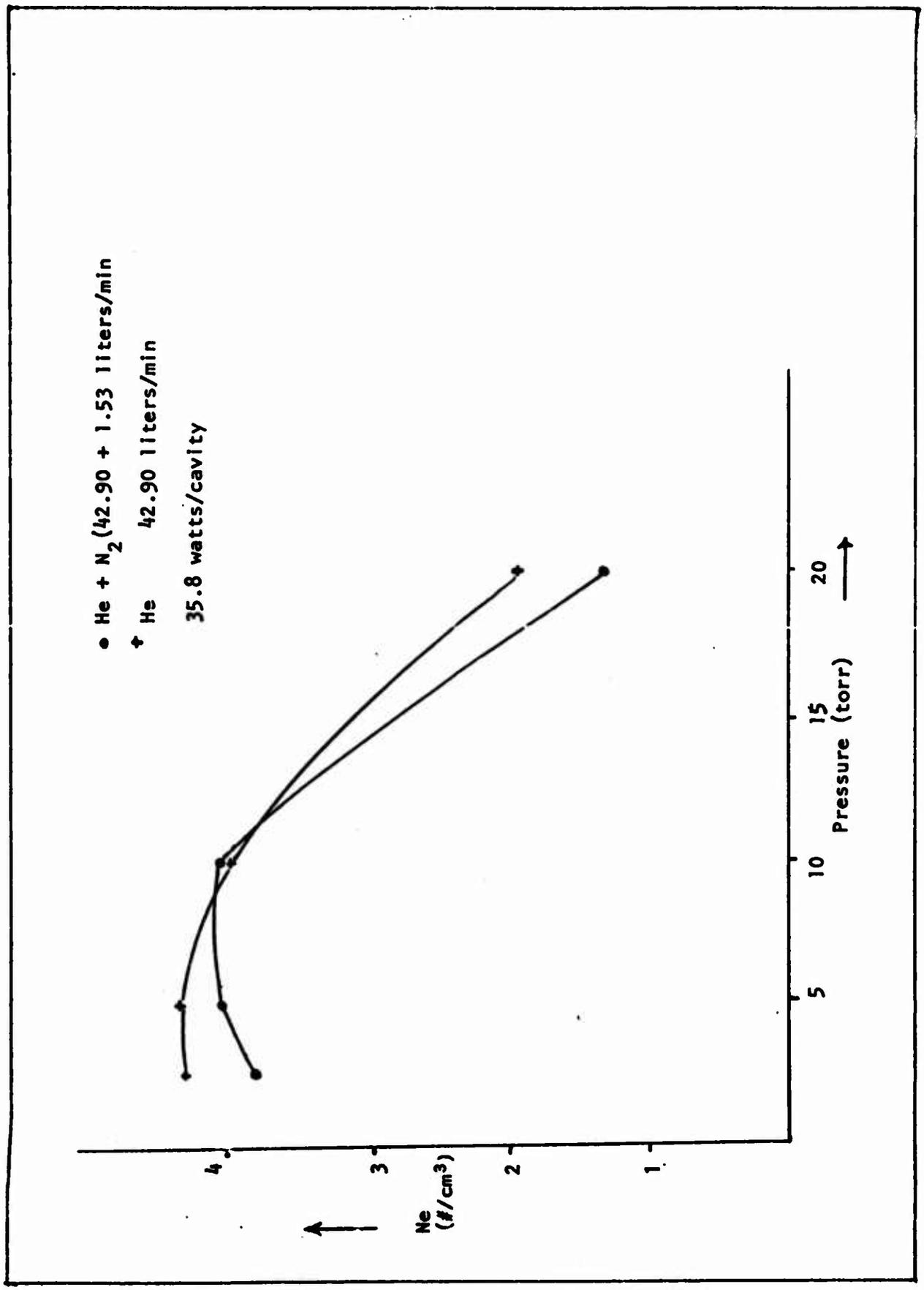

Fig. 13. Electron Number Density vs. Pressure III

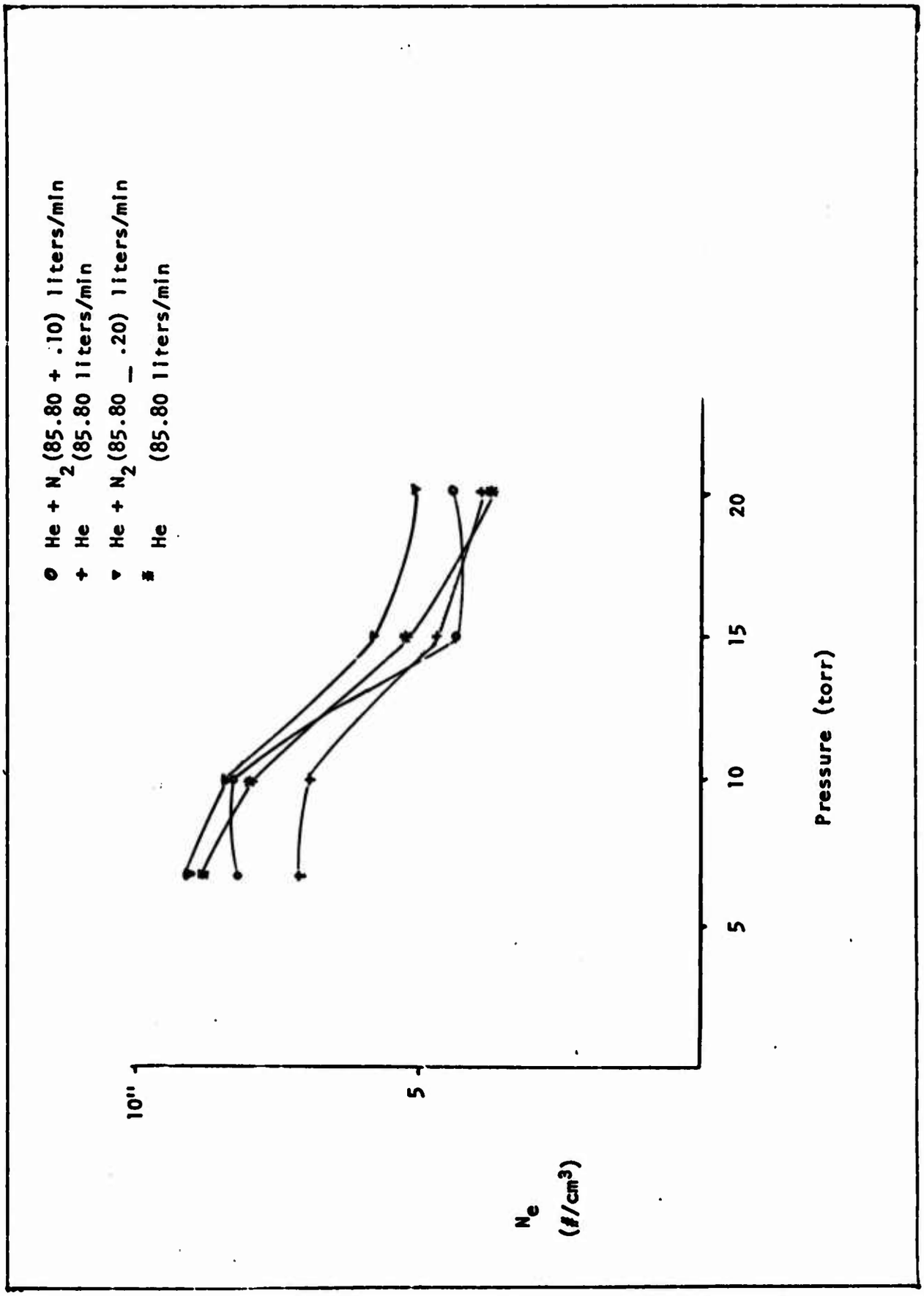

Fig. 14. Electron Number Density vs. Pressure for Helium-Nitrogn-IV

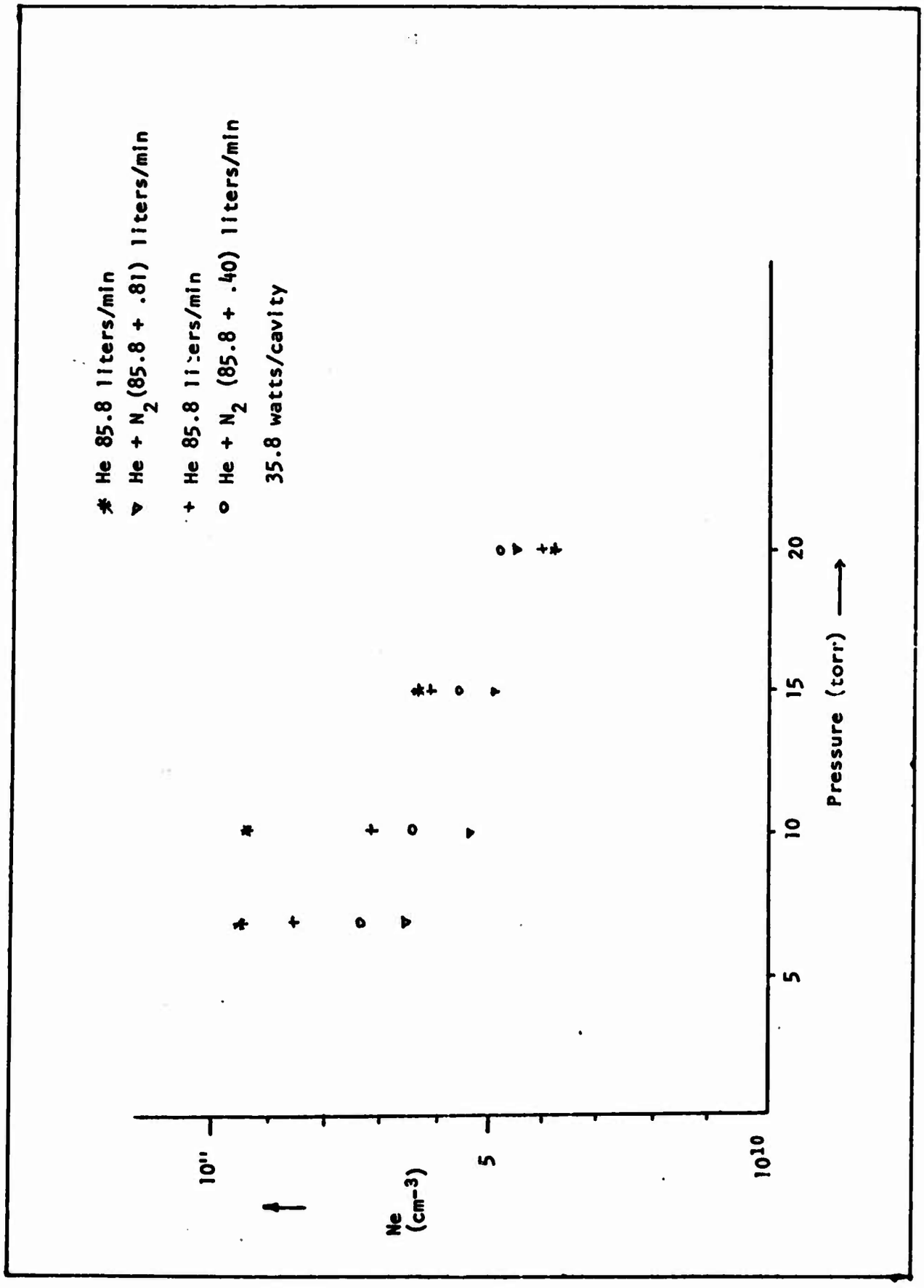

Fig. 15. Electron Number Density vs. Pressure for Helium-Nitrogen - V

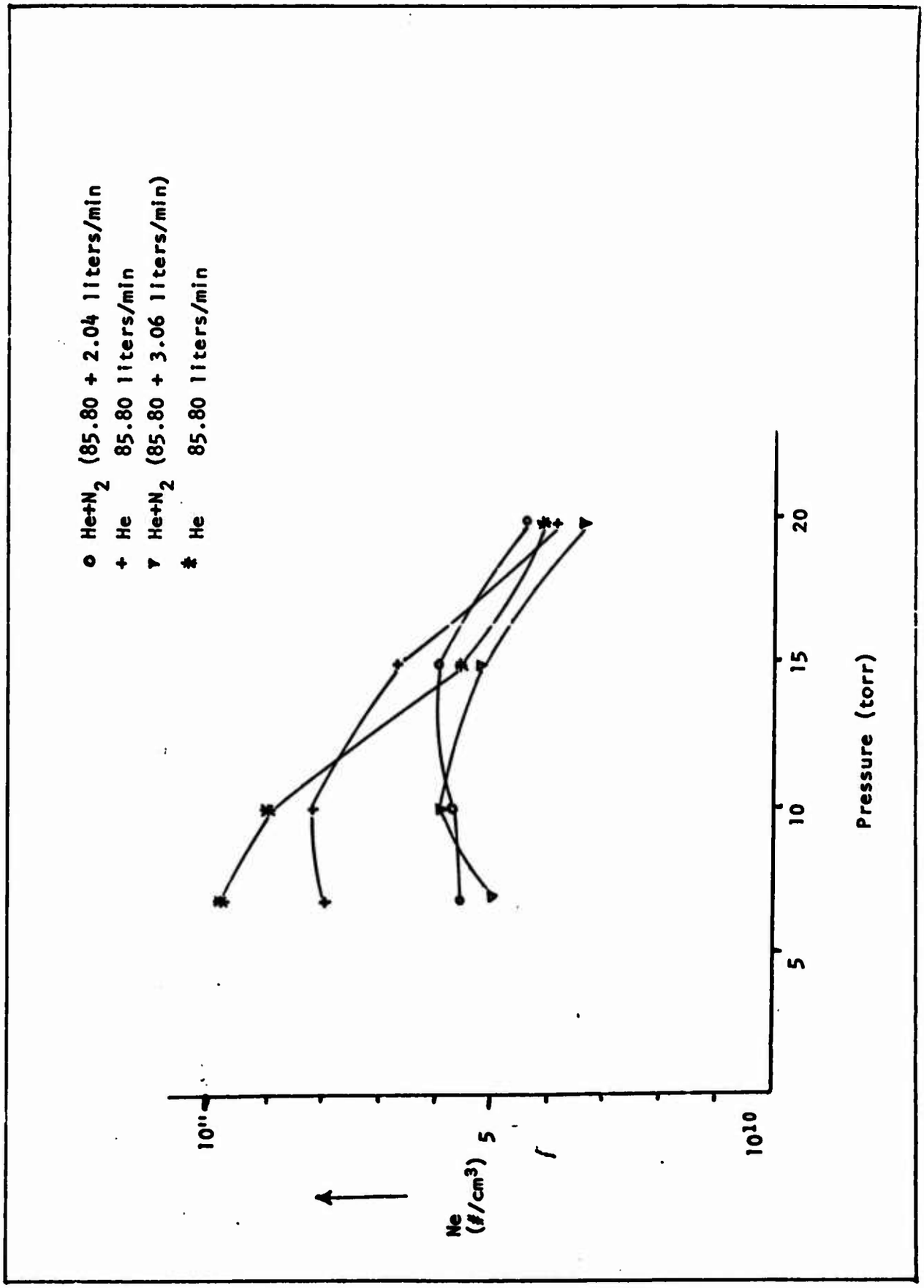

Fig. 16. Electron Number Density vs. Pressure for Helium-Nitrogen VI

IX. Experimental Results - Optical

The optical data was reduced using the following relation:

$$\frac{(C_{on\,off}W_{on\,off} - C_{on\,on}W_{on\,on}) + (C_{off\,on}W_{off\,on} - C_{off\,off}W_{off\,off})}{(C_{on\,off}W_{on\,off} - C_{off\,off}W_{off\,off})} \times 100 = \%\ \text{absorption}$$

The C's stand for the capillary discharge tube, the W's stand for the microwave power, and the subscripts stand for the condition of each (ex: $C_{on\,off}W_{on\,off}$ - capillary on, microwave off).

In the runs where nitrogen was added, two absorption measurements were taken; one for helium only, then one for helium and nitrogen. The percent absorption for each was plotted against the varying parameter to indicate the metastable destruction. Electron density curves taken at the same time are also plotted against the varying parameter, but not all optical measurements (the early data for helium only) were taken simultaneously with the electrical data.

Error bars show the mean value and one standard deviation each side for runs where multiple data points were taken. The charts indicate which points are multiple plots.

The nine graphs which follow indicate relative absorption percentages vs pressure, power or flow.

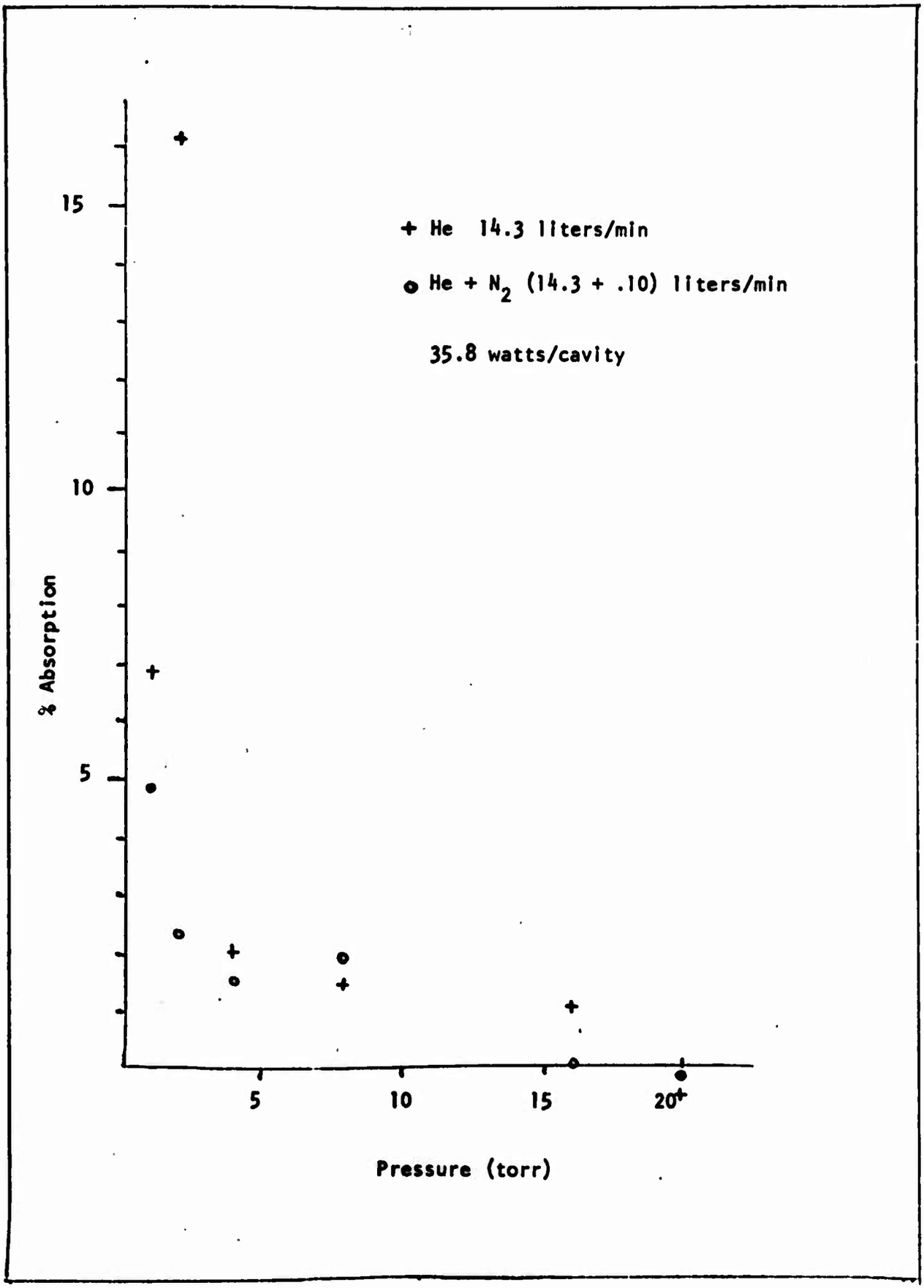

Fig. 17. Absorption vs. Pressure-1

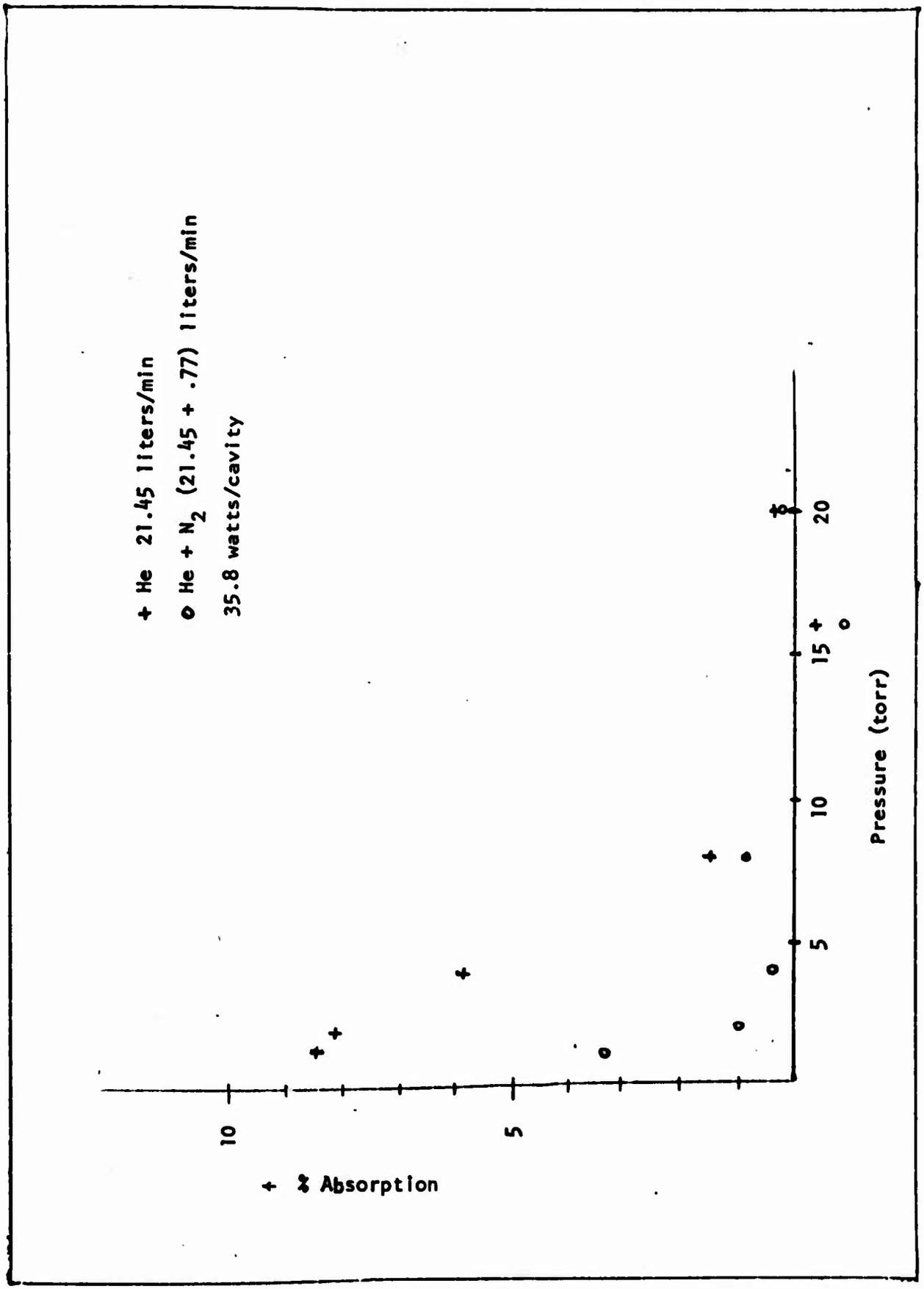

Fig. 18. Absorption vs. Pressure-II

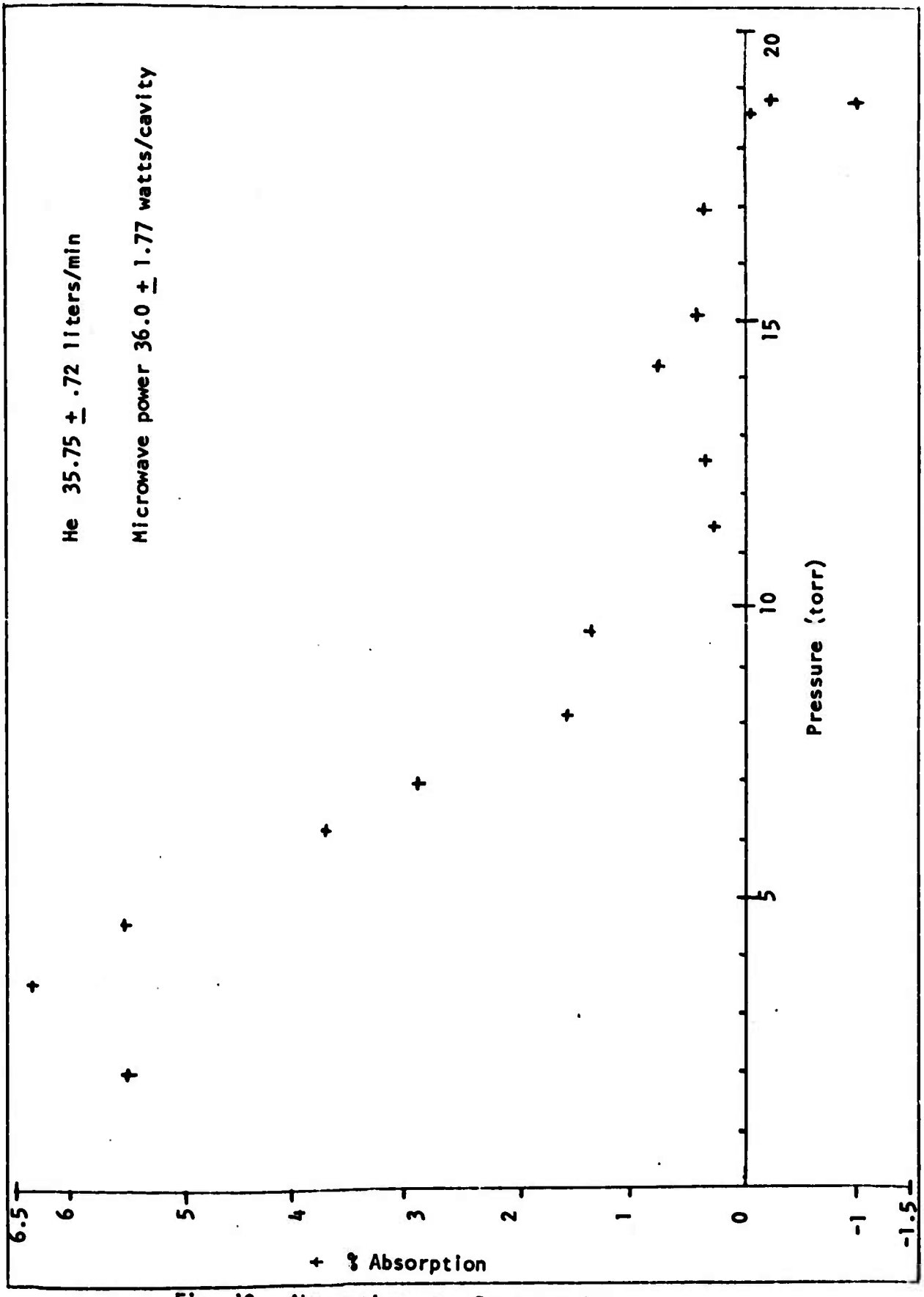

Fig. 19. Absorption vs. Pressure-III

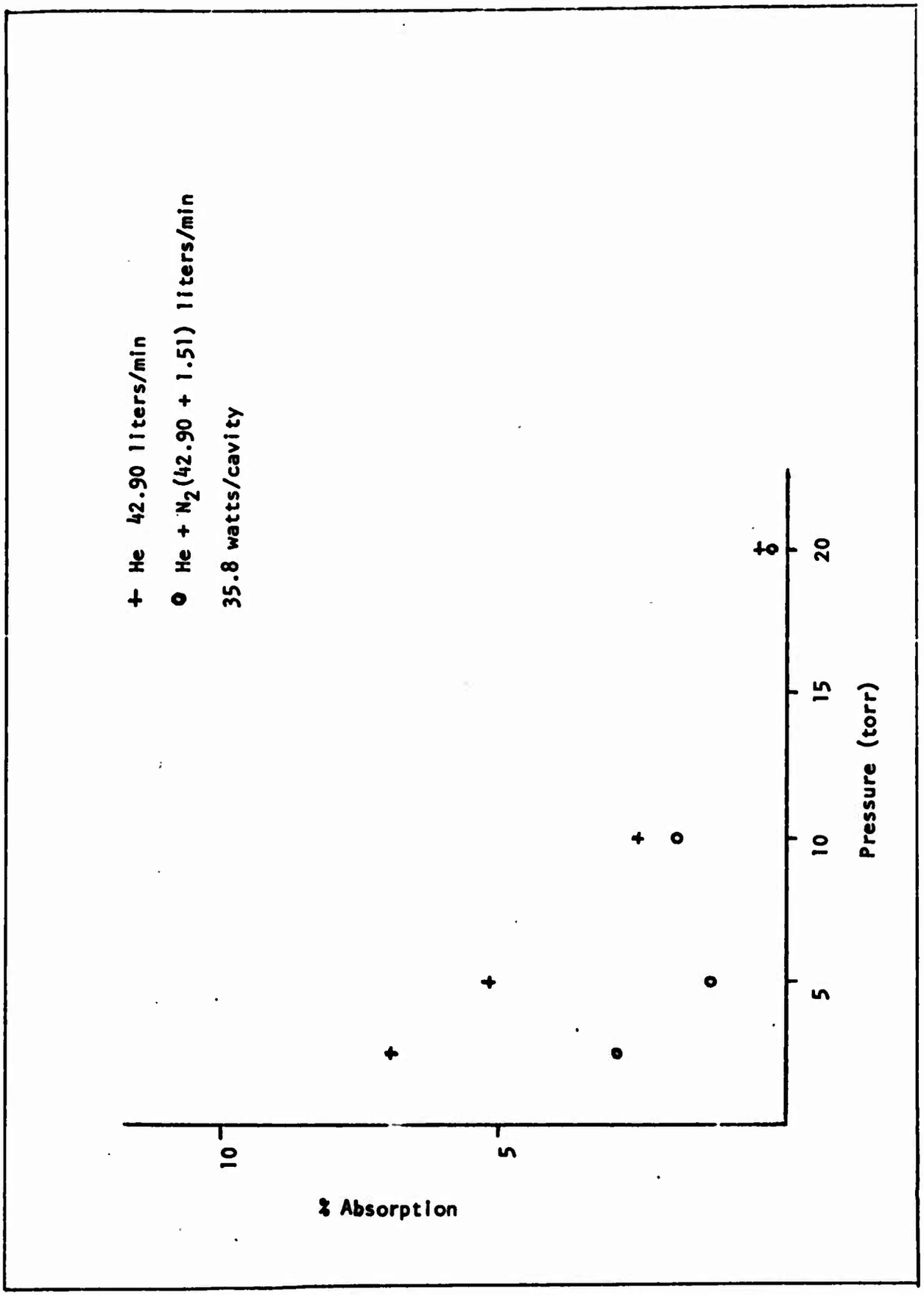

Fig. 20. Absorption vs. Pressure IV

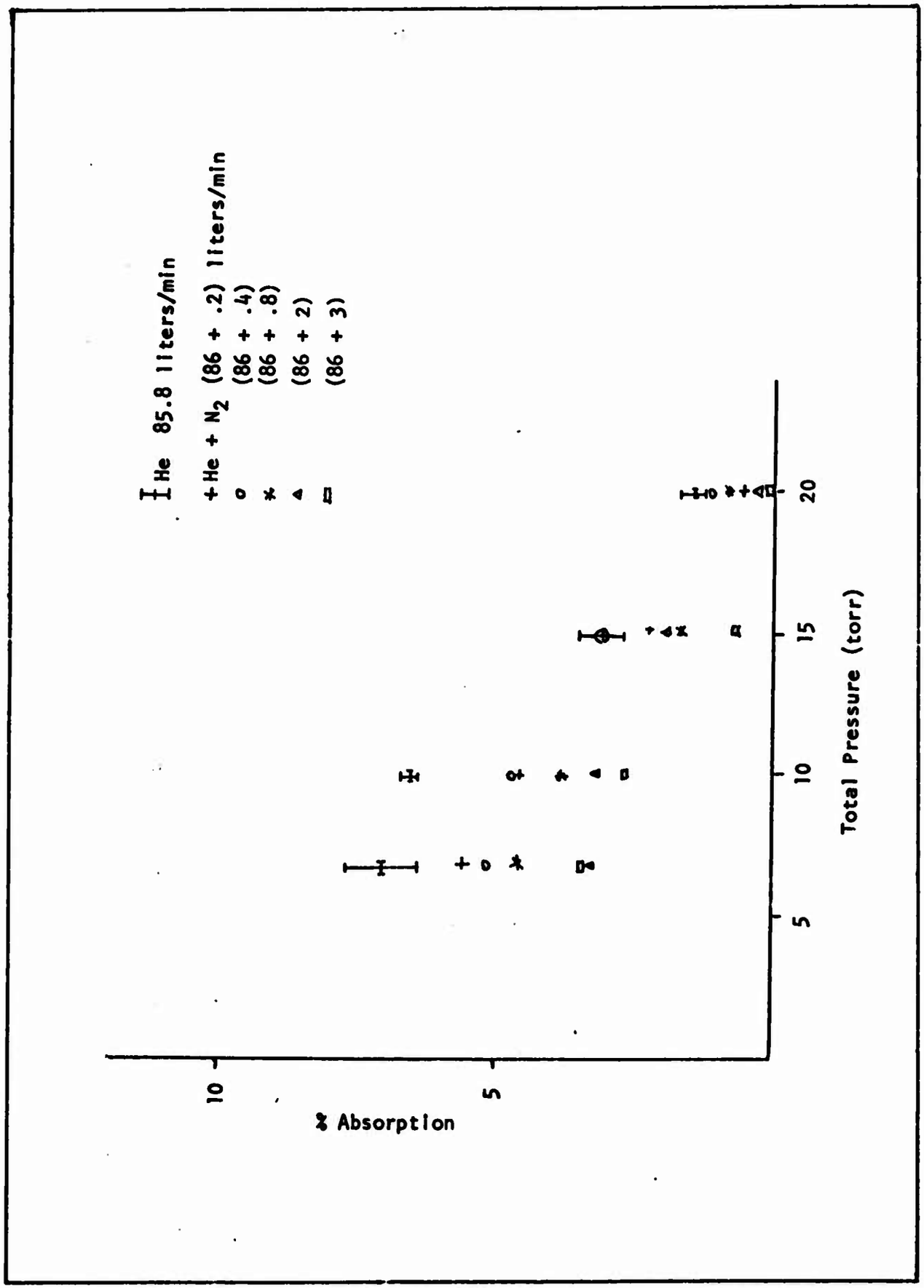

Fig. 21. Absorption vs. Pressure V

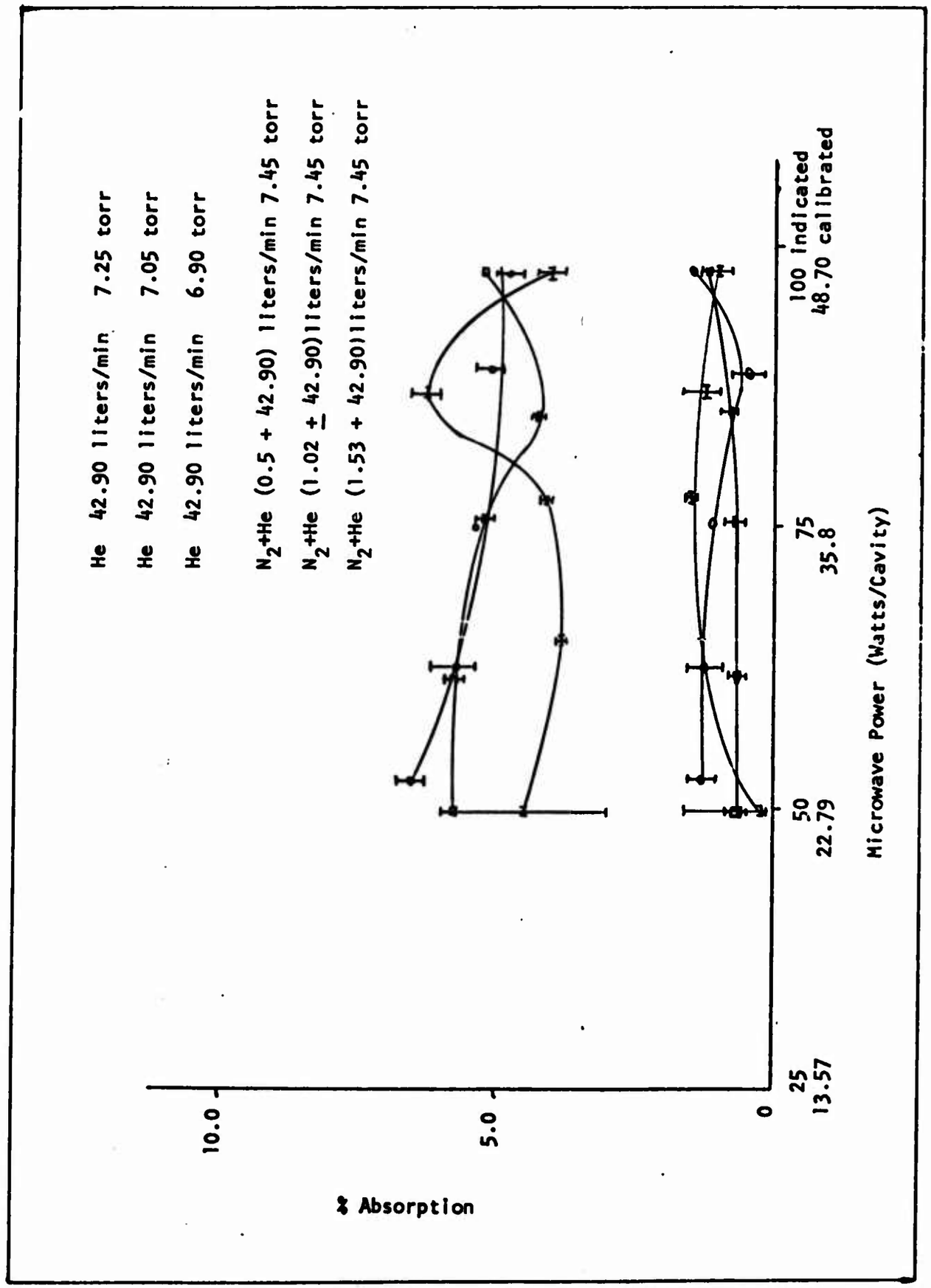

Fig. 22. Absorption vs. Power - I

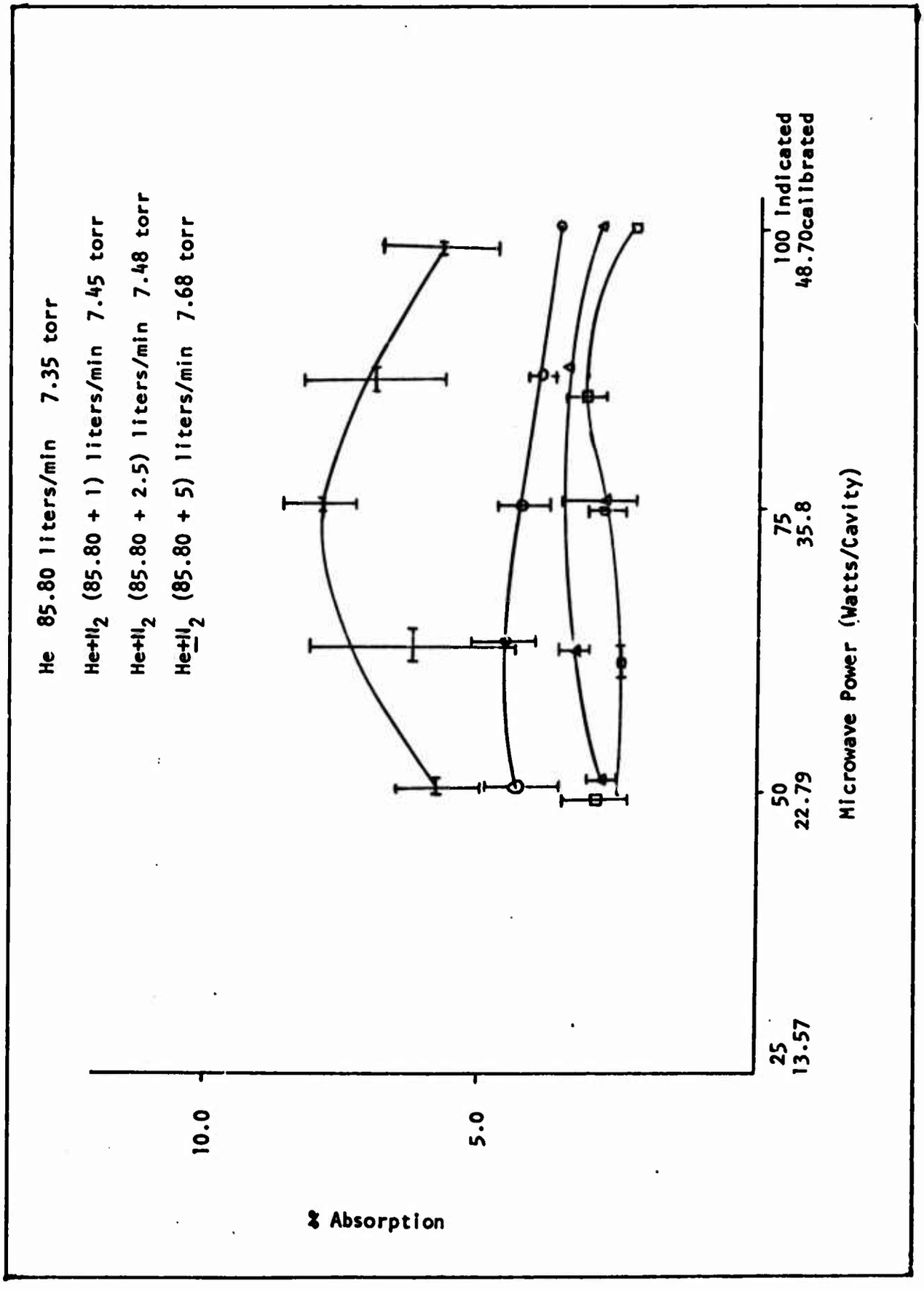

Fig. 23. Absorption vs. Power - II

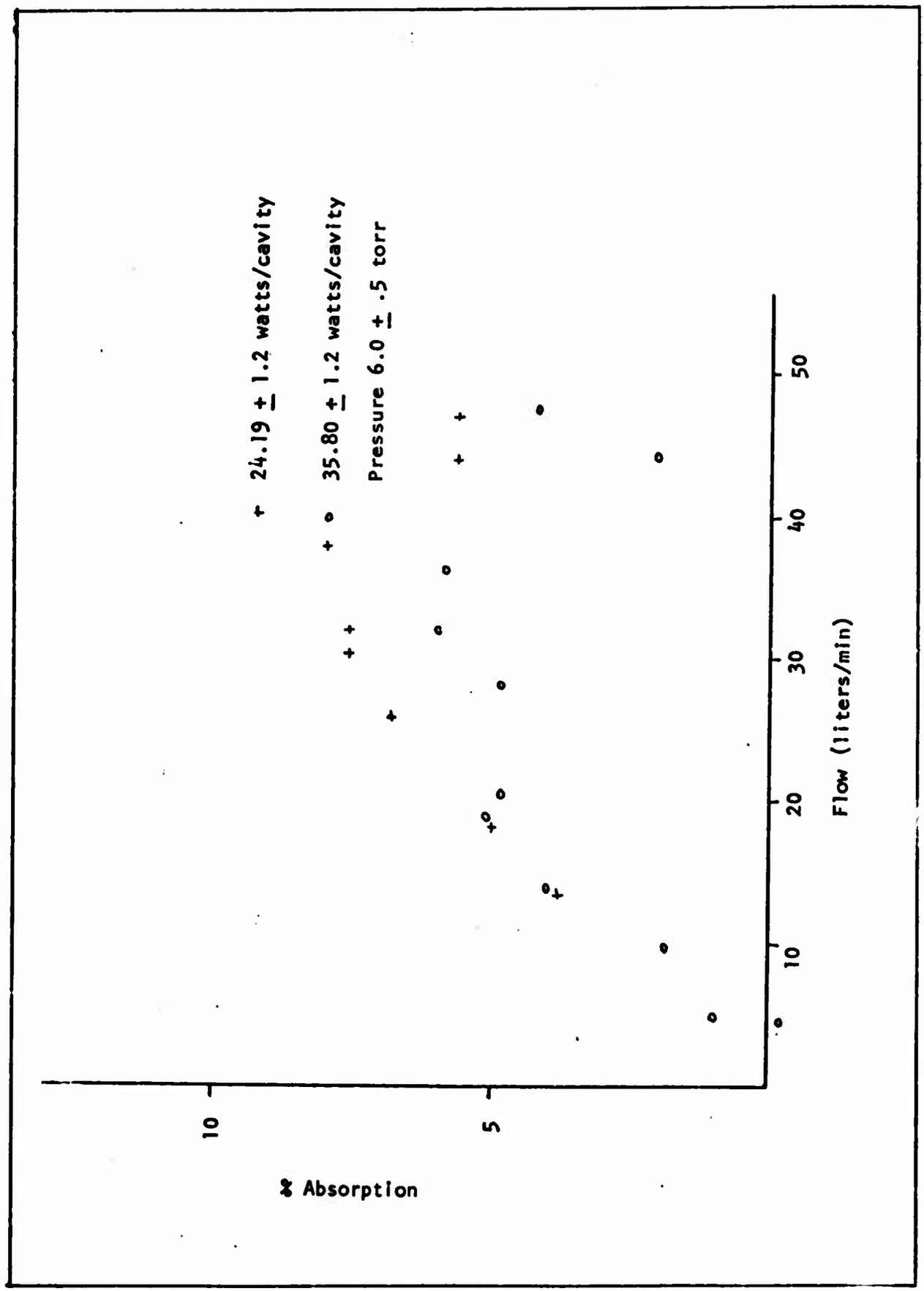

Fig. 24. Absorption vs. Flow - 1

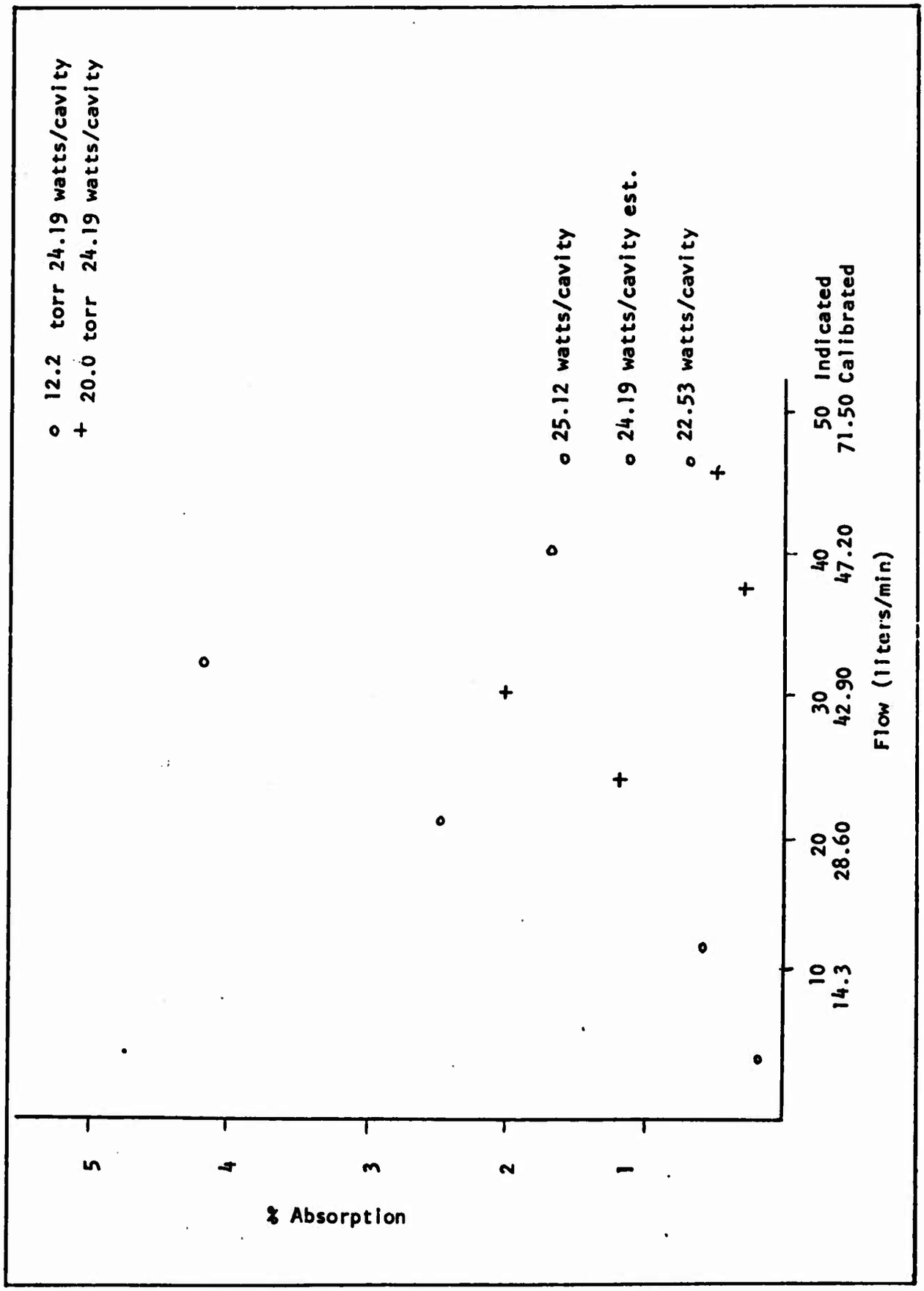

Fig. 25. Absorption vs. Flow - II

X. Comparison and Discussion

As can be seen from Figures 11-16 the electron density is dependent on the pressure and the reactant flow.

The apparent trend at 6-7 torr is for the electron density to rise in pure helium as more atoms are available per second to excite by the microwave cavity. This is reasonable since the cavity is becoming a more efficient exciting source. Additionally, the electron production is seen to drop off at higher pressures but at the same flow rate. With higher pressures, the plasma velocity is slowing considerably. The electrons then have more time to recombine hence their diminution.

Figures 17 through 21 display the metastable density as a function of pressure where percentage absorption is used as metastable indicator as was discussed earlier. As can be seen, an increase in pressure leads to a decrease in metastable density where the metastable is in its own gas. The addition of nitrogen decreases sharply the metastable density as expected. There are some further interesting points.

Figure 18 shows negative absorption at sixteen torr. Figure 19 shows negative absorption also at about 18.8 torr. And Figure 17 shows negative absorption at 20 torr. At the time these anamolies occurred the power was changed with no other change on the system to see if it was an error in the system. The negative absorption increased slightly and then decreased as power was decreased from 35.8 watts/cavity to 22.96 watts/cavity. The negative absorption uniformly decreased as the power was increased to 48.70 watts/cavity. The system

was shutdown completely and the run re-made at the specific power, flow, and pressure. The negative absorption appeared each time and at 35.75 ℓ/min and 35.8 watts/cavity varied over a pressure range from about sixteen to twenty-torr. No other measurements were made.

Figures 17 and 19 show a lower pressure (2-4 torr) peaking effect that could indicate the maximum number of metastables produced as a result of microwave excitation. This would indicate that the metastables do not reach a maximum number density immediately after microwave excitation but some short time later. A further indication of this effect is seen at higher velocities (lower pressure) where the metastable number density diminishes. At higher velocities, the He(2^1S)-electron collision process has not had sufficient time to create additional He (2^3S) metastables before the reactants have passed the probing beam.

The helium metastable-nitrogen interaction for varying power at constant pressure is shown in Figures 22 and 23. Also shown on the same graphs are the variation in metastable production for varying nitrogen concentrations. The metastable production is maximized for a particular power at a particular percentage of nitrogen mixed. This can be explained by recalling that as more energy goes into the electron gas, the electron distribution curve shifts to higher state.

Figures 24 and 25 show the metastable production variation with flow rate. Again peaks are exhibited.

Figure 24 shows the electron energy distribution peak discussed above coupled with a specific flow rate. The flow rate maximum represents the optimum number of molecules that the cavity can excite to a specific state (2^3S). The higher flow rate drop comes from the

extra speed with which the molecules must be moved through the cavity to maintain the same pressure. The lower flow rate drop indicates slower velocity, hence longer interaction time, hence fewer metastables.

From Figure 25 one sees that higher pressure decreases the maximum number of metastables but does not shift the flow rate maximum which was expected.

The calculations for the metastable density and electron density from Chapter V show the expected order of magnitude agreement with experiment for pure helium. In helium-nitrogen the electron density sample calculation at two torr agrees in order of magnitude with experiment also. It is apparent then that the analysis of Chapter V indicates the true reactive processes to an order of magnitude.

The analysis in Chapter VI showing a decrease in the metastable density with the addition of small amounts of nitrogen was expected and was confirmed by experiment. Not taken into account but demonstrated experimentally was the change of cross-section for the recombination of slow electrons and ions as the electron temperature decreases in the afterglow because of nitrogen addition. It was expected that the electron number density would increase markedly with Penning ionization in the afterglow as nitrogen was added. This was not entirely the case. Some increases were seen when the addition of nitrogen was less than 0.3% (Ref Figure 14). When the nitrogen addition became 0.5%, the cooling of the electron temperature by the nitrogen essentially reversed the electron creation process since more slow electrons and helium ions were recombining than electrons were being created from the Penning process. The net effect at greater than 0.5% nitrogen

addition was the destruction of metastables and the net recombination of electrons.

The importance of this finding is in the unexpected degree to which the nitrogen addition cools the electron temperature. Analyses following this work must account for the loss of electrons due to electron temperature cooling from the addition of other gases if correct predictions of Penning ionization with helium is expected.

XI. Conclusions and Recommendations

This experiment has shown that discharges in microwave cavities leads to the production of helium (2^3S) metastables densities of about 5×10^{10} metastables/cm^3. Further it has been shown that electron densities of about 5×10^{10} electrons/cm^3 can be readily produced up to twenty torr using the microwave cavity discharge. Thirdly, it has been shown that minute amounts of nitrogen added to the afterglow of a helium discharge increases the electron density due to Penning ionization.

One important discovery was the electron-ion recombination coefficient increase due to the addition of nitrogen in the helium afterglow. This recombination coefficient increase is due to the more rapid cooling of the electron temperature when nitrogen is added.

A second discovery was the observation of negative absorption on the 3889Å line in the pure helium afterglow at a 35.75 liter/minute flow rate, sixteen to twenty torr pressure, and 35.80 watts/cavity microwave power.

Because of the transonic nature of the flow, the undetermined velocity profile, the undetermined pressure profile across the reaction, and the unusual construction of the reaction chamber, modelling the plasma is extremely difficult. It is suggested therefore that a more conventional axial flow design be constructed and the experiment be repeated to better determine the metastable and electron production for conventional applications. It is further suggested that an optical cavity be built to test for stimulated emission on the 3889Å line where

negative absorption was seen. Lastly it is suggested that a Laser Doppler Velocimeter (LDV) be obtained to determine the areas of maximum turbulence for optimum mixing of the helium afterglow with a Penning gas.

Time prevented the attempted extension of this technique to atmospheric pressures.

Bibliography

1. Cold Cathode Discharge Tubes. J. R. Acton and J. D. Swift. Academic Press, 1963.

2. "Exciting Atoms in Decaying Optically Thick Plasmas". D. R. Bates, K. L. Bell, A. E. Kingston. Proceedings of the Physical Society (London) 91: 288-299 (1967).

3. "Cross Sections for the De-Excitation of Helium Metastable Atoms by Collisions with Atoms". E. E. Benton, E. E. Ferguson, F. A. Matsen, and W. W. Robertson. Physical Review 128, #1: 206-209 (October 1, 1962).

4. "The Measurement of Penning Ionization Cross Sections for Helium (2^3S) Metastables Using a Steady-State Flowing Afterglow Method." R. C. Bolden, R. S. Hemsworth, N. J. Shaw, and N. D. Twiddy. Journal of Physics B 3: 61-71 (1970).

5. "Measurements of Thermal-Energy Ion-Neutral Reaction Rate Coefficients for Rare-Gas Ions". R. C. Bolden, R. S. Hemsworth, M. J. Shaw and N. D. Twiddy. Journal of Physics B: Atomic and Molecular Physics 3:45-60 (1970) (London).

6. "Closed Cycle Performance of a High Power Electrical Discharge Laser". C.O. Brown and J. W. Davis. Applied Physics Letters 21: 480-481 (November 1972).

7. Basic Data of Plasma Physics. S. C. Brown. Technology Press (1959).

8. "Magnetically Stabilized Cross-Field CO_2 Laser". C. J. Buczek, R. J. Wayne, P. Chenausky and R. J. Freiberg. Applied Physics Letters. 16: 321-323 (April 1970).

9. "Electron Temperature Dependence of the Recombination Coefficient in Pure Helium". C. L. Cher, C. C. Leiby, and L. Goldstein. Physical Review 121: 1391 (1961).

10. "Chemiluminescent Reactions of $He(2^3S)$ with Nitrogen, Oxygen, Carbon Monoxide and Carbon Dioxide". M. Cher and C. S. Hollingsworth. Journal of Chemical Physics 50 #11: 4942-4949 (1 June 1969).

11. "A Fluid Mixing Laser". Terrill A. Cool. Applied Physics Letters 9: 12:418-420 (15 December 1966).

12. "Gain Measurements in a Fluid Mixing CO_2 Laser System". T. A. Cool and J. A. Shirley. Applied Physics Letters 14, #2: 70-72 (15 January 1969).

13. "Review of CW High-Power CO_2 Lasers". Anthony J. Demaria. Proceedings of the IEEE 61, #6: 731-748 (June 1973).

14. "Energy Exchange Processes in a Low Temperature N_2-CO Transfer Laser", N. Djeu. Chemical Physics Letters 15, #3: 392-395 (15 August 1972).

15. "Calculation of Cross Sections for Zero Activation Energy Processes by Simple Collision Models with Emphasis on the Penning Effect" by E. E. Ferguson. Physical Review 128, #1: 210-212 (October 1, 1962).

16. "Dissociative Recombination in Helium Afterglows". E.E. Ferguson, F. C. Fehoenfeld, A. L. Schmeltekopf. Physical Review 138, #2A: A381-A385 (19 April 1965).

17. "Influence of Plasma Kinetic Processes on Electrically Excited CO_2 Laser Performance". M. C. Fowler. Journal of Applied Physics 43: 3480-7 (August 1972).

18. "Rotational Excitation and Momentum Transfer Cross Sections for Electrons in H_2 and N_2 from Transport Coefficients," L. S. Frost, A. V. Phelps. Physical Review 127, #5: 1621-33 (September 1, 1962).

19. "Atmospheric Pressure Pulsed CO_2 Laser Utilizing Preionization by High-Energy Electrons", R. K. Gainsworthy, L.E.S. Mathias, CH.H. Carmichael, Applied Physics Letters 19:18-19 (July 1972).

20. "Enhancement of CO_2 Laser Power and Efficiency by Neutron Irradiation". T. Ganley, J. T. Verdeyen, G. H. Miley. Applied Physics Letters 18, #12: 256-269 (15 June 1971).

21. "Potential Energy Curves for N_2, NO, O_2 and Corresponding Ions". Forrest R. Gilmore. Journal of Quantum Spectroscopy and Radiative Transfer, 5:369-390 (1965).

22. "Plasma Stability of Electric Discharges in Molecular Gases." Roger A. Haas, Physical Review 8 #2: 1017 (August 1973).

23. Spectra of Diatomic Molecules. G. Herzberg, F.R.S. VanNostrand Reihold Company (1950).

24. Molecular Spectra and Molecular Structure. G. Herzberg. D. Van Nostrum (1960).

25. Foundation of Plasma Dynamics. E. Holt, R. Haskell. MacMillian Company. (1965).

26. Plasma Diagnostic Techniques. R. H. Huddlestone, S. L. Leonard. Academic Press: (1965).

27. "Metastable Measurements in Flow Helium Afterglow", R. W. Huggins, J. H. Cahn. Journal of Applied Physics 38, #1: 180-188 (January 1967).

28. "Helium Afterglow and the Decay of the Electron Energy." J. C. Ingraham, S. C. Brown. Physical Review 138, #4A: A1015-A1022, (17 May 1965).

29. "Ionizing Collisions of Two Metastable Helium Atoms (2^3S)" A. W. Johnson, J. B. Gerado. Physical Review A 7, 3:925 (March 1973).

30. "Ionization Growth and Breakdown". F. L. Jones, Encyclopedia of Physics XXII: 1-40, Springer-Verlac (Berlin) (1956).

31. "Observation of Laser Oscillation in a 1-atm (CO_2-N_2-He Laser Pumped by an Electrically Heated Plasma Generated via Photo-Ionization". J. S. Levine, A. Javan. Applied Physics Letter: 22:55-57 (January 1973).

32. Fractional Power Transfer as a Function of E/N into Vibrational Electronic, Metastable, and Ionic States (Personal communication). Bill Long. Aeronautical Research Laboratories, Wright-Patterson AFB, Ohio, October 1973.

33. Microwave Breakdown in Gases. A. D. MacDonald. John Wiley & Sons, (1966).

34. Collision Phenomena in Ionized Gases. McDaniel, E. W. John Wiley & Sons (1964).

35. Mobility and Diffusion of Ions in Gases. E. W. McDaniel, E. A. Mason. John Wiley & Sons (1973).

36. "Continuous-Wave CO_2 Laser at Atmospheric Pressure", R. McLeary W.E.K. Gibbs, Journal of Quantum Electronics of IEEE, QE-8: 596-597 (Paper Q.7) (June 1972).

37. Electronic & Ionic Impact Phenomena, Massey, H.S.W., E.H.S. Burhop, Clarenden Press: Oxford, England (1952).

38. "Behavior of He(2^3S) Metastable Atoms in Weakly Ionized Plasmas". P. A. Miller, J. T. Verdeyen, B. E. Cherrington, Physical Review A 4, #2: 692-700 (August 1971).

39. Partially Ionized Gases. M. Mitchner, C.H. Kruger, John Wiley & Sons (1973).

40. Fundamentals of Gaseous Ionization and Plasma Electronics, Essam Nasser. Wiley-Interscience (1971)

41. "Progress in High Pressure Electric Lasers". William L. Nighan. United Aircraft Research Lab Report, UAR-M107, September 1973.

42. "Lifetimes of Metastable States of Noble Gases", A.V. Phelps, J. P. Molnar, Physical Review 89, #6: 1202 (1953).

43. "Penning Ionization Optical Spectroscopy; Metastable Helium... Chlorine". W. C. Richardson, D.W. Setser, Journal of Chemical Physics 58, #5: 1809-1825 (1 March 1973).

44. "Reaction of Atomic Oxygen Ions with Vibrationally Excited Nitrogen Molecules", A. L. Schmetekopf, F.C. Fehesenfeld, G.I. Gilman, E.E. Ferguson. Planetary Space Science 15: 401 (1967).

45. "Manifestations of the Structure in Electron Energy Distribution Functions and Using it to Determine the Effective Cross Sections of Inelastic Processes". A. N. Soldatov, N.A. Prilezhayeva. Izvertiza Vysshikh Uchebnykh Zavedenig Fizika 11: 51-62 (1971).

46. Tables of Spectral Lines. Zaidei, A.N.

47. Absorption and Collision Broadening of the Mercury Resonance Line". M. W. Zemansky, Physical Review 36: 219-238 (1930).

APPENDIX A

Reproduction of Experimental I-V Curves

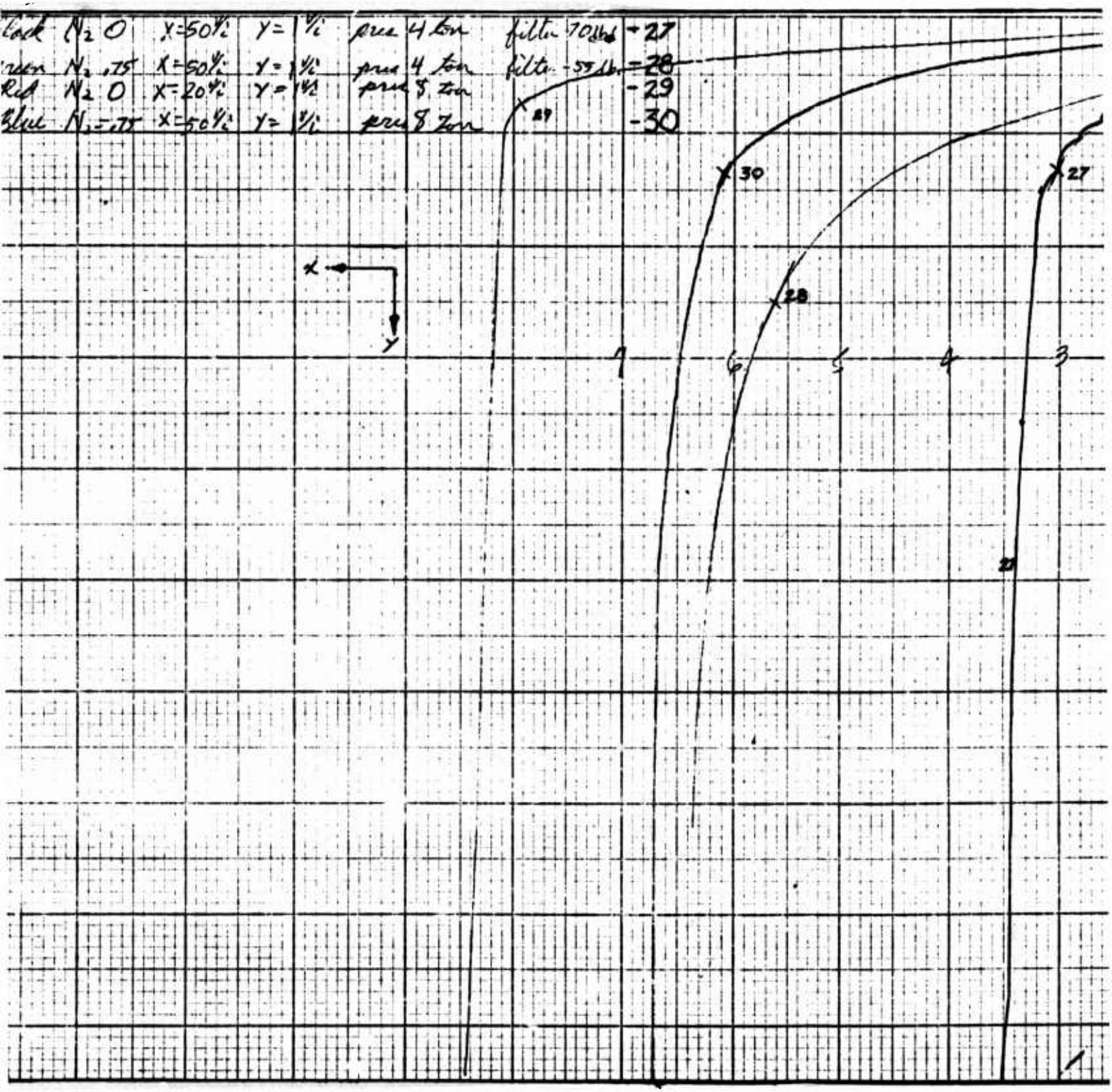
Black N_2O X=50% Y= % pres 4 torr filter 70 lbs -27
Green N_2 .75 X=50% Y= % pres 4 torr filter -55 lbs -28
Red N_2O X=20% Y= % pres 8 torr -29
Blue N_2 .75 X=50% Y= % pres 8 torr -30
x
y
30
28
27
1
6
5
4
3
2
1

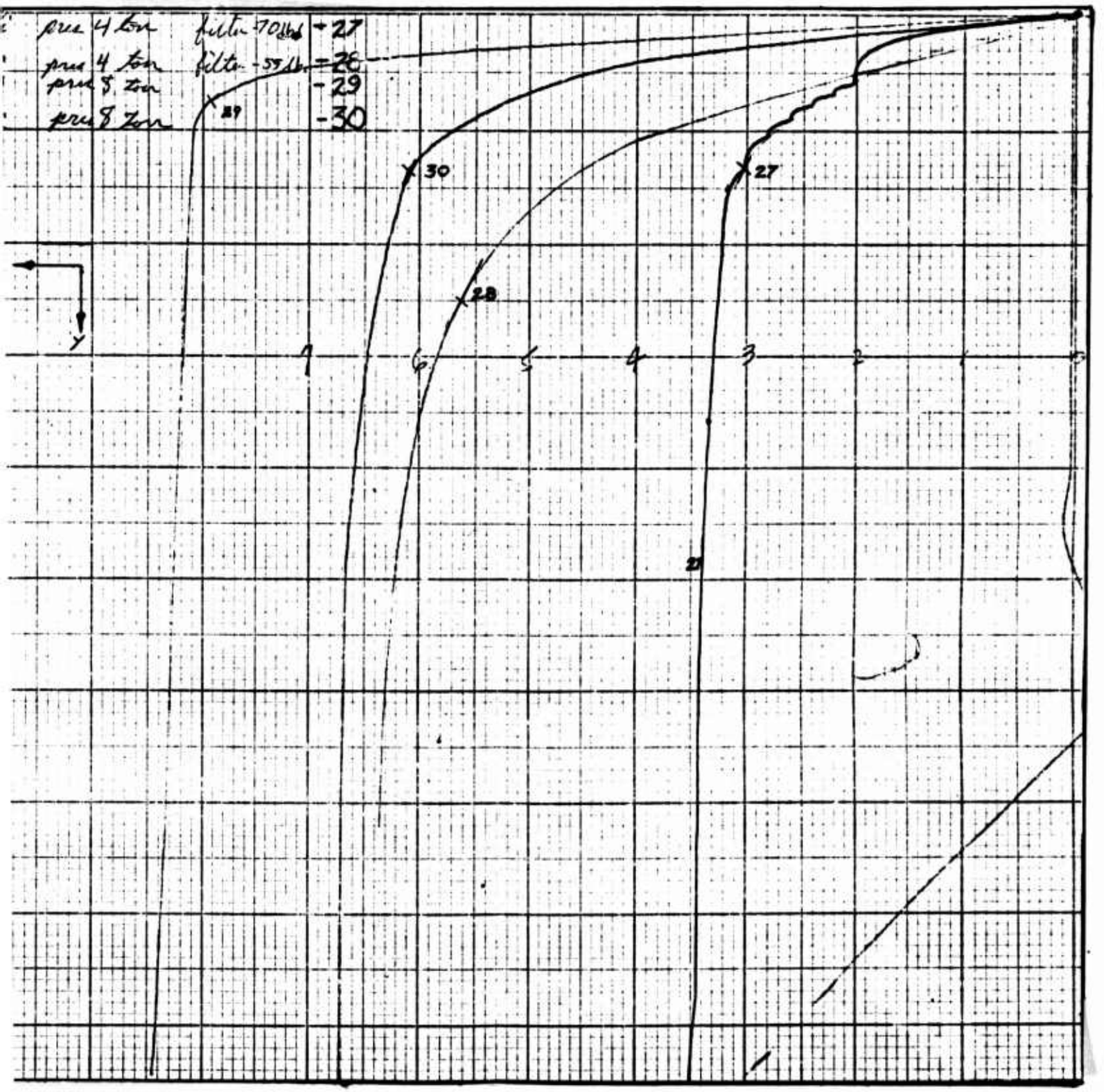
pre 4 ton filter 70 lbs +27
pre 4 ton filter 55 lbs -26
pre 5 ton -29
pre 8 ton -30
29
30
28
27
y
1
6
5
4
3
2

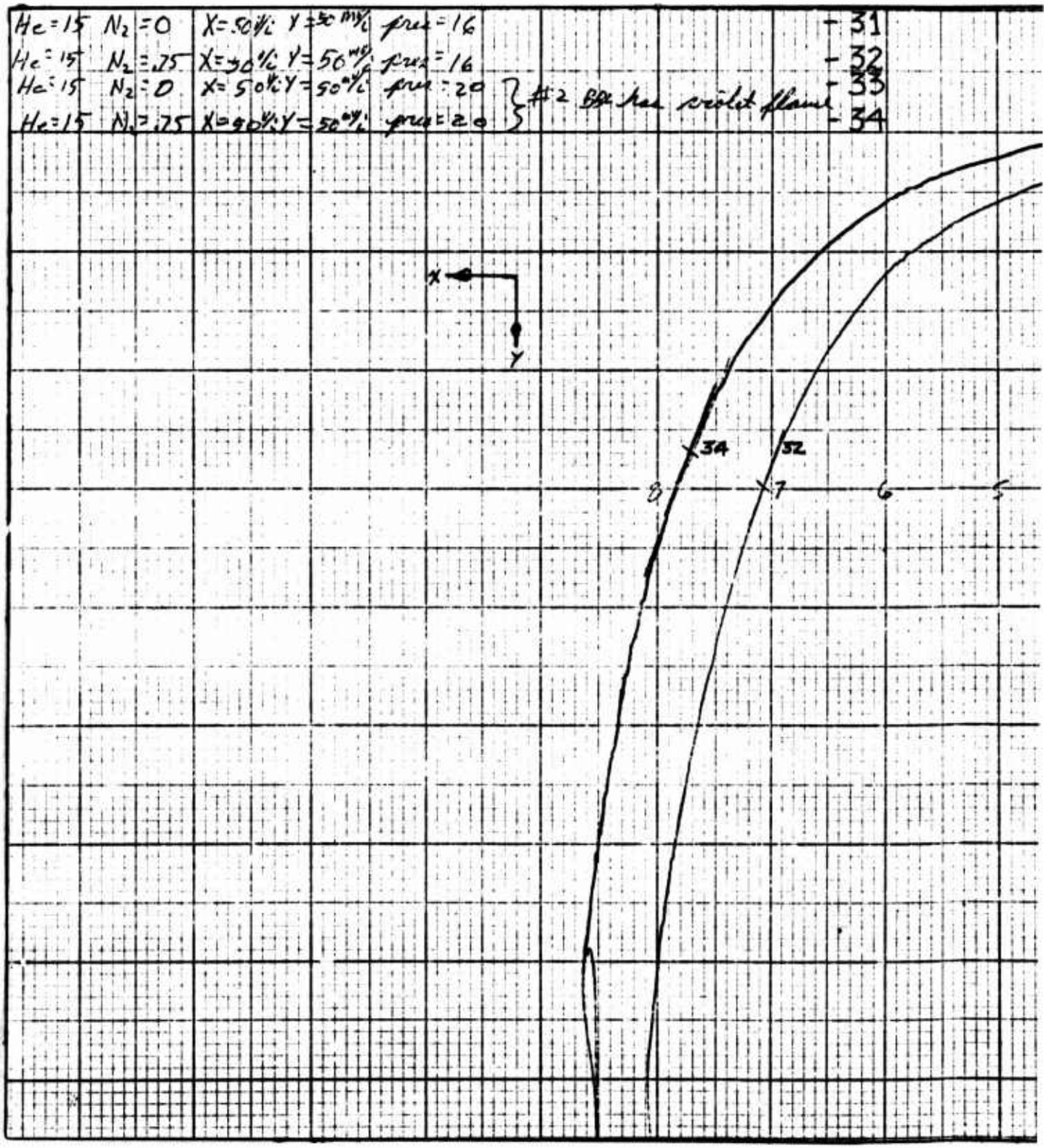
He=15 N2=0 X=50% Y=50% pres=16 - 31
He=15 N2=.25 X=50% Y=50% pres=16 - 32
He=15 N2=0 X=50% Y=50% pres=20 - 33
He=15 N2=.25 X=50% Y=50% pres=20 - 34
#2 Bar has violet flame
X
Y
34
32
8
7
6
5

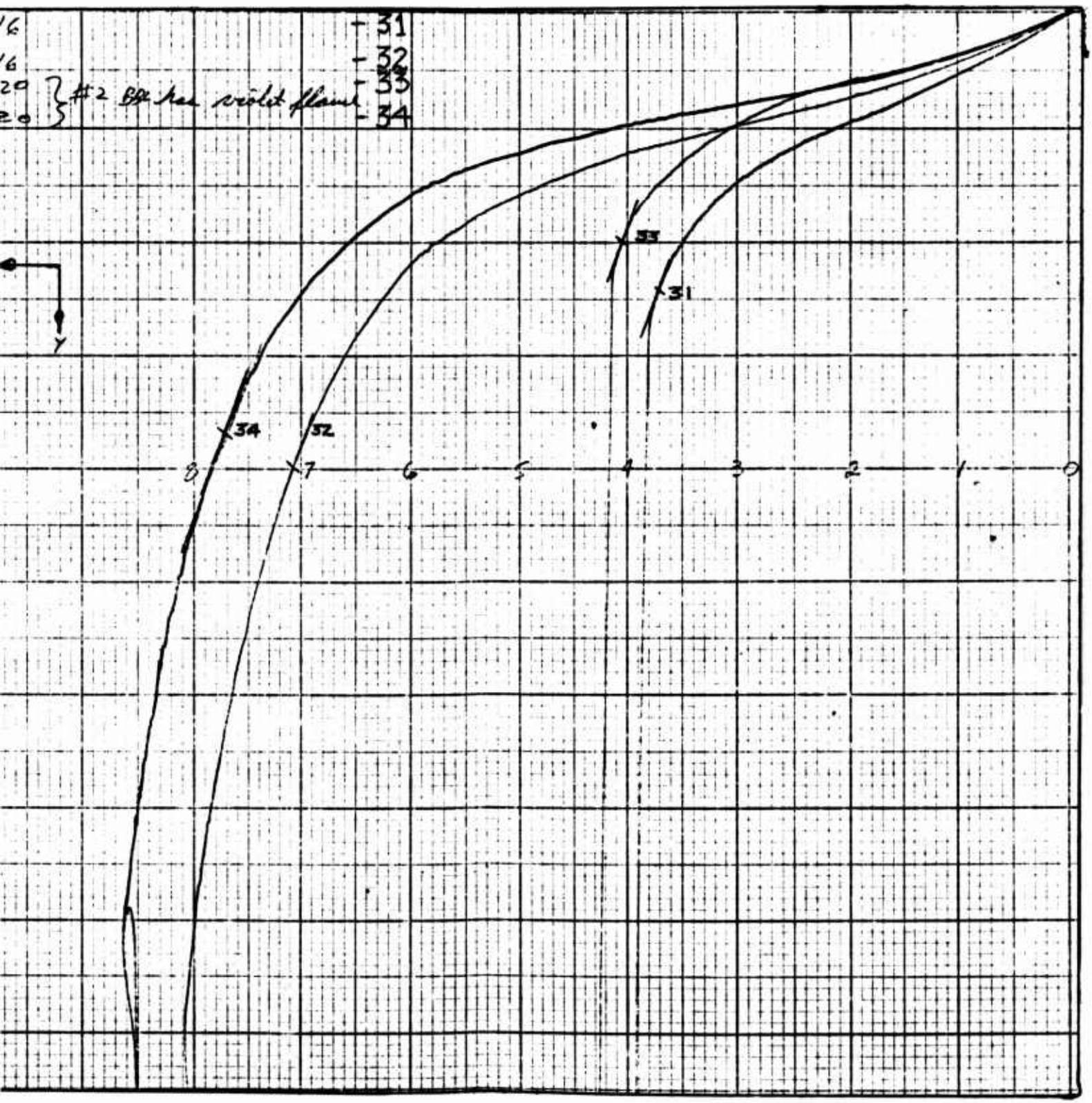
16
16
20
20
#2 Bk has violet flame
31
32
33
34
Y
34
32
33
31
8
7
6
5
4
3
2
1
0

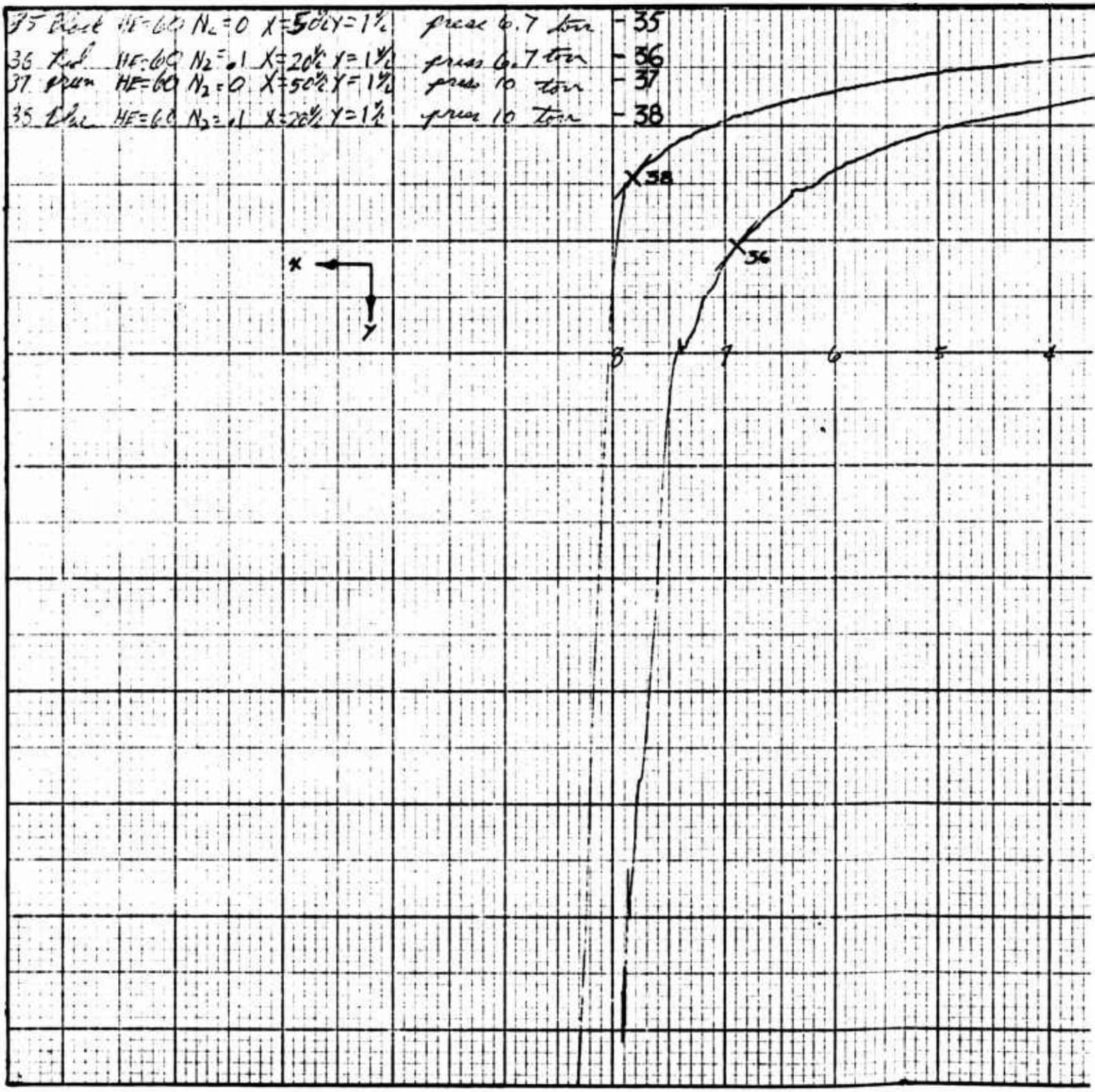
35 Blue HF=60 N2=0 X=50% Y=1½ press 6.7 torr
36 Red HF=60 N2=.1 X=20% Y=1½ press 6.7 torr
37 green HF=60 N2=0 X=50% Y=1½ press 10 torr
38 blue HF=60 N2=.1 X=20% Y=1½ press 10 torr
35
36
37
38
X
Y
8
7
6
5
4

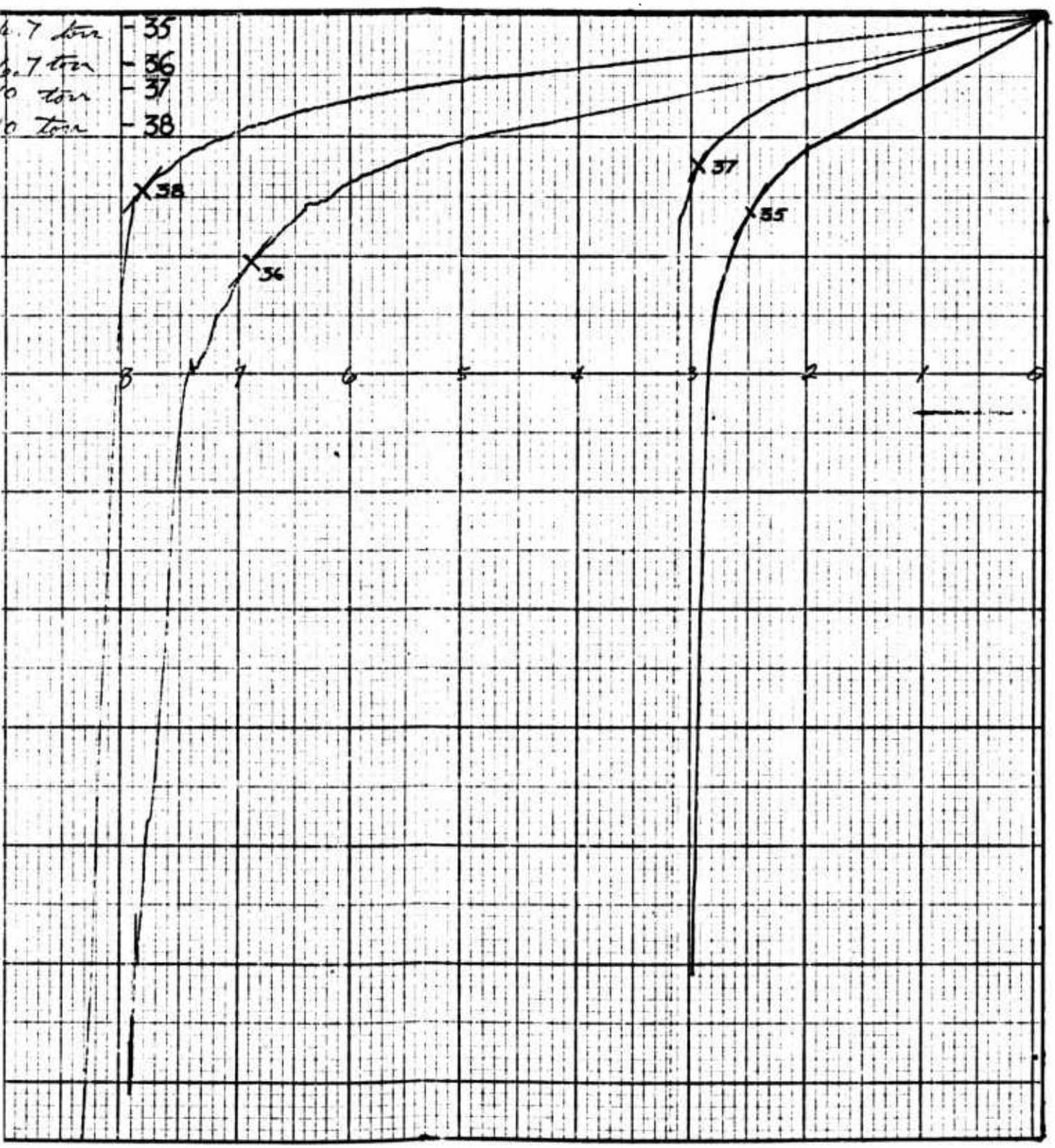
4.7 torr - 35
3.7 torr - 36
0 torr - 37
0 torr - 38
38
36
37
35
8
7
6
5
4
3
2
1
0

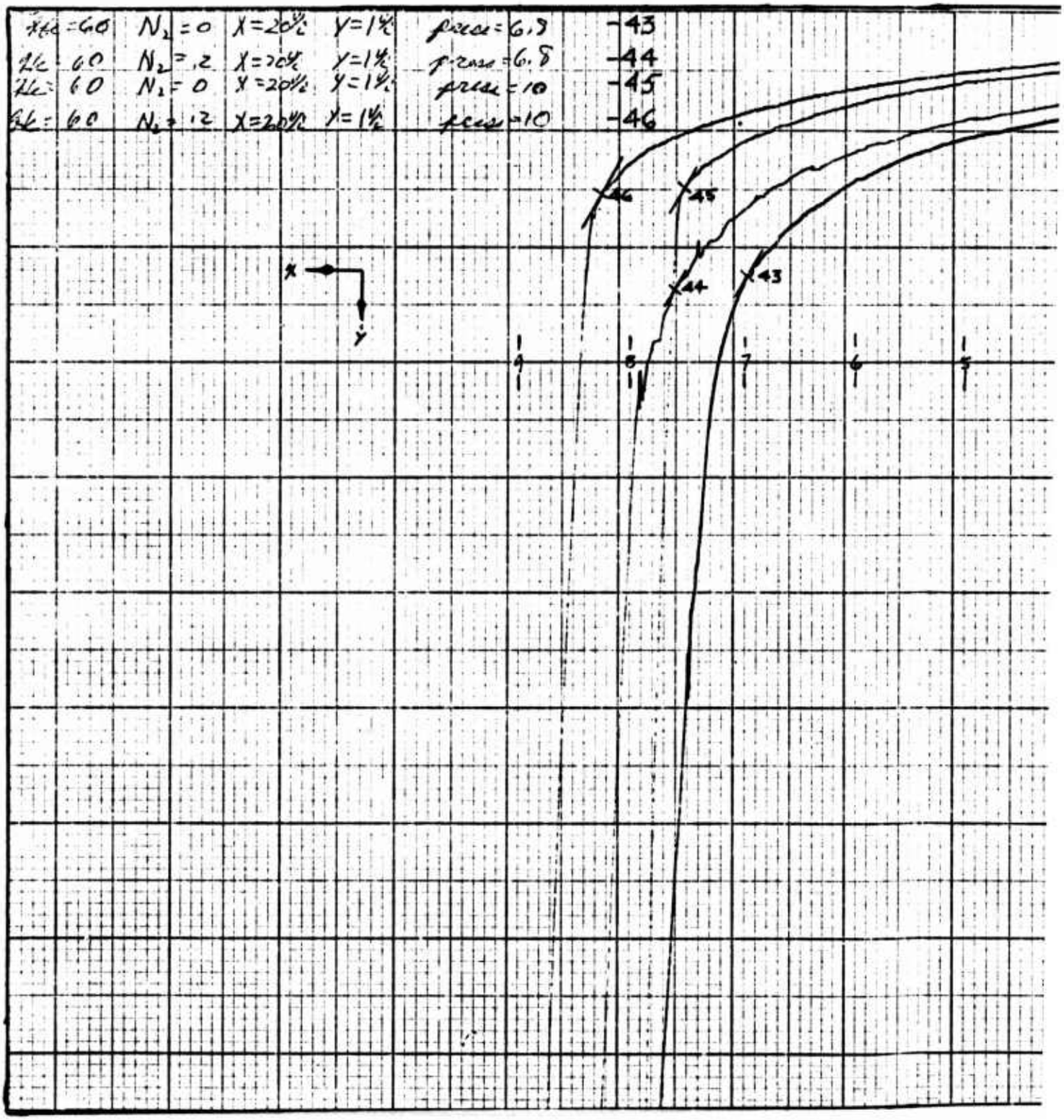
x_{tc} = 60 N_2 = 0 X = 20½ Y = 1½ press = 6.9 -43
2c 60 N_2 = .2 X = 20½ Y = 1½ press = 6.8 -44
2c 60 N_2 = 0 X = 20½ Y = 1½ press = 10 -45
2c 60 N_2 = .2 X = 20½ Y = 1½ press = 10 -46
X
Y
46
45
44
43
9
8
7
6
5

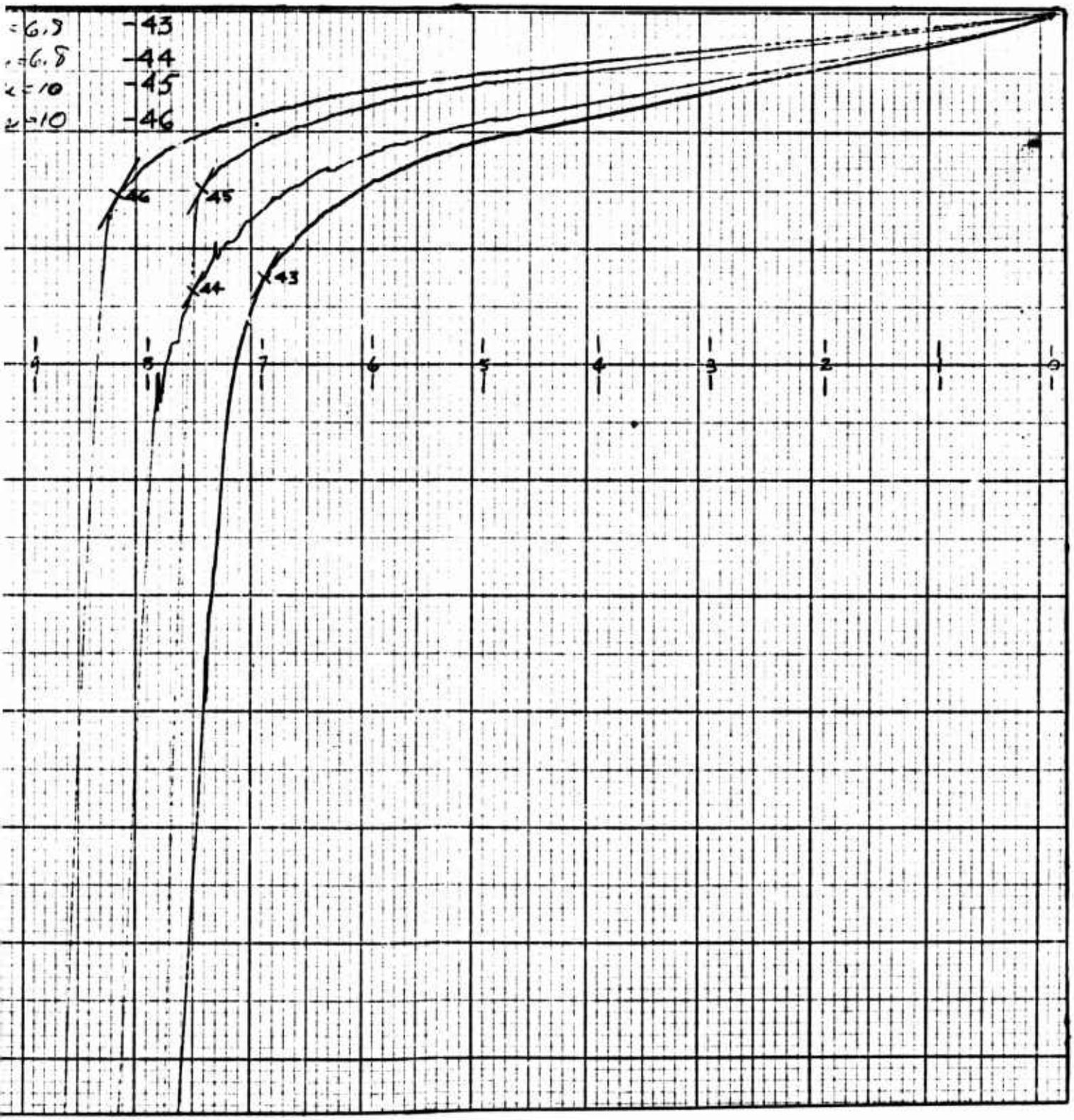
=6.9
=6.8
=10
=10
-43
-44
-45
-46
46
45
44
43
9
8
7
6
5
4
3
2
1
0

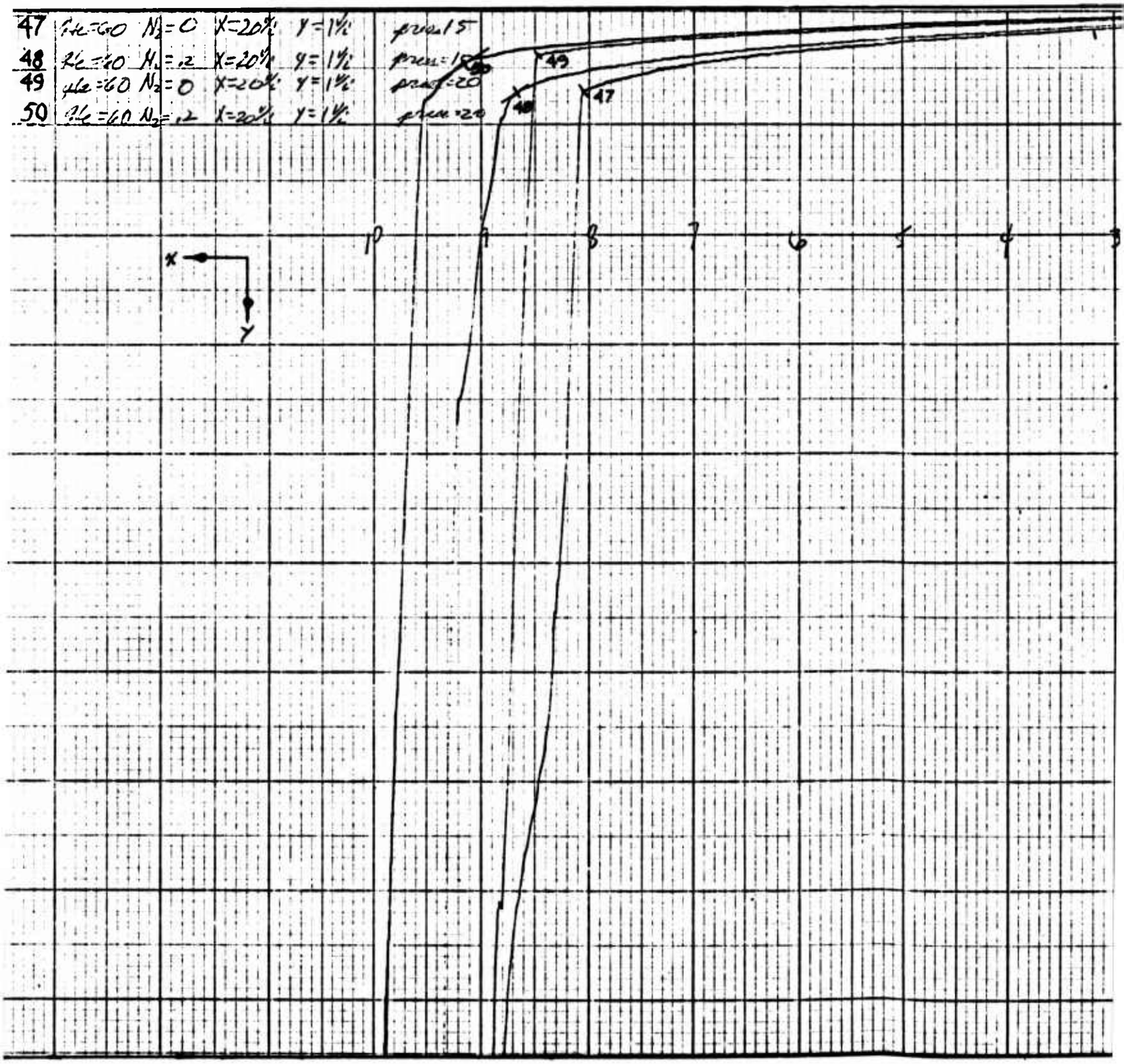
47 Re=60 N2=0 X=20% Y=1½ pres 15
48 Re=60 N2=.2 X=20% Y=1½ pres=18
49 Re=60 N2=0 X=20% Y=1½ pres=20
50 Re=60 N2=.2 X=20% Y=1½ pres=20
49
47
X
Y

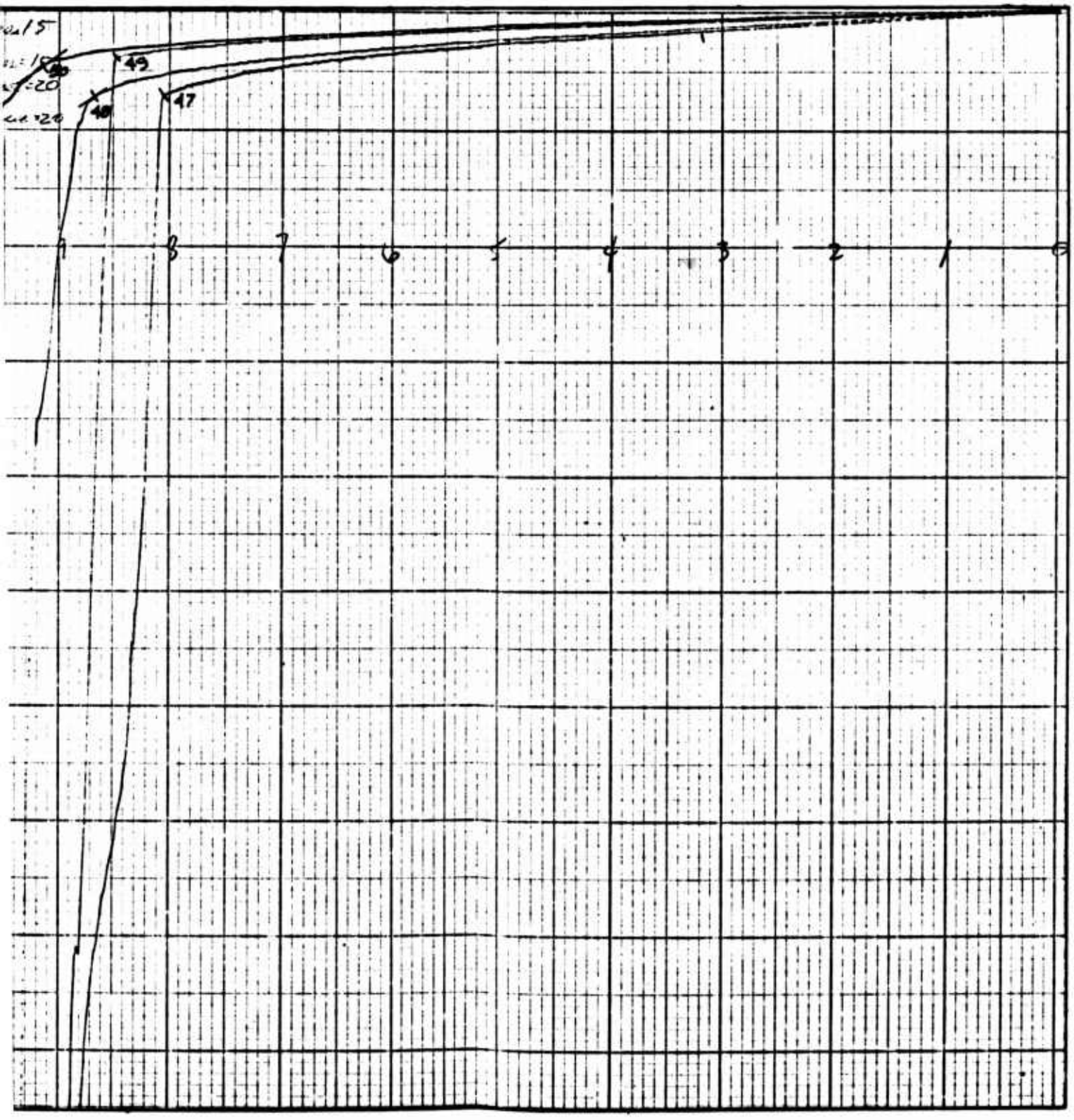
49
47
8
7
6
5
4
3
2
1

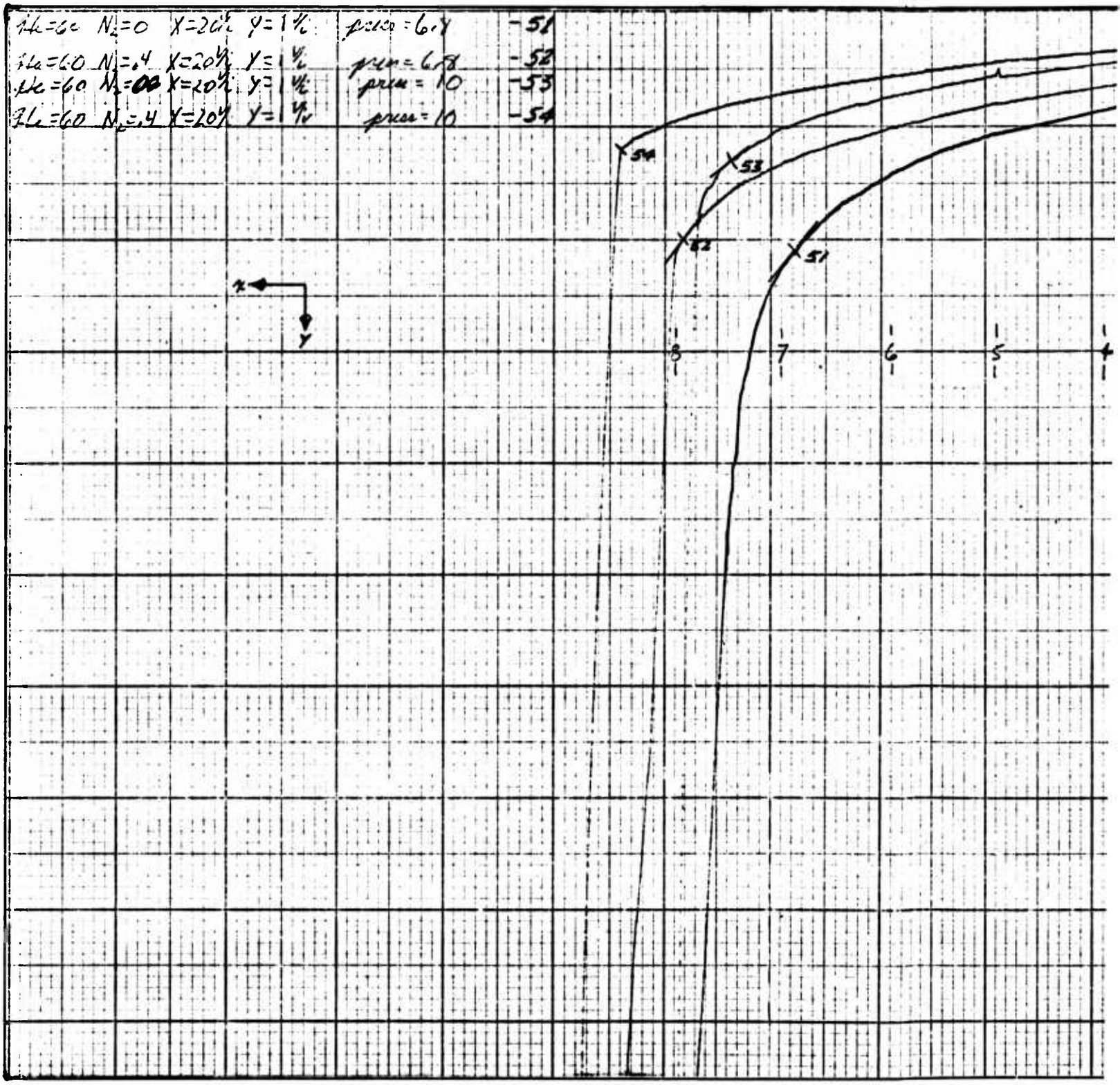
M_∞=6.0 N_2=0 X=20½ Y=1½ pitot=6.4 -51
M_∞=6.0 N_2=.4 X=20½ Y=1½ pitot=6.8 -52
M_∞=6.0 N_2=.8 X=20½ Y=1½ pitot=10 -53
M_∞=6.0 N_2=.4 X=20½ Y=1½ pitot=10 -54
54
53
52
51
x
y
8
7
6
5
4

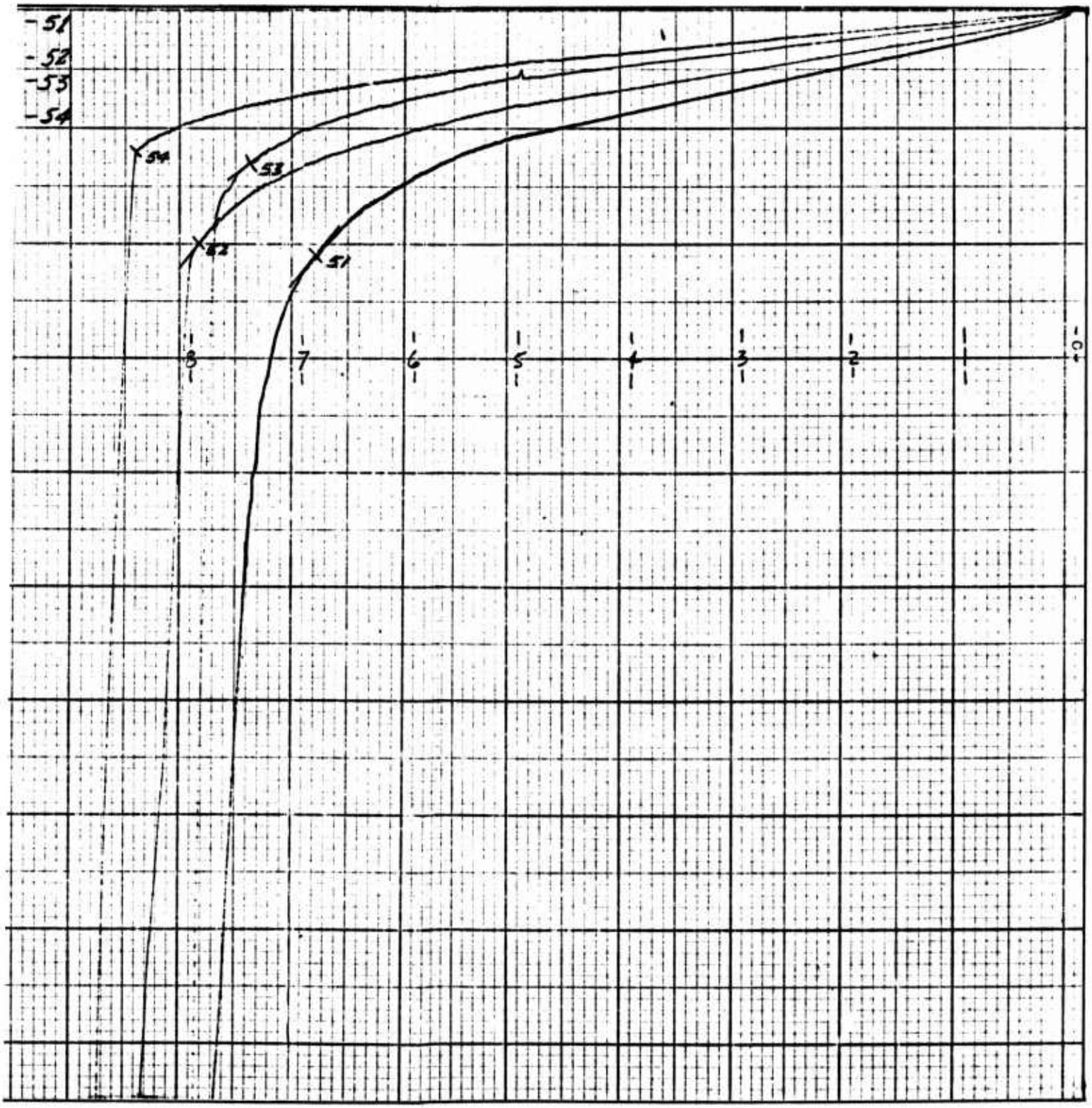
-51
-52
-53
-54
54
53
52
51
8
7
6
5
4
3
2
1
0

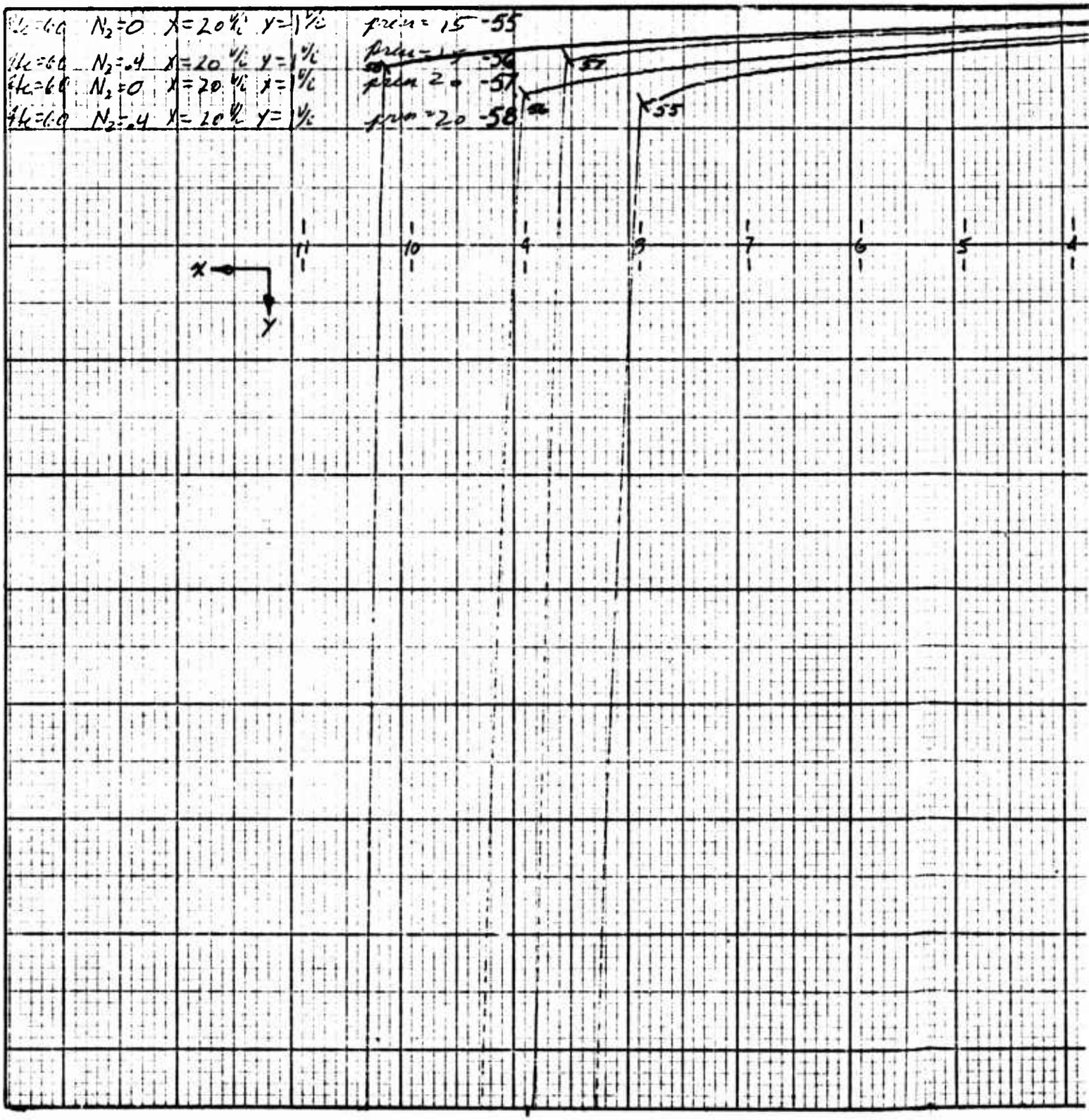
H_2=6.0 N_2=0 X=20% Y=1% p_{max} = 15 -55
H_2=6.0 N_2=.4 X=20% Y=1% p_{max} = 1 -56
H_2=6.0 N_2=0 X=20% Y=1% p_{max} = 2 -57
H_2=6.0 N_2=.4 X=20% Y=1% p_{max} = 20 -58
57
55
11
10
4
9
7
6
5
4
X
Y

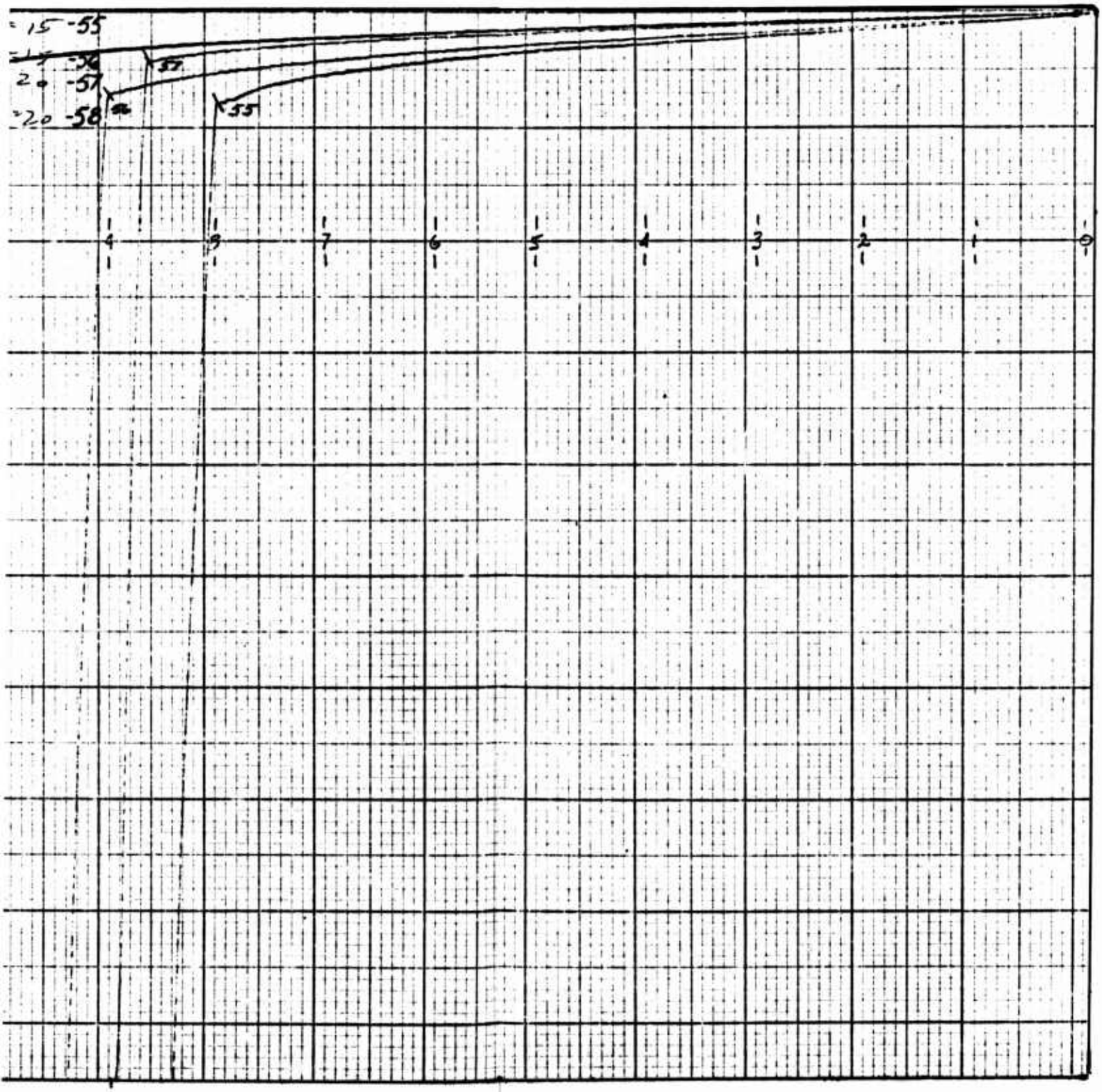
=15 -55
=1 -56
2 -57
=20 -58
55
55
4
3
7
6
5
4
3
2
1
0

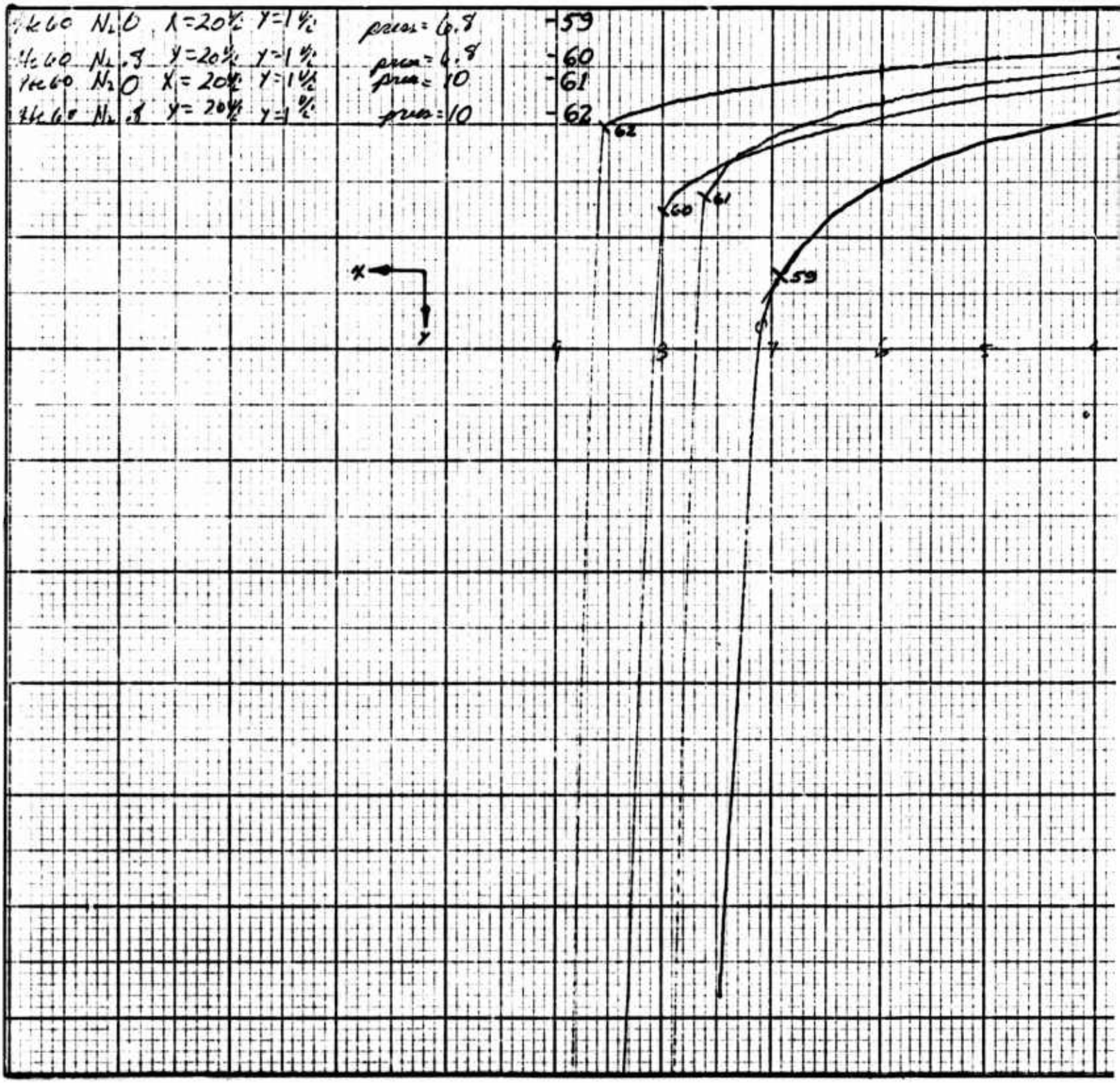
Hg 60 N2 O X=20½ Y=1½
Hg 60 N2 .8 Y=20½ Y=1½
Hg 60 N2 O X=20½ Y=1½
Hg 60 N2 .8 Y=20½ Y=1½
press = 6.8
press = 6.8
press = 10
press = 10
-59
-60
-61
-62
62
60
61
59
X
Y

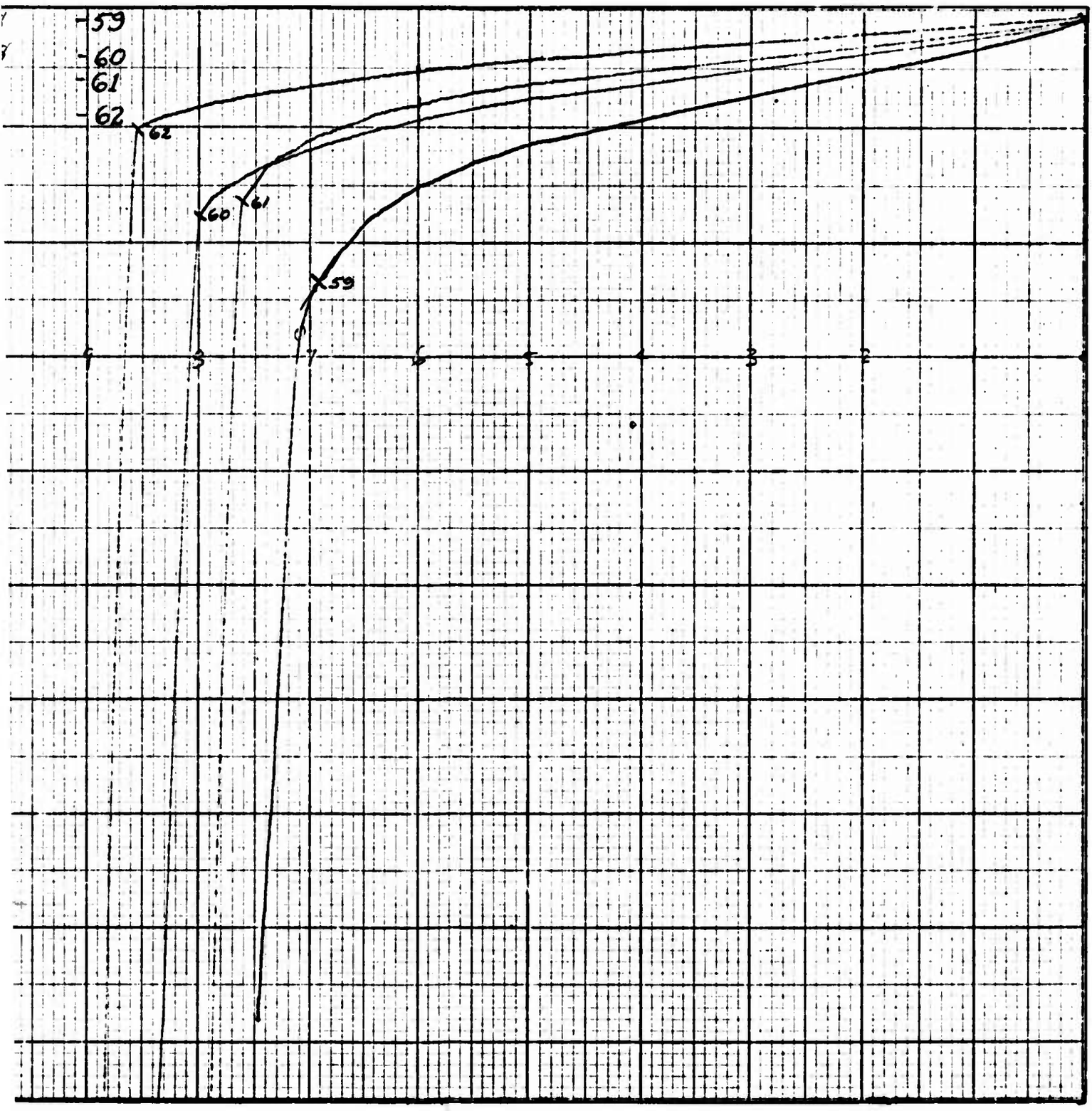
-59
-60
-61
-62
62
60
61
59

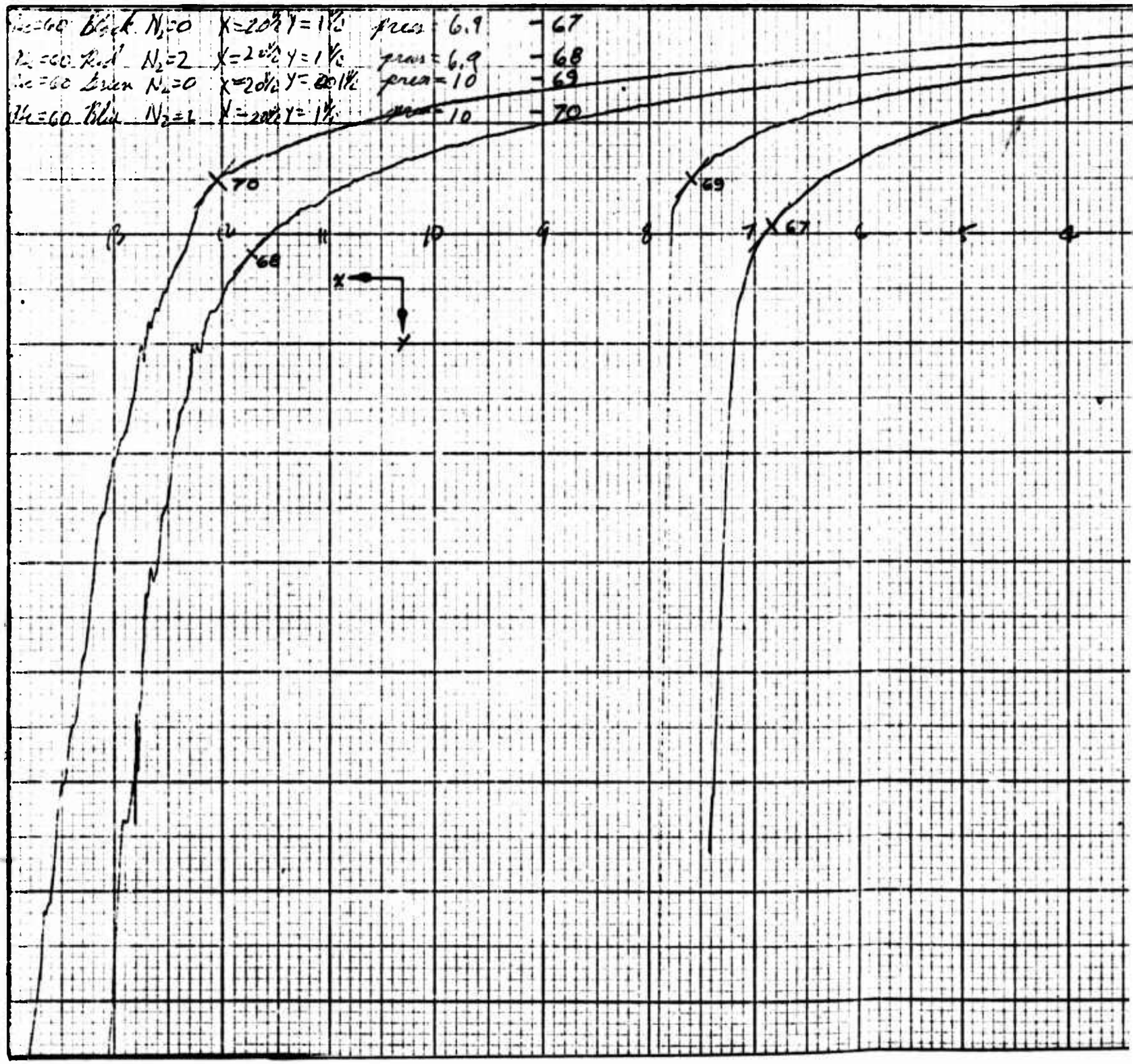
Black N_2=0 X=20½ Y=1½ press 6.9 – 67
Red N_2=2 X=20½ Y=1½ press 6.9 – 68
Green N_2=0 X=20½ Y=1½ press 10 – 69
Blue N_2=2 X=20½ Y=1½ press 10 – 70
70
69
68
67
X
Y

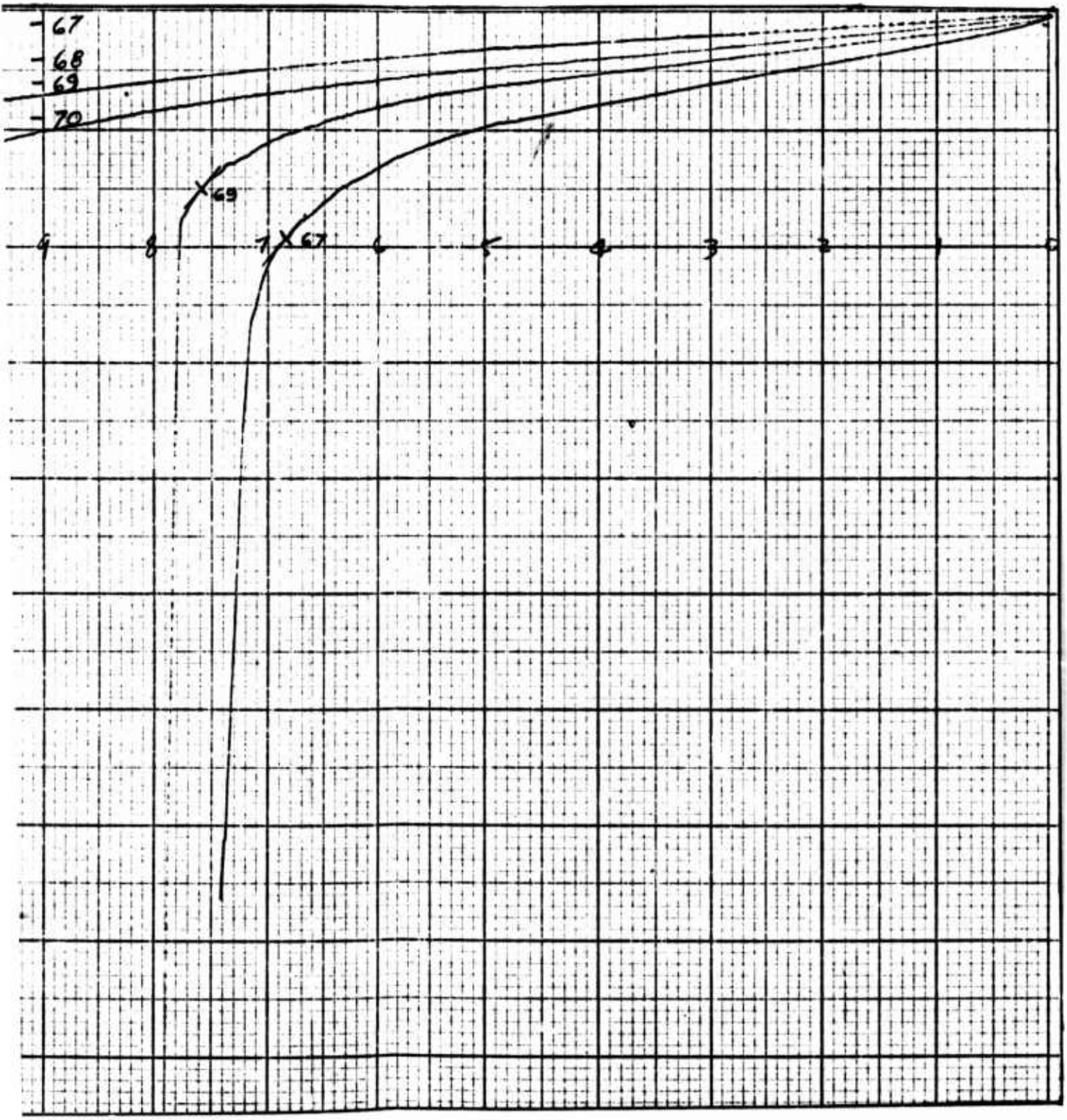
67
68
69
70
69
67
9
8
7
6
5
4
3
2
1
0

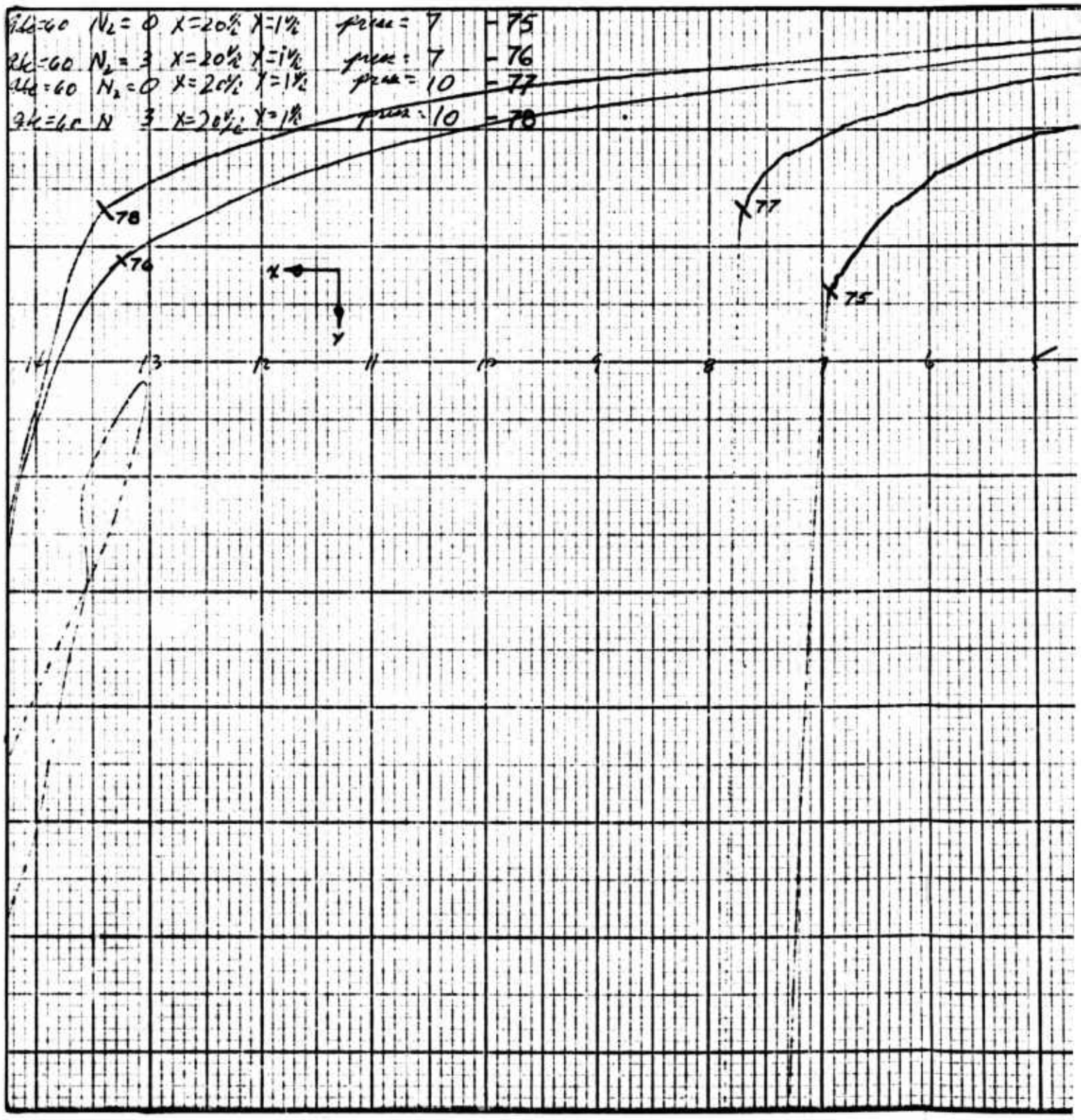
$\dot{m}_a$=60 N_2 = 0 X=20% X=1% p_{max} = 7 - 75
$\dot{m}_a$=60 N_2 = 3 X=20% X=1% p_{max} = 7 - 76
$\dot{m}_a$=60 N_2 = 0 X=20% X=1% p_{max} = 10 - 77
$\dot{m}_a$=60 N_2 = 3 X=20% X=1% p_{max} = 10 - 78
78
76
77
75
x
y
14
13
12
11
10
9
8
7
6

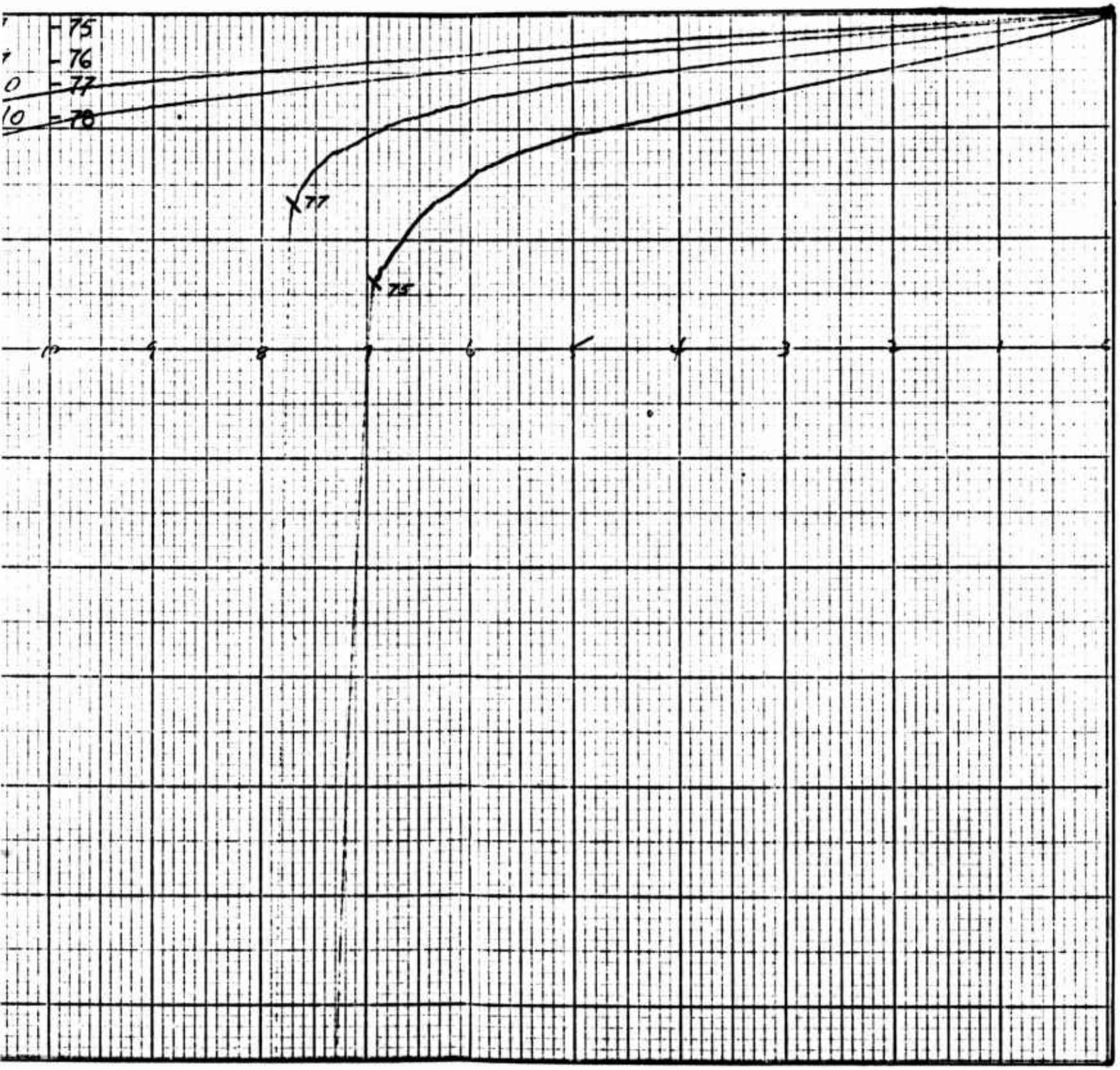
75
76
77
78
77
75
10
9
8
7
6
5
4
3
2
1

VITA

David Reginald Durham was born [redacted]. He graduated from [redacted] He received a Bachelor of Engineering Science in biological-mechanics from the University of Texas. After Officer Training School, he attended pilot training at Reese Air Force Base. He was married [redacted] He served as a pilot in Southeast Asia from August 1968 to August 1969. He subsequently served as an Aircraft Commander and Mission Instructor Pilot at McCoy Air Force Base, Florida. He entered the Air Force Institute of Technology in June 1972.